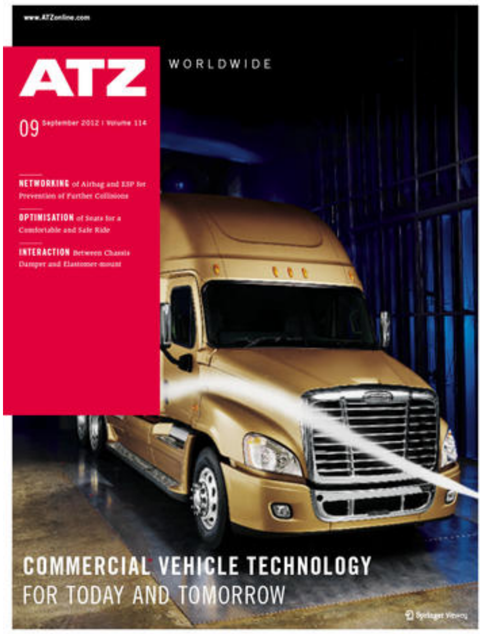


ATZ .worldwide 9/2012
http://www.atz-worldwide.com

www.ATZonline.com

# ATZ WORLDWIDE

09 September 2012 | Volume 114

**NETWORKING** of Airbag and ESP for Prevention of Further Collisions

**OPTIMISATION** of Seats for a Comfortable and Safe Ride

**INTERACTION** Between Chassis Damper and Elastomer-mount


## COMMERCIAL VEHICLE TECHNOLOGY FOR TODAY AND TOMORROW

Springer Vieweg

CONTENTS

COVER STORY

# COMMERCIAL VEHICLE TECHNOLOGY FOR TODAY AND TOMORROW

**4, 10** I The commercial vehicle industry has the task of developing technologies that satisfy both economic and ecological interests while at the same time addressing the conflicting demands of haulage efficiency and climate protection. In the run-up to this year's IAA Commercial Vehicles, RWTH Aachen University has developed a battery-powered electric bus as part of its Smart Wheels research project, with the aim of showing the possibilities of this concept for a vehicle with zero local emissions. Voith is offering the world's first secondary water retarder for long-distance trucks and coaches as an already available series development.






**COVER FIGURE** © Daimler Freightliner
**FIGURE ABOVE** © Mercedes-Benz

# USEFUL SOLUTIONS

*Dear Reader,*

Even though people complain about too many useful commercial vehicles in overcrowded cities and endless convoys of HGVs on motorways, they still want to enjoy North German beer in Bavaria and eat Bavarian yoghurt in Hamburg. This means plenty of business for haulage companies.

The latest economic figures are a clear indication of the continued success of commercial vehicle manufacturers and hauliers. "The last two years have seen a great recovery. In Western Europe, sales of heavy commercial vehicles (over six tonnes) in 2011 climbed to around 262,000 units," said VDA President Matthias Wissmann in the run-up to the $64^{th}$ IAA Commercial Vehicles, which will take place in Hanover from 20 to 27 September 2012. That is a huge rise of 31 per cent compared to 2009.

Under the slogan "Commercial Vehicles: Driving the Future", the IAA in Hanover will underline the innovative power of the industry and the efficiency of commercial vehicles. One example of state-of-the-art technology is the Mercedes-Benz Actros. This truck has been optimised in every detail from its powertrain to its rolling resistance and aerodynamics. As a result, the Euro VI version of the Actros now consumes only around 26 litres of diesel per 100 kilometres – 4.5 per cent less than its Euro V compliant predecessor – in spite of lower emission levels.

Diesel emissions are today; electromobility is tomorrow. What the future state of technology might look like is shown by RTWH Aachen University in its innovative "Smart Wheels" project described on page 4. The two institutes ika and Isea have developed an electric bus with recharging intervals that enable it to achieve the daily driving range of urban bus routes. ika produced a prototype while Isea developed the battery system and an innovative fast charging unit.

In spite of all the euphoria surrounding technical developments and economic data, the commercial vehicle industry is nevertheless feeling the impact of the national debt crisis in European countries. The VDA expects new registrations of heavy trucks in Western Europe to total between 256,000 and 250,000 over the year 2012. That would be a drop of two to four per cent compared to the previous year. Looking beyond Europe, Brazil will also see a fall in its figures due to the introduction of a new exhaust standard and economic factors. China is having a break from expansion this year with a slight drop of three per cent.

Careful planning is therefore the order of the day. But one thing is certain: the IAA, with more exhibitors and a larger area than 2010, will have the right answers and will present useful solutions for the transport market of today and tomorrow.

Best regards,

Michael Reichenbach

**DIPL.-ING. MICHAEL REICHENBACH,**
Vice-Editor in Chief
Wiesbaden, 7 August 2012




# ELECTRIC MINIBUS FOR PUBLIC TRANSPORT

As part of the SmartWheels project funded by the Federal Ministry of Economics and Technology, two institutes of RWTH Aachen University have developed a battery electric minibus to demonstrate the potential of electric vehicles in public transport. The Institute of Automotive Engineering Aachen (ika) built the prototype vehicle based on a Mercedes-Benz Sprinter City 65. The Institute for Power Electronics and Electrical Drives (ISEA) has developed the battery system and an innovative quick charging device.


AUTHORS

**DIPL.-ING. FELIX TÖPLER**
is a member of the scientific staff in the drivetrain department at the Institute for Automotive Engineering at RWTH Aachen University (Germany).

**UNIV.-PROF. DR.-ING. LUTZ ECKSTEIN**
is Director of the Institute for Automotive Engineering at RWTH Aachen University (Germany).

**DIPL.-ING. GERRIT GEULEN**
is a member of the scientific staff in the electronics department at the Institute for Automotive Engineering at RWTH Aachen University (Germany).

**DIPL.-ING. JÉRÔME HOMANN**
is a member of the scientific staff and Manager Design and Prototyping Drivetrain at fka Forschungsgesellschaft Kraftfahrwesen Aachen mbH (Germany).

## MOTIVATION

The public transport system allows wide-scale and low cost mobility [1]. Most of the vehicles used in public transport in Germany are powered by diesel engines. Alternatives are natural gas, fuel cells or hybrid drives as well as electric drive systems, which are supplied with energy from a battery or a corresponding infrastructure (trolley busses).

Compared to other alternatives, electric drive systems have no local emissions and a low noise level. However, batteries have a relatively low energy density, which means that these vehicles will have a significantly shorter range than a vehicle powered by an internal combustion engine or a fuel cell. Compared to various commercial vehicles, such as those for long-distance transport, city buses have a low average speed and a shorter daily mileage. As city buses are used on fixed routes with only few changes over time, only a limited number of charging stations would need to be installed, thus reducing the necessary investment costs.

With the possibilities provided by a quick charging device, the average daily mileage can be reached with a few charging stops. ❶ shows the average moving velocity of a selected city bus line as well as an overland connection close to the city of Aachen [2]. The average moving velocity is defined as the average speed without standstill phases.

The inner city cycles are driven in the city area of Aachen and the overland cycles with a significant elevation profile between Aachen and the Eifel mountains. The objective was to demonstrate the performance of the electric drive system and to determine the actual range of the test vehicle in real driving conditions as well as the required charging time.

## TEST VEHICLE

The test vehicle was an electric minibus with a passenger capacity of around 25 people, ❷. The diesel engine and the automatic gearbox of the series-production vehicle were replaced by a hybrid synchronous motor with a maximum power of 150 kW. A single-stage planetary gear with a transmission ratio of 4.5 is flanged to the electric machine and connects the new propulsion system to the rear axle taken from the series-pro-

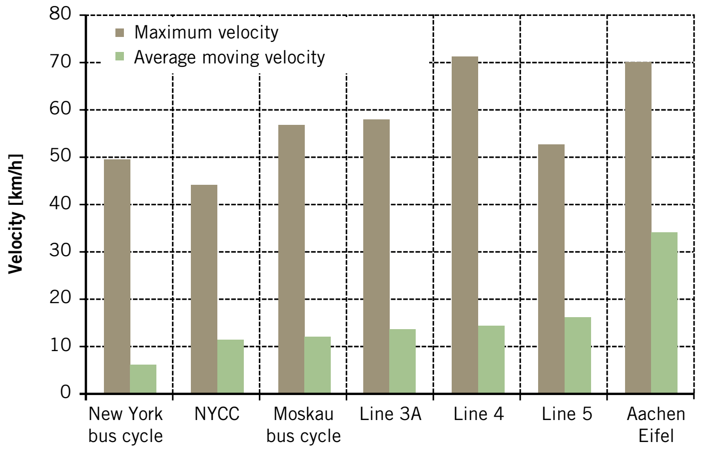


❶ Examples of bus cycles and urban city driving cycles

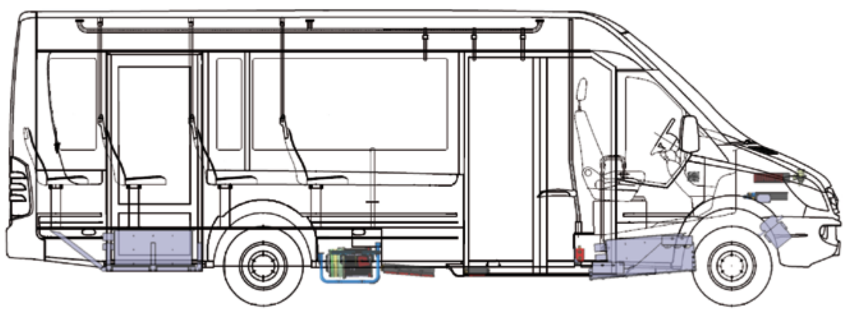

❷ Prototype of a electric-powered minibus

duction vehicle. The characteristics of the test vehicle are shown in ❸. Compared to the series-production vehicle, the passenger capacity is reduced due to the higher curb weight and the changed weight distribution.

The replacement of the propulsion system requires small modifications to the body of the minibus. The passenger cabin remains unchanged and does not differ from the diesel-powered model. The battery consists of two blocks of the same size, which are electrically connected in parallel and are also cooled or heated from a common liquid circuit in parallel. A PTC heating element installed in the battery circuit serves to heat the battery at low temperatures. Via a heat exchanger, the PTC can also be used for heating the interior. Since the heating requirements are much higher for a bus compared to a passenger car, due to the large interior volume and the frequent stops, an additional diesel-powered heater is also used as well as in the series-production vehicles.

The fuel is supplied from an auxiliary tank with a capacity of about 30 l. This ensures that the range in winter is not reduced by constantly using the electric heater. The high-voltage components of the drivetrain (electric motor, drive inverters, DC/DC converter) are liquid cooled in a further closed cycle. The waste heat is not used because both cooling circuits of the motor and the batteries are at a low temperature level. Moreover, due to the high efficiency, the power losses are considerably lower than in an internal combustion engine.

To ensure that the vehicle can pull away from a standstill on an incline of more than 20 % with maximum load or even overload, the powertrain is designed in such a way that the maximum traction force corresponds to that of the series-production vehicle in first gear. The maximum speed of 74 km/h is only slightly below that of the series-production vehicle (80 km/h) and is sufficient for a city bus. Changing the drive characteristics towards a higher top speed or a higher traction force at lower speeds can be achieved by using one of the other available differential gears from the series-production vehicles.

❹ shows the positioning of the new drive components added in the engine compartment and underbody area. The drive unit, which consists of an electric machine and a planetary gear, is installed in the space of the optional retarder. The drive inverter and the high-voltage distributor box are installed under the low-floor section between the longitudinal beams. The front battery block is located behind the front axle in the space of the 12-V battery, the automatic transmission and the offset gearbox of the diesel-powered model [3].

The high-voltage battery can be charged at any normal household socket via an

| CHARACTERISTICS | DATA | UNIT |
|---|---|---|
| Seats | 12 + 1 | – |
| Standing places | 10 to 15 | – |
| Curb weight | 4040 | kg |
| Maximum velocity | 5650 | kg |
| L × W × H | 7700 × 1993 × 2845 | mm |
| Motor power | 150 | kW |
| Maximum rotational speed | 12,000 | rpm |
| Battery capacity | 45 | kWh |
| Usable SOC range | 15 to 95 | % |
| Maximum discharging current | 400 | A |
| Maximum charging current | 160 | A |
| Charging time at 230 V | 12 | h |
| Charging time at 400 V DC | < 1 | h |
| Maximum velocity | 74 | km/h |

❸ Vehicle data of the test vehicle with battery electric propulsion; the number of standing places depends on the equipment and the seating arrangement

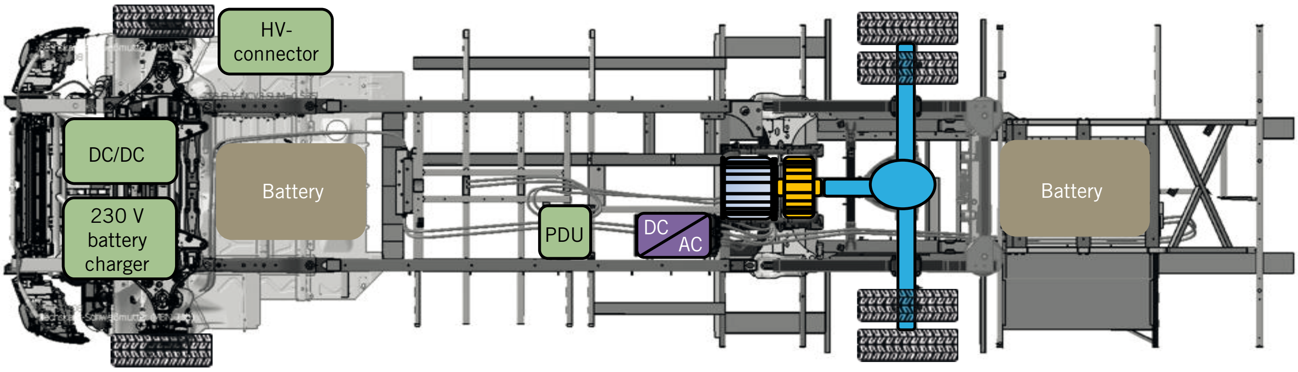


❹ Structure of the electric-powered bus



onboard 230 V charger. For an energy requirement of approximately 35 kWh, the maximum charging power of 3 kW results in a charging period of 12 h. In order to increase the availability and daily mileage of the vehicle, ISEA has developed a quick charging option within this project. A bipolar socket with the mechanical structure of a CHAdeMO standard plug is installed in the vehicle and allows a charging power of up to 64 kW at 400 V DC. During the charging process, the plug is connected directly to the high-voltage intermediate circuit. By using the quick charger, the time required for recharging the batteries can be reduced to 45 min. However, it depends on additional parameters such as the battery temperature and state of charge.

Driving torque is transferred only to the rear axle, as in the series-production vehicle. This might restrict recuperation, so that the slip of the drive wheels is limited during braking. Recuperation can be activated manually by the driver in three stages by actuating the gear selector lever. The brake characteristics correspond to the retarder of the series-production vehicle. The maximum braking power is 60 kW. There are no changes in the hydraulic braking system compared to the series-production vehicle. However, an electric pump generates the vacuum required in the brake booster.

## TEST DRIVES IN REAL TRAFFIC

Testing of the vehicle began in September 2011 on several city bus routes in Aachen. In addition, an overland bus line from Aachen to the Eifel region was selected to investigate the influence of an inclination profile and higher average speeds in overland driving. ❺ shows the energy consumption of the test drives on different bus routes. In addition, the maximum range of a single battery charge and the maximum daily mileage for a particular route, when a quick charging station is available, was specified. A daily operation time of 18 h was assumed.

Each route was driven at least twice with different load conditions to determine the maximum and minimum energy consumption. The vehicle was loaded with water-filled ballast dummies and sandbags up to the maximum weight limit. During the tests, all data, which were transferred via a CAN bus, were recorded and subsequently evaluated. Among other things, this data shows the ratio of recuperation to propulsion. The fifth column of ⑤ illustrates the ratio of the energy volume taken from the battery and recharged during the recuperation phases.

Bus routes in cities have a great potential for recuperating energy due to road congestions and short distances between stops, which leads to many braking phases. Based on the information provided by the bus routes investigated, the average travel distance between two stops is between 200 and 300 m and each stop has an average stopping time of 20 to 30 s [4].

❻ shows in detail the energy balance of Line 4 driven without a payload. The red arrows represent the power loss in the components emitted as waste heat into the surrounding environment. As recuperation allows only limited deceleration and is reduced at low speeds because of drivability, part of the kinetic energy

| CYCLE | ROUTE LENGTH; DRIVING TIME | ALTITUDE DIFFERENCE | MINIMUM/MAXIMUM ENERGY CONSUMPTION IN kWh/100 km | RATIO RECUPERATION TO PROPULSION (AT BATTERY) | RANGE PER CHARGE (35 kWh USABLE) | MAXIMUM km PER DAY WITH QUICK CHARGER (OPERATING HOURS 5 TO 23 O'CLOCK) |
|---|---|---|---|---|---|---|
| Line 3 (Ringline) | 11.2 km; 0:39 h | 132 m | 43 to 56 | 0.19 to 0.25 | 62 to 81 km | 202.5 km |
| Line 4 | 12.5 km; 0:56 h | 159 m | 50 to 60 | 0.20 to 0.22 | 58 to 70 km | 180 km |
| Line 5 | 29.6 km; 1:43 h | 268 m | 47 to 52 | 0.16 to 0.19 | 67 to 74 km | 216 km |
| Aachen – Eifel – Aachen | 74 km; 2:00 h | 1000 m | 38 to 42 (51 to 54 uphill; 26 to 29 downhill) | 0.17 to 0.21 (0.09 to 0.1 uphill; 0.25 to 0.32 downhill) | 83 to 90 km | 450 km |

❺ Results of the test drives on various bus routes

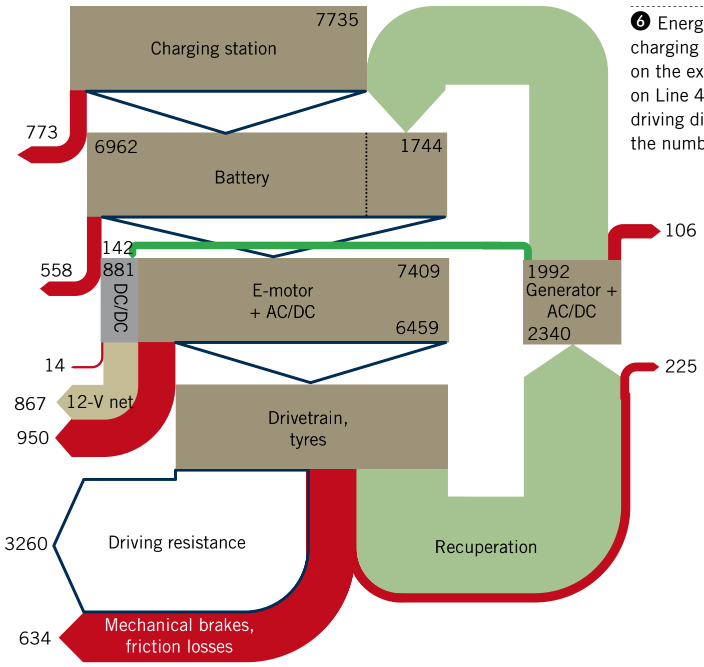


❻ Energy balance from charging station to the wheel on the example of a test drive on Line 4 (travel time: 56 min, driving distance: 12.5 km, all the numbers in Wh)

of the vehicle must be converted into heat by the mechanical friction brake. The numbers shown in the figure represent the energy flow in Wh for a distance of 12.5 km. The upper numbers in the "Electric motor + AC/DC" and "Generator + AC/DC" block are for the DC side of the converter and the lower numbers show the energy supplied to and taken from the electric machine.

The energy required in this example is 50 kWh per 100 km. The minimum and maximum energy consumption during the test was 38 kWh and 60 kWh per 100 km. The energy losses incurred in the battery and the charging station during charging are not included in these figures. The losses shown in ⑥ are based on the assumption that the battery has an efficiency of 95 % and the charging station 90 %.

In order to recharge the energy needed for balancing the state of charge to 7735 Wh, by using a quick charging station with a power of 60 kW in optimum conditions, a period of less than 8 min is required. In normal operation, the regular breaks at the ends of a line can be used to recharge the battery. At the end of the day, the battery can be fully charged overnight and preconditioned for the next day.

## SUMMARY

A prototype battery-powered electric minibus for public transport has been developed and tested in real traffic by ika and ISEA, two institutes of RWTH Aachen University. It was shown that, with a quick charging infrastructure and several charging stops, the average daily mileage of a city bus can be reached. For an overland line with a higher average speed, despite a significant elevation profile, more than 400 km can be covered within 18 h of operation. The measured energy consumption compared to a diesel-powered bus of the same size shows a considerable saving in energy costs. A significant saving of $CO_2$ emissions is also possible. However, the value depends on the energy costs for electricity and diesel production and the resulting costs and emissions.

### REFERENCES

**[1]** Reim, U.; Reichel, B.: Öffentlicher Personenverkehr mit Bussen und Bahnen 2007. Statistisches Bundesamt, Fachserie 8, Reihe 3.1 – 2008
**[2]** Homann, J.; Eckstein, L.: Smart Wheels Electric Bus – A Concept for Electric Mobility in Public Transportation. 20. Aachener Kolloquium für Fahrzeug- und Motorentechnik, 2011
**[3]** Mathar, S.; Rothgang, S.; Sauer, U.; Eckstein, L.: Gesamtfahrzeugintegration von Traktionsbatterien: Herausforderungen und Lösungsansätze Kraftwerk Batterie, Aachen, 2011
**[4]** Kunze, A.: Konzeptuntersuchung zu einem elektrisch betriebenen Stadtbus im ÖPNV. Diplomarbeit, ika, Aachen, 2010

## THANKS

The project was carried out in a cooperation between ika and ISEA. On behalf of the ISEA's project team, we would like to thank Univ.-Prof. Dr. rer. nat. Dirk Uwe Sauer, Dipl.-Ing. Benedikt Lunz and Dipl.-Ing. Susanne Rothgang. Both institutes would like to thank the Federal Ministry of Economics and Technology for supporting and funding the project.

# NEW SECONDARY WATER RETARDER FOR COACHES AND TRUCKS

In order to improve driving safety, modern continuous braking systems have been a standard feature for trucks and coaches for many years. The most established system in this field is the secondary retarder, which is fitted to the majority of long-distance trucks and coaches. With the new Aquatarder SWR, Voith offers the world's first secondary water retarder for commercial vehicles to utilise the cooling water as operating medium and to be fully integrated into the vehicle cooling system.



## INTRODUCTION

For decades, commercial vehicle retarders, on which development is based on the hydrodynamic principle by Professor Föttinger, have been using oil as operating medium. Braking energy that is converted into heat is dissipated into the cooling circuit of the vehicle by high-performance heat exchangers. The world's first water retarder was the Primary Water Retarder Voith Aquatarder PWR. The technically complex retardation technology has been the basis for a long-term cooperative partnership between Daimler and Voith. This cooperation has resulted in the development right through to series maturity of the Secondary Water Retarder for commercial vehicles: the new Aquatarder SWR. This secondary water retarder requires only one medium: the cooling water of the vehicle, for both for hydrodynamic energy conversion and for energy dissipation. This paper describes the development, its technical challenges, and the eventual application of the secondary water retarder in the new Mercedes-Benz Actros.

## GOALS

Legislative, economic and ecological requirements make high demands on the design engineers of drivelines in commercial vehicles. In industrial applications, water has been used as an operating medium for quite some time, for example in water turbines, couplings or water retarders in offshore operations. The installation space required for such applications can, however, not be transferred to high-performance brakes in commercial vehicle drivelines. Here, installation space and weight have to be as low as possible. Small installation spaces call for the addition of a step-up gear. The latter allows the rotating parts of the retarder to run at twice the propshaft speed – with the operating medium reaching flow speeds of over 100 m/s. For the surfaces of the components subjected to the flow of cooling water this means at certain operating pressures, there is a strong tendency towards cavitation. Getting this cavitation under control through suitable materials and flow designs was another challenge of the development project.

As a closed unit, the engine cooling system does not allow any connections to the atmosphere. The goal pursued by Daimler and Voith was therefore to integrate the water retarder completely into the engine cooling system. The adaptation to the diesel engine was eventually achieved by the readiness of both development partners to introduce substantial

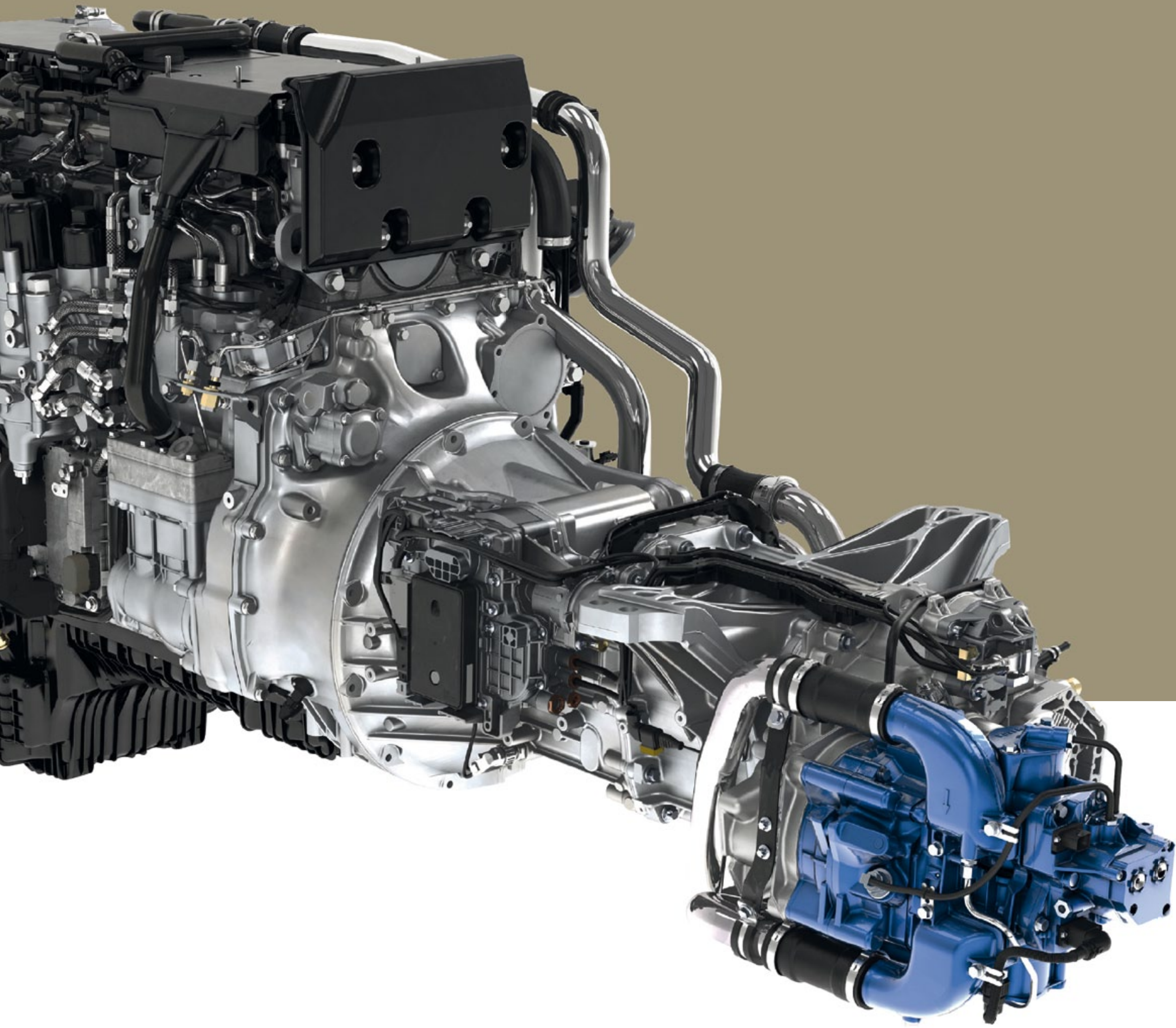




AUTHORS

**DIPL.-ING. (BA) THOMAS OHR** is Project Manager Aquatarder SWR in the Business Unit Driveline at Voith Turbo in Crailsheim (Germany).

**DIPL.-ING. M. SC. DIETER LAUKEMANN** is Head of Development Retarder in the Business Unit Driveline at Voith Turbo in Crailsheim (Germany).

**DR.-ING. TILMAN HUTH** is Technical Director of the Business Unit Driveline at Voith Turbo in Crailsheim (Germany).

**DIPL.-ING. (FH) FRANK STEFFENS** is Project Manager Secondary Water Retarder and Team Leader for Construction Retarder, Take-offs and Transfer Gearbox in the Transmission Development at Daimler Trucks in Stuttgart-Untertürkheim (Germany).

technical modifications, which were necessary in view of the latest technological aspects of Euro V to Euro VI engines and retarders, ❶.

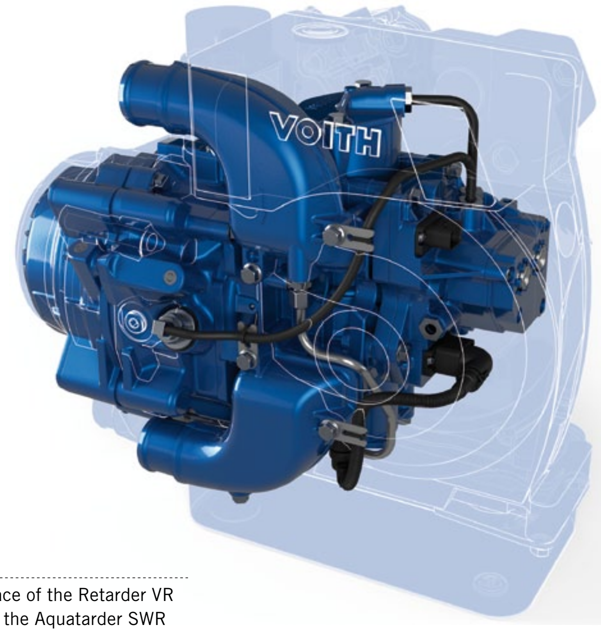


❶ Comparison of installation space of the Retarder VR 115 HV (predecessor model) and the Aquatarder SWR

### OPERATING PRINCIPLE AND DESIGN

The secondary water retarder operates on the basis of the "hydrodynamic principle" discovered by Herrmann Föttinger. Here power is transmitted by fluid via a pump and a turbine. Pump and turbine face each other in the shape of a rotor and a stator, ❷. The rotor, which is driven by a step-up gear, rotates in proportion to the vehicle speed. If there is fluid in the hydrodynamic circuit, it is accelerated by the rotor and directed into the stator. Through the stator, the flow impulse is redirected into the rotor, where it counteracts the rotary motion. As the stator is rigidly connected with the housing, he cannot transmit power. The kinetic energy of the fluid is completely converted into heat. Conventional retarders use oil as operating medium. In oil retarders, braking energy is dissipated to the vehicle cooling system via a heat exchanger. The water retarder utilises the cooling agent as its operating medium thus the heat exchanger can be omitted.

The braking torque of the retarder is controlled by the filling level of the hydrodynamic circuit: the higher the filling level, the stronger the braking torque. The degree of filling is controlled by a hydraulic valve that is directly connected to the vehicle's cooling circuit. During idling, the cooling agent flows past the hydrodynamic circuit, ❸ left. In order to switch the retarder on, the valve is actuated with compressed air. The valve piston leaves its resting position and opens a cross section to the retarder circuit. The cooling fluid flows through the stator into the space between stator and rotor, and from there via openings in the stator back to the hydraulic valve. The valve tappet opens a wide aperture at the throttling point. A spring below the valve piston acts against the pneumatic pressure. This also allows a partial opening of the inlet into the hydrodynamic circuit, resulting in a partial flow through the hydrodynamic circuit. The remaining cooling agent flow occurs via a bypass. In this way, even relatively low braking torques, which are, for example, required during Tempomat (constant-speed) operation, can be generated, ③ centre. Another advantage of the valve is that the filling process can be precisely controlled. As a result, possible pressure fluctuations in the cooling system can be kept at a minimum. If higher braking torques are required, the pneumatic pressure increases and the valve opens the full inlet aperture. The valve tappet throttles the outlet orifice, ③ right. The pressure to the outlet – and therefore the filling level in the retarder – are increased. In this state, the retarder acts like a second pump in the cooling system. During braking, the volume flow is increased via the retarder. Consequently, high braking torque is dissipated via the cooling system. The water retarder therefore requires fewer downward shifts than an oil retarder. In order to end the braking process, pneumatic pressure is released; the hydraulic valve moves back into its resting position.

The pumping effect of the hydrodynamic circuit depends on the degree of filling. At a filling level that would produce too much drag torque the hydrodynamic circuit is not drained any further. Complete drainage of the circuit occurs via the peripheral wheel pump driven by the retarder shaft. After the draining process, the peripheral wheel pump is

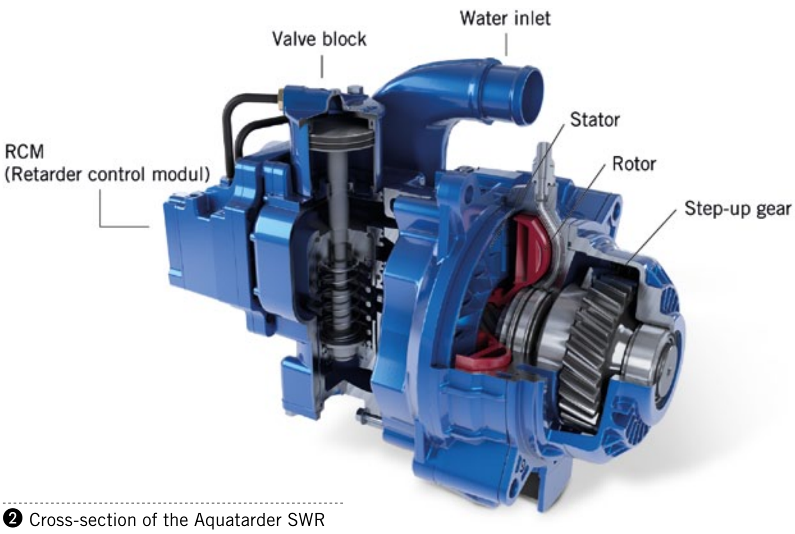


❷ Cross-section of the Aquatarder SWR

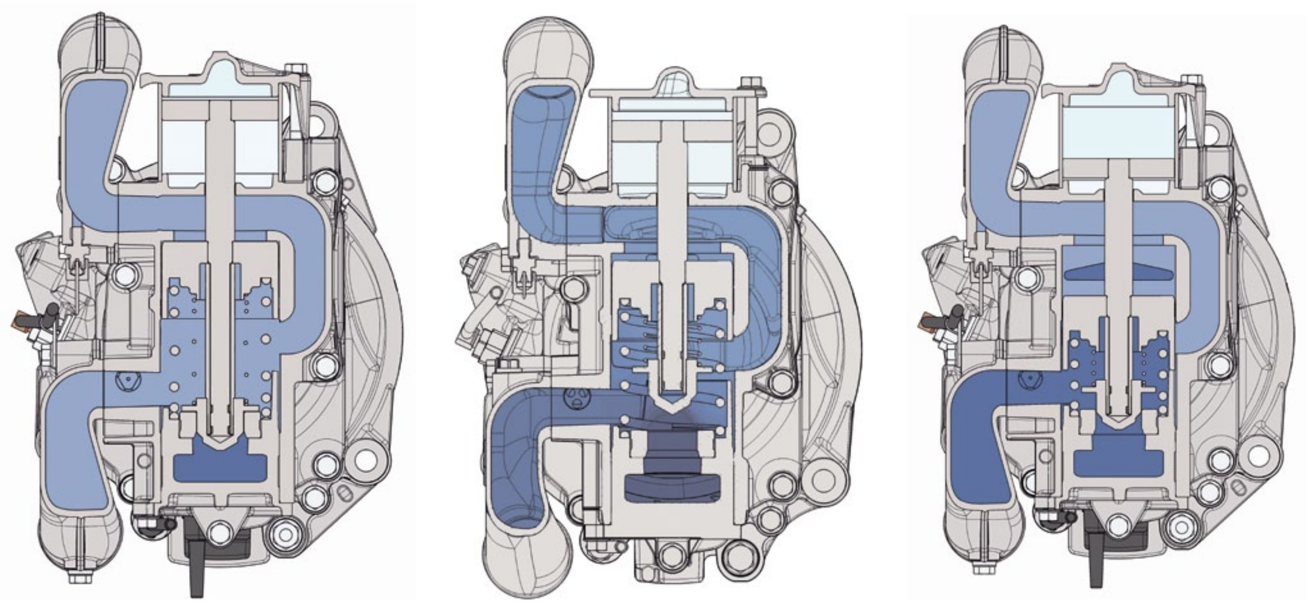

❸ Operating principle of control valve at the Aquatarder SWR (left: idling; centre: low braking stage; right: braking operation)

briefly shut, in order to minimise power uptake. Due to the pumping effect of the water retarder in the cooling system there is no need for large apertures in the connecting lines of the retarder. It is also possible to integrate the secondary water retarder into the cooling system in parallel, and not – as usual with oil retarders – in series. Compared to a vehicle without retarder, a parallel retarder arrangement ensures that there is no increased resistance of the cooling system. This also means that driveline losses are consistently reduced.

Special attention had to be paid to the development of the seal for the cooling agent side of the retarder shaft. The sealing effect is realised by a double-acting slip ring, ❹. One slip ring seal blocks the sealant from the atmosphere, the other slip ring seal blocks the sealant from the operating chamber. The sealant is used for lubricating the sliding surfaces if the retarder is drained. Due to the small installation space, the two sliding surfaces are arranged coaxially with a common counter ring. The bearing system of the retarder shaft consists of two tapered roller bearings. It is lubricated with oil from the transmission.

## MINIMISING POWER LOSSES

In order to reduce power losses, the technological solution for oil retarders is an atmospheric connection of the centre of the meridian flow, while the retarder is switched off. This ensures almost complete drainage and drag losses are kept at a minimum. For a water retarder, such a connection to the atmosphere would mean, however, that air might penetrate into the cooling circuit. The consequences are possible local overheating of the engine or a reduced throughput of cooling agent. In order to eliminate this risk, the technology had to be further developed. To allow further reduction of the drag torque while the water retarder is idling, a rotor shift was added. A spring brings this case the rotor to a position away from the stator. The increased distance between stator and rotor during idling ensures that hydrodynamic valve losses are reduced.

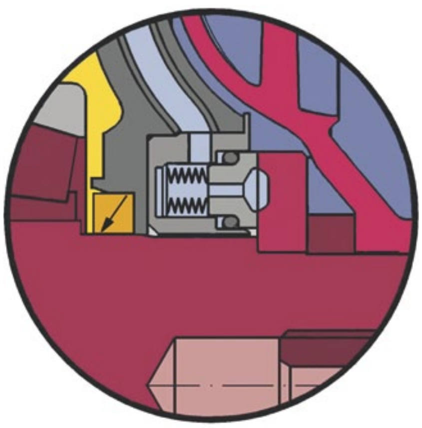

❹ Schematic cross-section of slip ring seal

## INSTATIONARY PROCESSES IN THE PRESSURE SYSTEM

As the retarder is largely drained in idling operation, ❺ left, impermissible compression waves are introduced to the cooling system when the system is switched on. In order to prevent this, the vehicle manufacturer specified that the necessary amount of coolant had to be provided without any additional volume from the series-produced compensation tank. Due to a compact design and optimum arrangements of valves and channels close to the retarder, the filling volume could be reduced to approximately 2 l. The manufacturer's request was therefore met. In addition, pressure fluctuations can be reduced to a minimum due to the excellent control accuracy of the hydraulic valve. In order to prevent pressure shocks to the cooling system when the retarder is switched off, ⑤ right, the volume has to be directed back into the compensation tank without generating pressure peaks in the cooling system. Vehicle tests on the DAG power test station ensured the development and validation of optimum parameters for the valves, as well as for the entire control system, for fast switching behaviour.

The development team was aware of the possible consequences of cavitation on the retarder components especially on bladed parts of the circuit from previous applications of water-operated

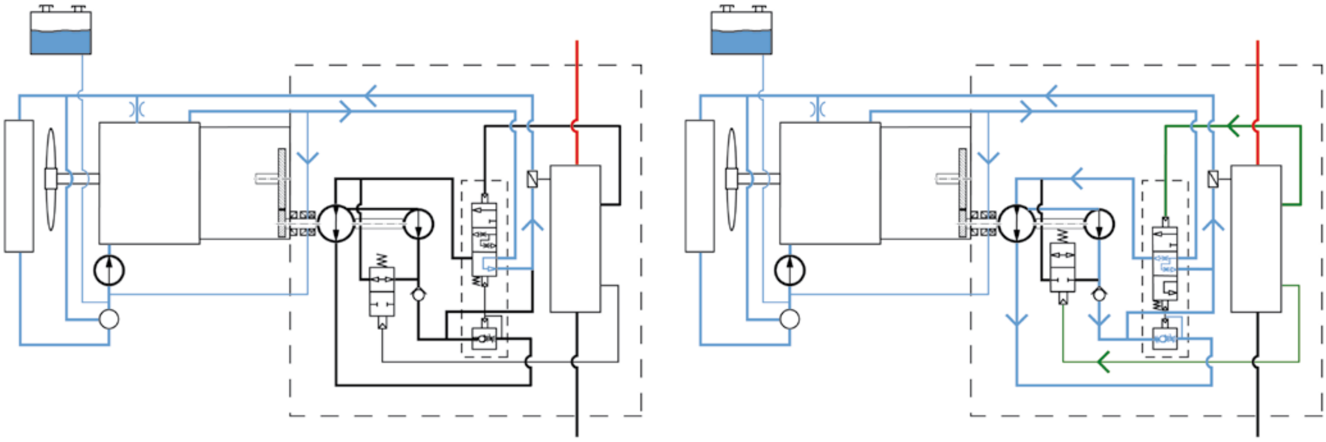

❺ Water flow during idling and braking operation

brakes. Initial tests with conventional materials and component geometries confirmed this risk. In order to find a solution, comprehensive endurance runs on the test stand were required. The step-by-step adaptation of the blade and torus geometry of rotor and stator, as well as more resistant materials, finally managed to get the phenomenon under control.

## INTEGRATION INTO THE OVERALL VEHICLE SYSTEM

The following aspects are of particular importance when comparing the innovative water retarder with a conventional oil retarder:

: fluid characteristics
: low application efforts
: resistance in the cooling circuit
: weight
: service friendliness
: quality
: costs
: sustainability.

For the energy balance, the physical characteristics of the cooling medium are also more favourable compared to oil, for example the high density, the high specific thermal capacity an the low, nearly temperature-independent viscosity. The higher density results in improved braking torque on the filling rate. The specific thermal capacity is nearly twice as high. Combined with the higher density, this results in a significantly increased specific energy dissipation capability. The water retarder can therefore be operated on a lower temperature level and at lower temperature differences whatever the cooling circuit of the vehicle requires. Apart from that, the thermal design of the cooling circuit is the same as that for the water circuit of oil retarders.

As a fluid, water has clear advantages due to its low viscosity, as the braking effect of the retarder is not generated by shearing forces, but because of hydrodynamic forces. The temperature-insensitive viscosity improves the cold braking behaviour of the retarder. Moreover, because of the absence of the medium oil there is also no need for the heat exchanger stage oil to water. Significant weight advantages as well as no extra expense for the high-performance heat exchanger are the result.

In summary, the characteristics of the cooling water allow the construction of a compact and powerful retarder with a weight of just 42 kg and a braking output of 520 kW. In combination with the vehicle engine brake, the available braking power can therefore be as high as 750 kW, ❻. The actual power limit is not prescribed by the water retarder but by the maximum cooling output of the vehicle itself. Due to the pumping effect of the retarder, and the consequently increased coolant flow, the retarder increases the continuous braking output by 20 to 30 % compared to the predecessor model. ⑥ shows that the combination of engine brake and water retarder can increase the braking output by up to 164 %, depending on the selected gear stage.

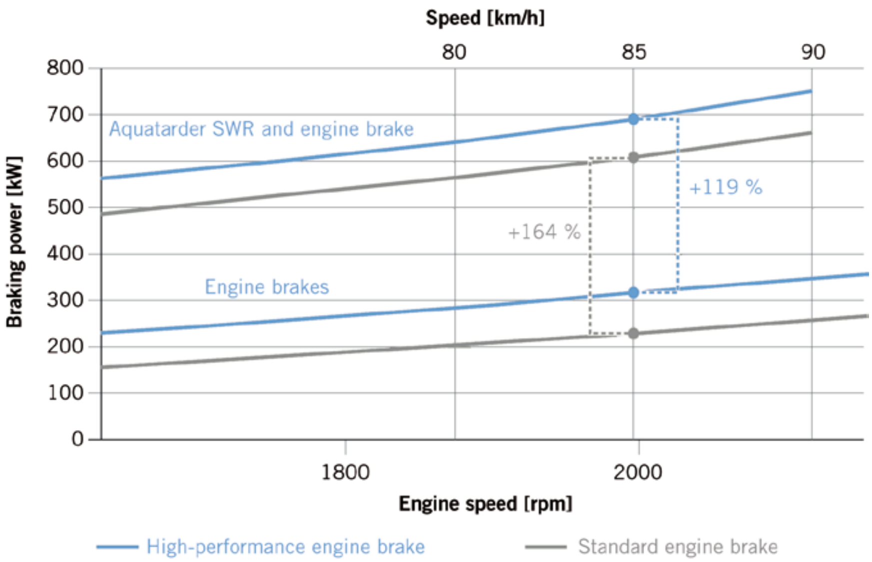


❻ Comparison of continuous braking output of OM 471 engine brakes with and without Aquatarder SWR

## CONTROL AND OPERATING CONCEPT

The electronic control system of the retarder, the retarder control module (RCM), communicates with the brake management of the vehicle via a CAN-Bus interface. The temperature and pressure sensors of the system permanently monitor all operating conditions. This protects the driveline components and also the cooling circuit. It goes without saying that the retarder system is an integral part of the vehicle diagnostics system. The operating concept has been designed for maximum efficiency and highest possible user comfort. Apart from manual operation via the multi-function lever at the steering wheel, the concept can also be applied for foot operation and integration into the tempomat function. The desired speed of heavy commercial vehicles remains constant on upward and on downward gradients.

## APPLICATION AND BENEFITS

The cooling water-based, highly integrated retarder does not require any separate service intervals for changing the operating fluid or carrying out other maintenance work. Compared with a secondary retarder of the same power class, the secondary water retarder offers more braking comfort and efficiency, as well as a gain in payload of about 35 kg. With the absence of oil as an operating medium and the low amount of additionally required cooling water, the retarder offers not only commercial but also ecological benefits. The retarder utilises generated heat for heating the vehicle and keeps the engine temperature at optimum levels during coasting, which, in turn, helps to adhere to existing $CO_2$ emission regulations.

## SUMMARY

Daimler and Voith have used their cooperative technical partnership to take water retarder technology for heavy commercial vehicles to series maturity. The Aquatarder SWR is the first commercial vehicle retarder worldwide to utilise the cooling water as operating medium and to be fully integrated into the vehicle cooling system. The market-ready development is an important contribution to the adherence to future commercial and ecological requirements. This innovation is setting standards for wear-free continuous brakes in terms of weight, performance, service-friendliness and customer benefits. With its comfortable integration into the vehicle management, the application goes beyond its utilisation as a continuous brake for driving on downward gradients. Today's requirements on continuous braking systems can only be met by the combination of engine brake and retarder.


## THANKS

The authors would like to thank Dipl.-Ing. Jürgen Vollmar, Dipl.-Ing. Albrecht Köllermeyer, Dipl.-Ing. Bernhard Schropp and Dipl.-Ing. Matthias Noske, all at Daimler AG, for their support.

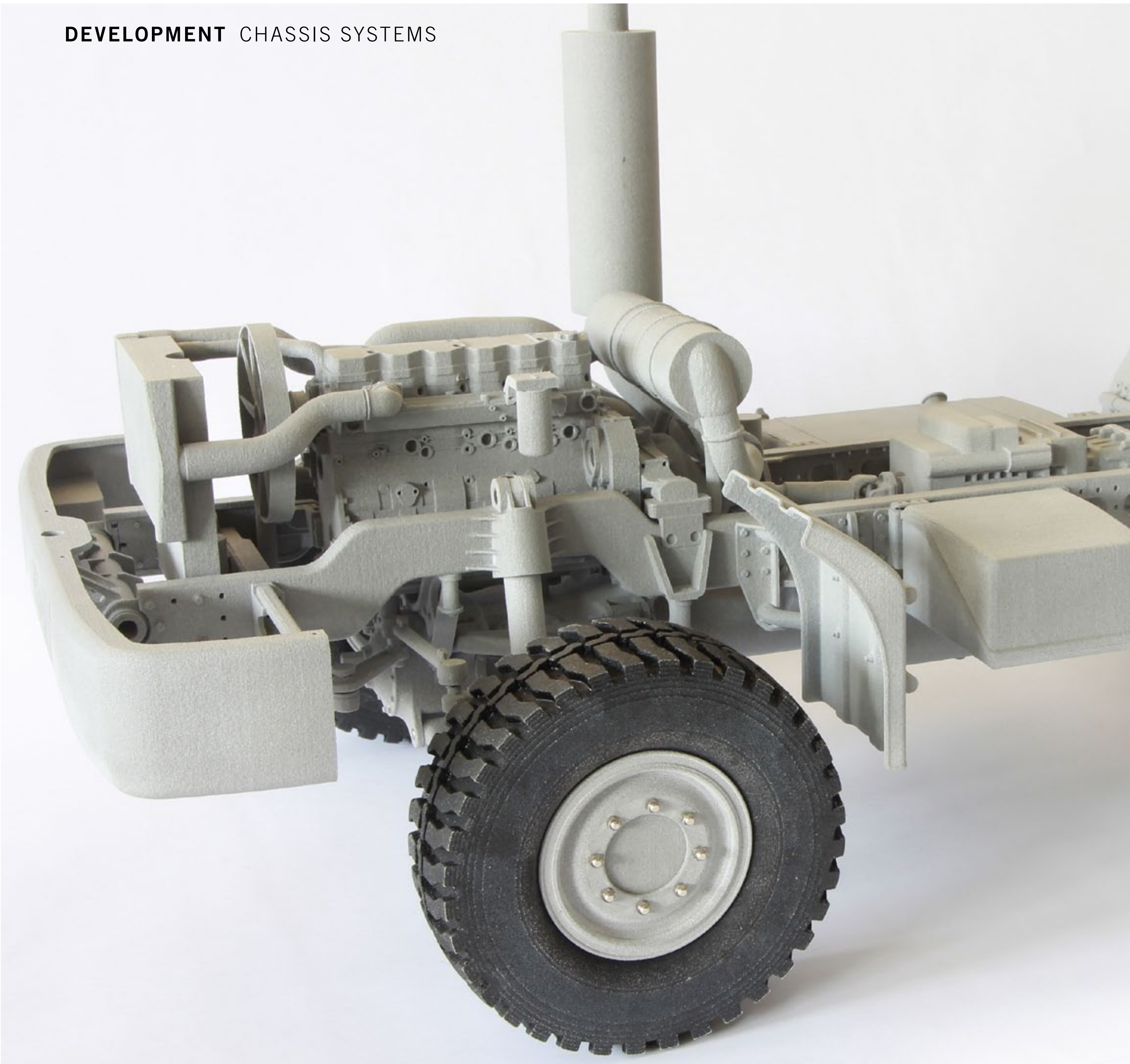



# LIGHTWEIGHT CHASSIS FRAME WITH INDEPENDENT WHEEL SUSPENSION FOR LIGHTWEIGHT TRUCKS

Today's chassis frames in trucks with rigid axles have big unsprung masses limiting driving comfort and stressing the road surfaces. In the course of a research project that was sponsored by the German Federal Ministry of Economics and Technology, the engineers from Gratz Engineering designed a lightweight chassis frame concept with a centre tube and independent wheel suspension to increase the vehicle load capacity and reduce the road surface stress.

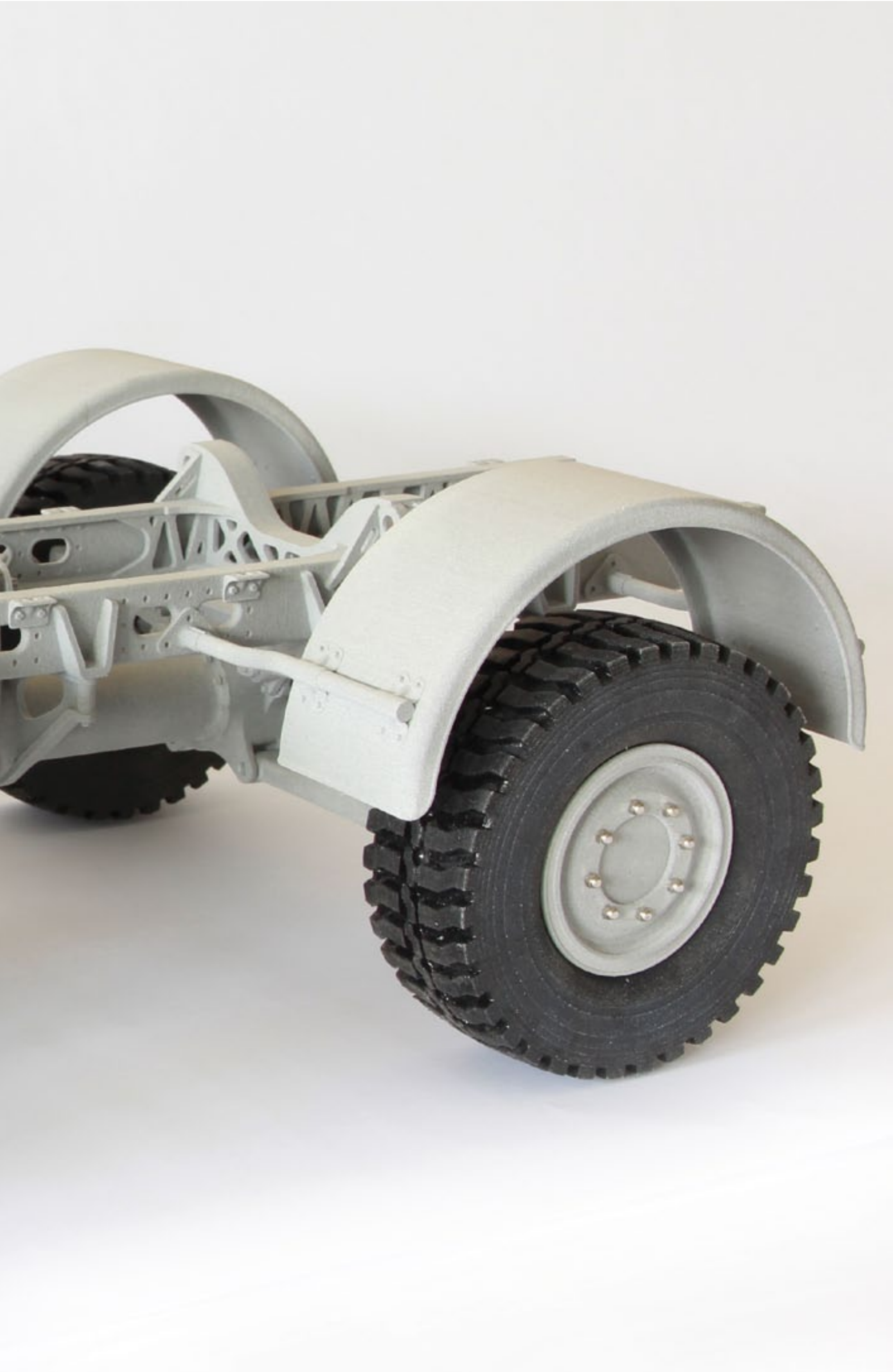

AUTHORS

**DIETMAR INGELFINGER**
is Head of Vehicle Design Department at Gratz Engineering in Weinsberg (Germany).

**DIPL.-ING. (FH) MANUEL LIEDKE**
is Project Manager ULTC at Gratz Engineering in Weinsberg (Germany).



## MOTIVATION

Commercial vehicles are supposed to transport persons and goods safely and efficiently. Here, efficiency is determined by the ratio of usable space to total package dimensions and of load capacity to total weight. Dimensions and weight are limited by law. State-of-the-art trucks have regular chassis frames with flat-spring or air-suspended rigid front and rear axles. The disadvantages of these vehicles are: their huge unsprung mass, driving on uneven pavement causes their wheels to interact, toe and camber cannot be directly influenced through applied wheel forces or driving situation dependent compression movements, and their space requirements (due to their massive and flexible cross members relative to the structure). Larger utility vehicles generally have a ladder-like supporting frame with side and cross members. A ladder frame is unable to absorb forces generated by an independent wheel suspension (IS); there are no suitable load application points for absorbing lateral forces. When connecting an IS to a ladder frame, there are certain limitations, mostly regarding achievable spring travel. In contrast to the continuous rigid axle that is state-of-the-art, this project realised a lightweight chassis design (Ultra Light Truck Chassis, ULTC) featuring a centre tube and independent suspension for the weight range from 5.5 to 12 tons in vehicle class N2, with a 4×4 chassis for various wheel bases. One

❶ Centre tube frame

characteristic feature of independent wheel suspension compared to axle bracket solutions is a reduced unsprung mass. The quality of suspension and driving comfort are better, the lower the unsprung mass is in proportion to the sprung mass. Also, the road itself is adversely affected by dynamic wheel load fluctuations generated by heavy axle bodies, while the wheels are more resilient with an independent suspension. Due to these reduced unsprung masses, forces caused by vertical acceleration are also lower. Therefore, a reduction of unsprung mass in case of independent suspension results in reduced driver stress, improved driving comfort, while at the same time it protects the transport load and road surface.

## VEHICLE CATEGORY

In order to design and construct a chassis for the ULTC project, it was necessary to decide for a vehicle category and the relevant permissible maximum weight. The engineers chose to use a 12-ton chassis with the lowest possible wheel base and additional all-wheel drive as a basis for testing. This approach led to a chassis with a very complex package space. However, other variations, for example 6×6 and 4×2, were also taken into consideration to ensure that the solutions and concepts found would lead to a modular system.

## WEIGHT SAVING

A centre tube frame was developed under this project as opposed to a heavy ladder frame that takes up a lot of space. Despite its lightweight design, a centre tube frame allows great moments of inertia and section moduli that effect high flexural and torsional rigidity. Accordingly, high-strength materials must be used: high and higher-strength steels for example, such as sheets of TRIP (Transformation Induced Plasticity) for wishbones (tensile strength of 780 N/mm² at 21 % elongation at break A80). The newly developed centre tube frame is shown in ❶. Two longitudinal members have been arranged laterally above the centre tube to incorporate the cabin and further structures and bodywork. Furthermore, the rear part of the longitudinal members can be adjusted to the relevant load or bodywork so that any additional supporting frame can be omitted. Chassis and bodywork forces pass directly in the centre tube. The centre tube frame allows an integral construction method, as shown in ❷ with the differential serving. The drive is produced via articulated cross shafts. They were designed for the maximum articulation angle to remain below that of the drive shaft so that increased wear is not to be expected. Wheel suspension on the centre tube frame is realised by double wishbones, ❸. The effective forces and momentums were determined on the basis of five relevant load cases and used for the strength calculation with the finite elements method (FEM) programme Ansys V12. A topology optimisation was carried out for a structure detection. Such optimisation led to the concept of a two-shell element which, due to its closed structure, features a great moment of inertia and section modulus.

## KINEMATICS DESIGN

For this design, special attention was paid to robustness and service life as this is top priority in utility vehicles, for instance, regarding the tyre wear. During compression, the camber was to be negative and positive during rebound in order to counteract to the articulation angle of the drive shaft and increase its

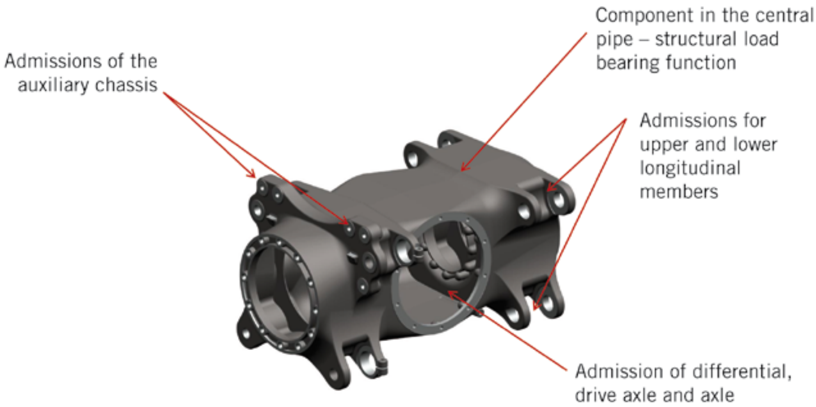


❷ Integral structure using the differential casing by way of example

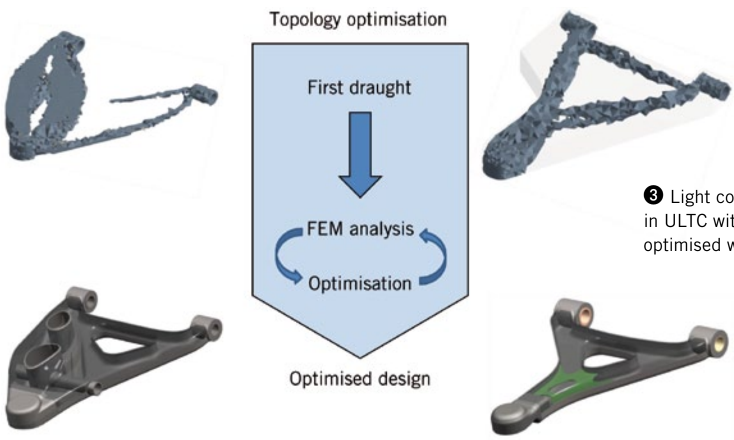


❸ Light construction in ULTC with topology-optimised wishbones

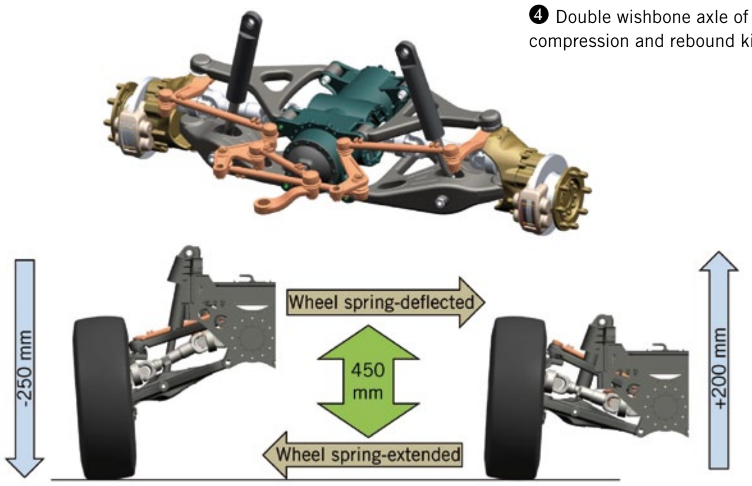


❹ Double wishbone axle of the ULTC with compression and rebound kinematics

transmission capacity. Mainly during the compression phase, the track gauge was to be kept as low as possible to reduce tyre chafing on the road surface and to prevent excessive tyre wear. Furthermore, steering forces are to be kept low as well. To achieve this goal, the upper wishbone was designed shorter than the lower and with a positive inclination angle. This causes the camber to be negative during the compression phase and to be positive during the rebound phase. The roll centre is close to the road surface and the articulation angle of the drive shaft is reduced. To increase road clearance, the lower wishbone was aligned parallel to the road surface. Thereby, a ground clearance of 429 mm below the axle was achieved for the all-wheel drive variants. The results for compressed and rebound states are shown in ❹.

## RESULTS

In the course of this project, a lightweight chassis concept with independent wheel suspension was developed for the 5.5 to 12 ton weight class (vehicle class N2 with a gross vehicle weight rating of up to 12 tons) with a 4×4 chassis, ❺. The ULTC's kerb weight is about 5150 kg. Compared to other vehicles of the N2 class with conventional 4×4 chassis and rigid axles, this means an average weight saving of 4 to 6 %. However, the savings potential is even higher because many component parts have not yet been optimised, for example the wheel mount, the steering parts or the gear box. According to the FEM analysis, the frame can be even lighter. One important target of this independent suspension project involved the unsprung masses: They should be lower than comparable rigid axles. The ULTC's unsprung mass for one axle is 436 kg (consisting of wishbones, wheel mount, brake, drive shaft, piston spring, reduction gear, complete steering system, without wheels.) A comparison between this independent wheel suspension and a comparable rigid axle resulted in significant savings of about 20 %. Further advantages are:

- No stabilisers are necessary due to hydropneumatic suspension. Because a stabiliser would work against a unilateral compression with a maximum travel of 450 mm, it could not be used anyway. Therefore, the rolling motion is actively compensated by the hydropneumatic system that also prevents a kinematic change of the camber while driving around curves.
- The wheels can compress individually and do not mutually influence each other.
- An independent wheel suspension can be fitted into the package of a utility vehicle or van better.
- With the position of the roll centre varying and thus an influence on the roll momentum being possible, kinematics design options have increased compared to a rigid axle.

An independent wheel suspension improves comfort. The portion of unsprung mass is reduced in particular, because the axle transmission is incorporated in the frame.

Independent wheel suspension and simultaneous utilisation of hydropneumatic suspension allows for skyhook suspension. Finally, development results correspond to a modular system which leads to simplification and cost savings due to identical component parts: Front and rear axle, with the exception of the parts of the steering system, feature the same component parts. Thus, a chassis with several axles is easily realisable. Identical wishbones can be produced for either side.

## SUMMARY

With a compression travel of about 80 mm in general, available travel is minimal. Unless when air springs are used, no

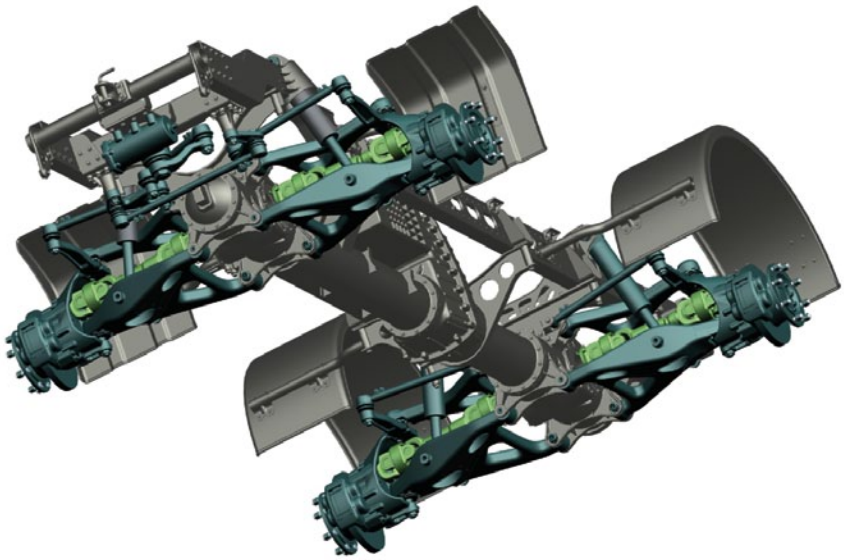

❺ ULTC (4×4) as project result

adjustment of the spring rate to the various load conditions occurs. The current unsatisfactory situation, especially the increased roadbed damage caused, led to this ULTC development project: Lightweight trucks with independent wheel suspension are considered to be me more road-friendly.

Comparing the two concepts of rigid axle and independent wheel suspension under technological aspects, the rigid axle's benefit is that it is simple and cost-effective in design, production and maintenance. Its drawbacks, however, are its relatively high package size and space requirement in the vehicle, its heavy design with an unsprung mass (without wheels) of up to 750 kg with an axle load of 8 tons and the fact that the driving dynamic parameters of camber, spreading, castor angle and wheel toe can be configured to a limited extent only. In contrast, independent wheel suspension is actually much more complicated and cost-intensive than a rigid axle. However, it offers the benefit of saving weight and its driving dynamic parameters and wheel suspension sizes are almost unlimited. Thus, the concept adapts well to any prevailing conditions. The wheels on an axle do not influence each other as they do on a rigid axle. The entire axle transmission (differential casing) does not participate in the compression movement so that the unsprung masses are clearly reduced. With an independent wheel suspension, because the axle transmission and the axle bracket do not participate in the compression and rebound movement, required space should be less than with a leaf-spring package. This should provide more options for better packaging, for example for exhaust gas after-treatment components. Instead of the ladder frame using much space and adding weight, a centre tube frame was used to allow for more road clearance (all-wheel variant) or to improve the loading height.

## THANKS

The authors wish to thank the EuroNorm Quality Assurance and Innovation Management GmbH for the support in the project that was sponsored by the German Federal Ministry of Economics and Technology on the orders of the German Federal Parliament. The authors also thank the co-authors and colleagues at Gratz Engineering GmbH in Weinsberg: Dipl.-Ing. (FH) Rolf Weyrauch, Dipl.-Ing. (FH) Uwe Becker, Dipl.-Ing. (FH) Sebastian Ritter and Michael Bürger as well as the managers of Gratz Engineering GmbH in Weinsberg, Dipl.-Ing. (FH) Klaus Schächtele and Dipl.-Ing. (FH) Peter Gratz.
Gratitude be also expressed to Dr.-Ing. Klaus Mager from Ingenieurbüro Mager in Bad Dürrheim for the administrative support in the project.

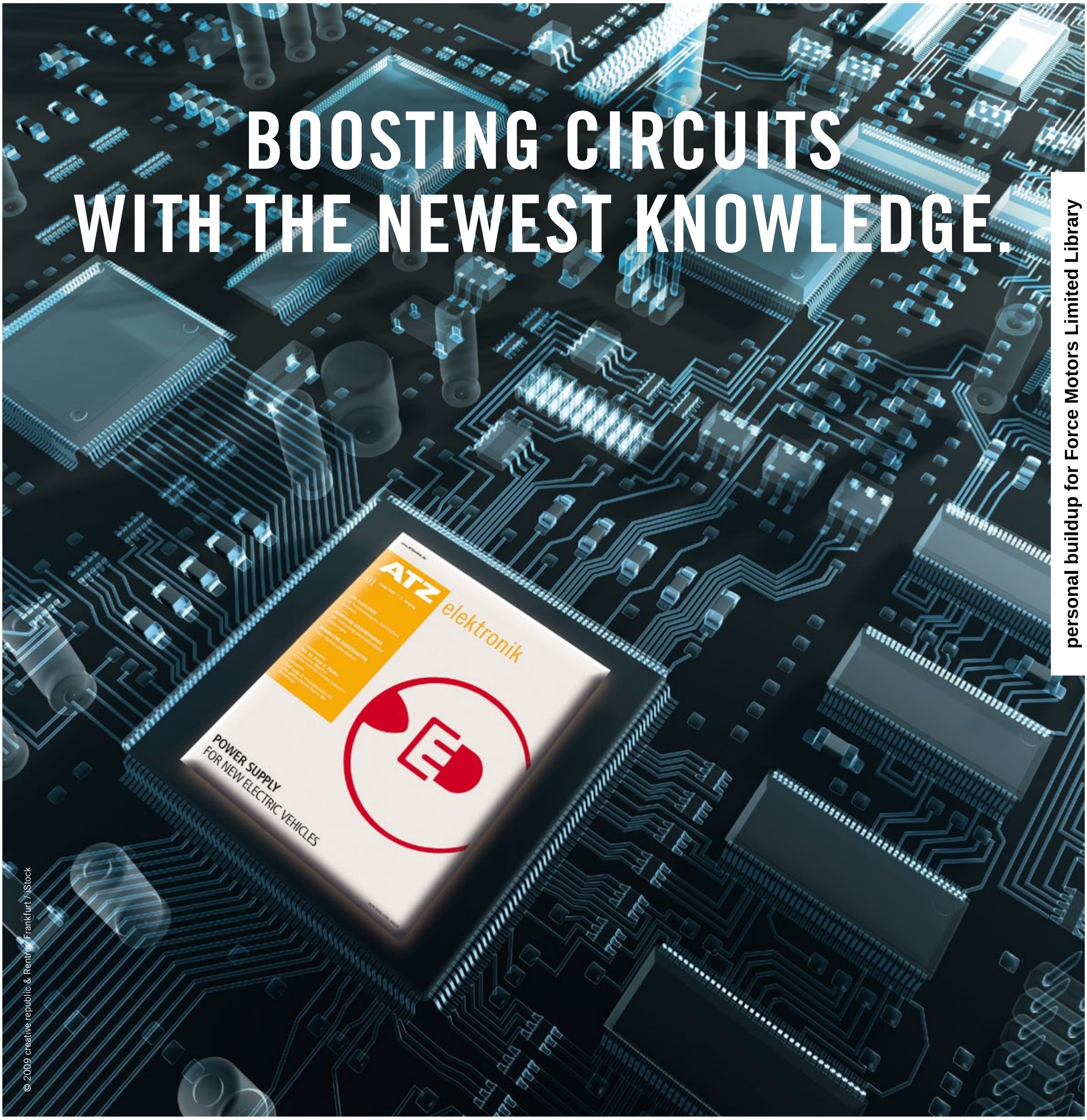
BOOSTING CIRCUITS
WITH THE NEWEST KNOWLEDGE.
ATZ
elektronik
POWER SUPPLY
FOR NEW ELECTRIC VEHICLES
© 2009 creative republic & Rentrop Frankfurt / iStock

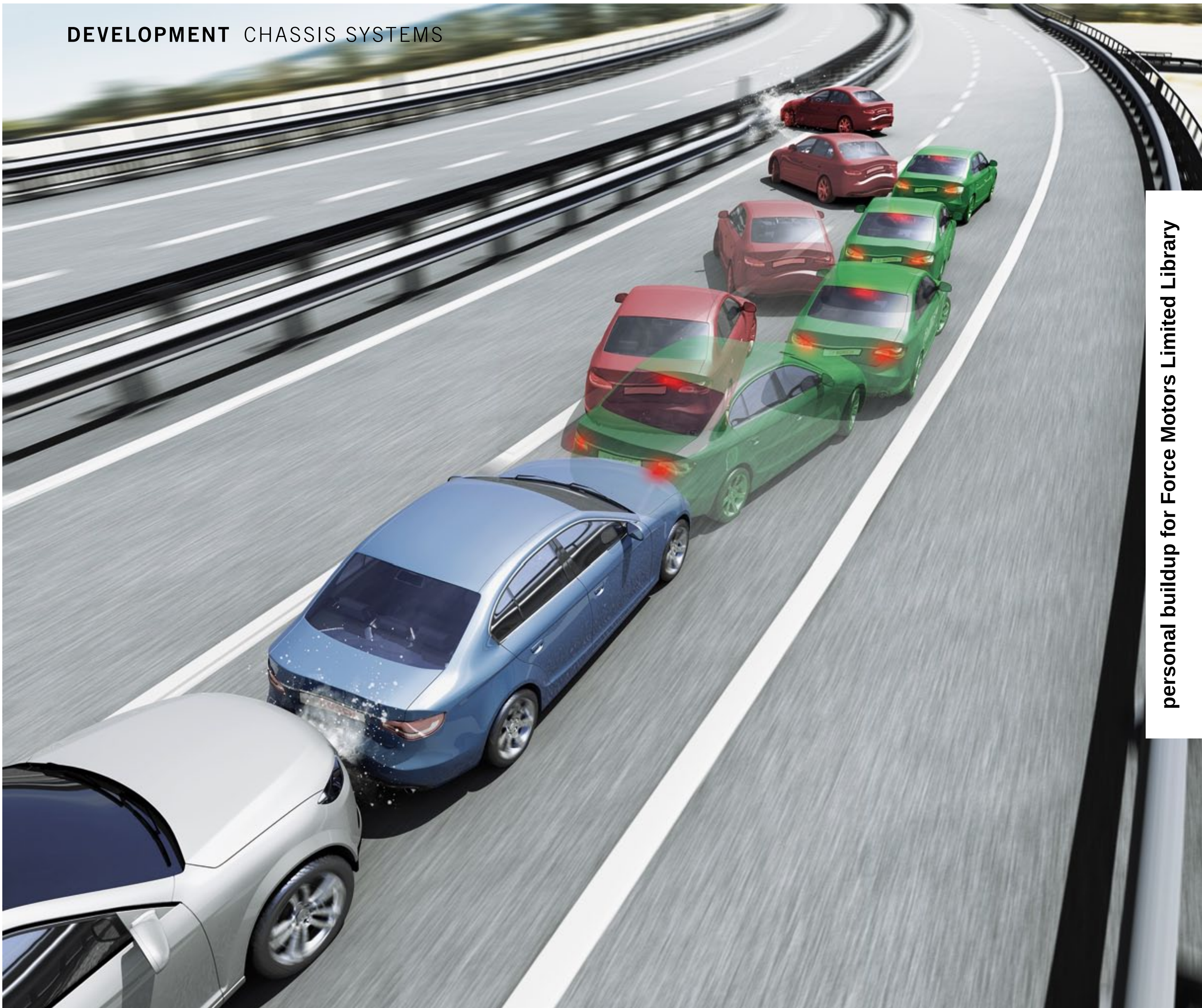



# NETWORKING OF AIRBAG AND ESP FOR PREVENTION OF FURTHER COLLISIONS

With the skilful networking of airbag and ESP Bosch succeeded to integrate an emergency braking system with which devastating subsequent collisions are avoided partly after accidents. The assistance system Secondary Collision Mitigation (SCM) is based on sensor fusion, intervenes automatically and does not break off if the data transfer is disturbed by the first impact.

AUTHORS

**DIPL.-ING. ALEXANDER HÄUSSLER**
is Director Engineering Systems Vehicle Motion and Safety in the area Chassis Systems Control at the Robert Bosch GmbH in Stuttgart (Germany).

**DIPL.-ING. RALF SCHÄFFLER**
is Development Engineer at Engineering Systems Vehicle Motion and Safety in the area Chassis Systems Control at the Robert Bosch GmbH in Stuttgart (Germany).

**DIPL.-ING. ANDREAS GEORGI**
is Senior Manager for Vehicle Safety and Assistance Systems at Corporate Research and Advanced Engineering of the Robert Bosch GmbH in Stuttgart (Germany).

**DR.-ING. STEPHAN STABREY**
is Development Engineer for Vehicle Safety and Assistance Systems at Corporate Research and Advanced Engineering of the Robert Bosch GmbH in Stuttgart (Germany).


## ACCIDENT-FREE DRIVING

As the automotive industry aims to achieve accident-free driving, it is constantly developing more powerful driver assistance systems that support the driver in critical situations and assist in avoiding crashes. Even in normal driving situations, factors that can affect safe driving can be monitored. For example, current systems can detect an increase in the driver's fatigue and recommend a break.

Critical driving situations, such as an imminent collision, can be detected at an early stage using assistance systems with the aid of surround sensors. The driver is initially given staged warnings. Then, if necessary, he is aided by automatic emergency braking and avoidance assistance. In addition, active safety systems such as ESP can stabilise the vehicle, within physical limits, during a critical driving manoeuvre. In the past, support was only provided by passive safety systems, such as airbags, should a crash occur.

Studies show that many of these initial collisions cause secondary collisions, on which the driver can have a significant impact. Each crash is a rare event for the driver and, after the initial impact, results in an extended period of shock. In this situation, the driver is hardly capable of reacting and is often also affected by resulting injuries. This is where the Secondary Collision Mitigation (SCM) function comes into play.

Networking of airbag information with ESP initiates an automatic delay after the initial collision. Secondary collisions can therefore be avoided, or at least the consequences of the accident can be significantly reduced. An important element of the development of this function was conducting a detailed analysis of accident data as part of accident research. An evaluation of statistically relevant situations was performed (effect field analysis) with subsequent benefit and risk analysis. The results of this analysis influenced the function design.

## FROM EFFECT FIELD ANALYSIS TO BENEFIT AND RISK EVALUATION

Real accident data shows that approximately one in four accidents resulting in physical injury, involved multiple collisions. The support of a function that avoids secondary collisions (SCM) is extremely beneficial, particularly in primary collisions where the airbag trigger threshold has been reached. For accidents in Germany which result in physical injury, the field of effect for this is 15 % (46,000 accidents per year). The accident database Gidas (German In-depth Accident Study) [1] provides the option of systematically evaluating such functions in terms of fields of effect, benefits and risks.

The functional benefit for the passenger car could only be exactly determined for slightly more than half of relevant Gidas accidents. The change in path due to system-initiated brake actuation was calculated. Elements such as the street condition, driver reactions and the vehicle rotation were taken into consideration in the calculation. As ❶ shows, in 2.6 % of all accidents brake actuation helps avoid a secondary collision, and in 3.6 % it results in a significant reduction in speed. In 1.8 % of all accidents, the function has no benefit; that means in these cases the driver had used the brakes optimally or the gap between collisions was very small.

In approximately one half of the accidents addressed by SCM (7 % of all accidents) the exact benefit could not be calculated. In these cases, the vehicles had either left the roadway in the primary collision or a secondary collision occurred with a moving vehicle. The effect of SCM in these "drifting" accidents is low, because wheels braking on a loose surface can only add a minimal amount of added deceleration. Additional detailed individual case analyses showed that in accidents involving secondary collisions with moving vehicles, there is also a significant functional benefit.

Because SCM is activated when the trigger threshold is reached, even in accidents with only one collision per vehicle, and the vehicles are delayed accordingly, this effect must also be examined for potential risks. To do this, more than 2700 additional accidents from the Gidas database were examined with respect to the effects of the change in path after an initial collision. The result of the risk analysis was that full braking is beneficial in almost all impact situations. Only in frontal collisions was a reduction in braking deceleration recommended to achieve an optimum benefit/risk ration.

## FUNCTION DESIGN

The function design is essentially based on the benefit and risk analysis per-

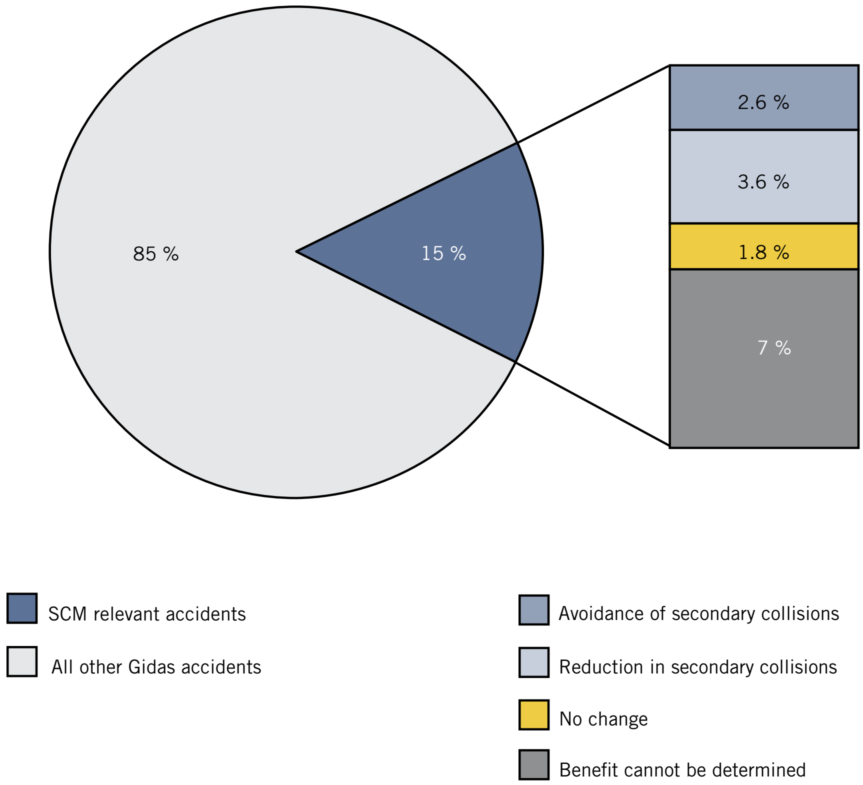


❶ SCM benefit analysis for passenger cars, based on 3148 representative accidents from the Gidas database

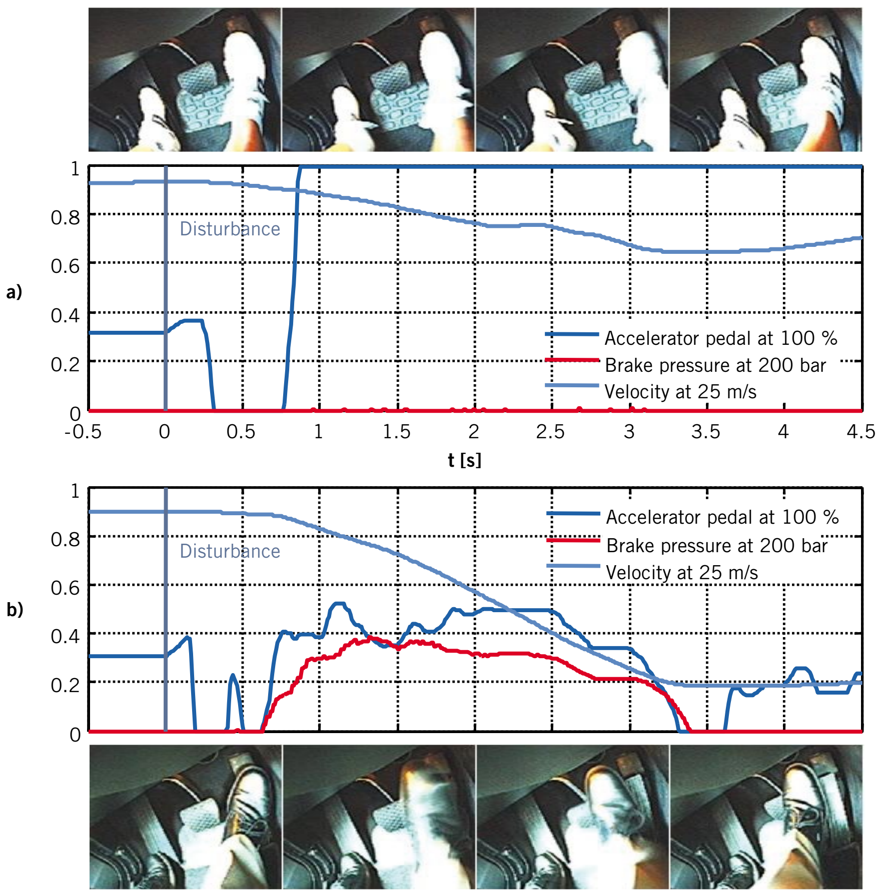


❷ Driver reactions in initial collision simulated by steering impulse; "pressing down" of the acceleration pedal (a), simultaneous activation of acceleration and brake pedal (b)

formed as part of accident research. The impact force required for the trigger, as well as the braking deceleration, depending on the impact situation, was derived from this. The functional parts for evaluating the impact force and impact situation are incorporated in the airbag electronic control unit. The braking pressure required to achieve the braking deceleration is calculated in the ESP electronic control unit.

The braking deceleration generated is determined according to the guidelines for functional safety (ISO 26262) and the safety requirements for the entire system. These are derived based on the probability and the effect of faulty functional behaviour and must be taken into consideration when SCM functions are incorporated in the two electronic control units. With regard to the secure transmission of the trigger signal from the airbag electronic control unit to the ESP electronic control unit, it must be noted that the vehicle network can be destroyed by an accident. If such a malfunction occurs after the SCM trigger, the braking deceleration initiated by the airbag electronic control unit can no longer be aborted. The trigger signal must therefore be sufficiently verified for transmission errors before the braking deceleration is initiated.

For example, this can be achieved using a special handshake mechanism between the airbag electronic control unit and ESP electronic control unit, whereby the SCM is only triggered in the ESP electronic control unit when the electronic control units have mutually calculated a checksum correctly. With regard to the acceptance of driver assistance systems, in addition to functional safety, transparent system behaviour for the driver as well as the option to be able to overrule automatic system interventions are of central importance. The interplay between automatic brake actuation by SCM and driver behaviour after an initial collision was therefore studied extensively in a test person study [2].

Although the forces affecting the vehicle in the steering intervention used during a safe simulation of an initial collision were considerably smaller than in a real collision, significant problems were observed while coping with the surprise situation.

The evaluation of driving and brake pedal actuation yielded important results as part of development of an intuitive overrule strategy. In addition to the expected reaction of "foot off the acceleration and braking pedal", a "pressing down" of the acceleration pedal was also observed, ❷ (a), as well as the simultaneous activation of acceleration and brake pedal, ② (b). Using the video recording of a camera installed in the footwell, this unexpected behaviour was traced to active inertia forces. Evaluation of motion sequences clearly shows that the test people affected take their foot off of the acceleration pedal and want to brake, but due to the effect of inertia forces are unable to move their foot to the brake pedal.

For a driver to overrule a SCM intervention, that means end the automatically triggered deceleration, the simple actuation of the acceleration pedal is not a suitable criterion. Based on the acceleration and brake pedal actuation sequence, the erroneous operation described before can be detected so that cancelation of the SCM intervention by the driver only occurs after intentional acceleration pedal actuation.

It can be assumed to be a driver request if a driver reacts initially with strong braking and then reduces the braking pressure again after regaining control. In this instance, the driver could be very confused if the vehicle continues to decelerate due to SCM intervention, despite pressure on the brake pedal being reduced. To avoid unexpected driving behaviour such as this, an SCM intervention is ended even if the driver brakes strongly.

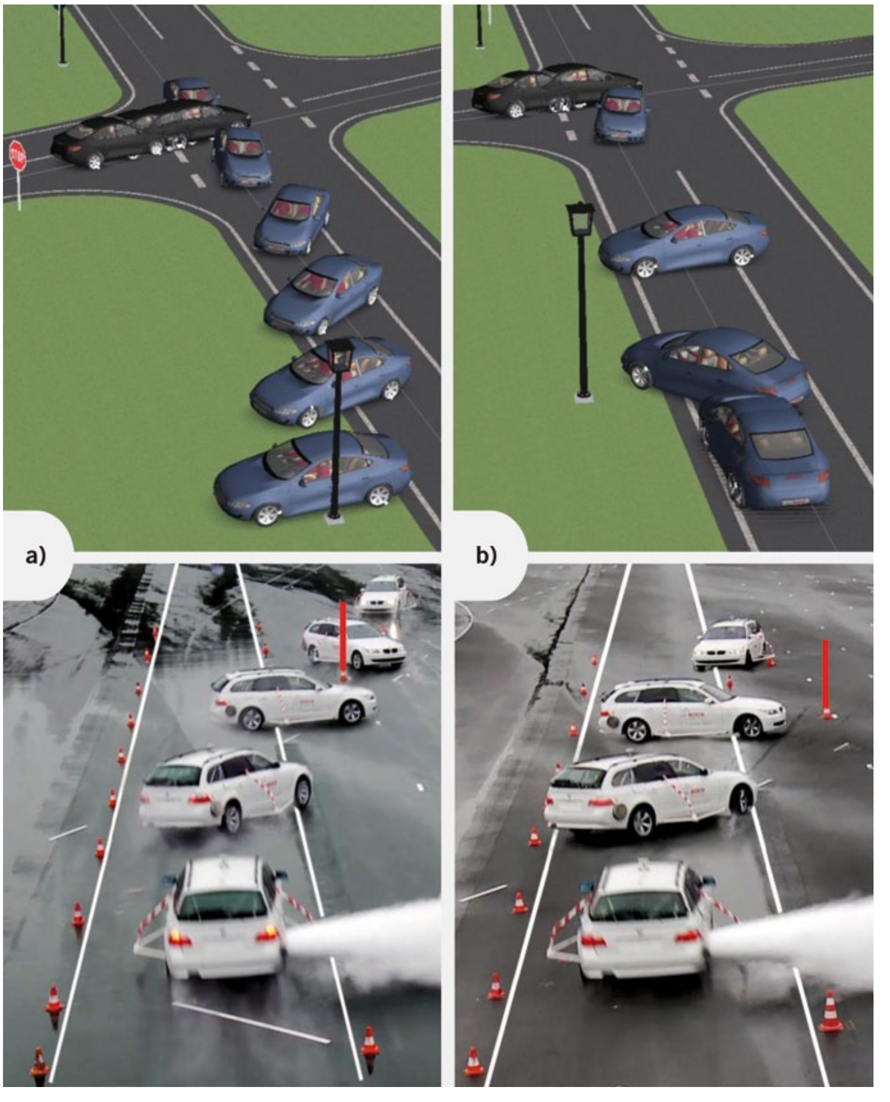


❸ Reconstruction of a specific real accident from the Gidas database in simulation (upper row) and in a driving test (lower row): without intervention of the SCM (a), with intervention of the SCM (b)

## VALIDATING THE FUNCTION

To analyse the potential of driving safety functions, such as SCM, that intervene in vehicle motion after an initial collision, a special test vehicle was built by the central research centre at Robert Bosch GmbH. With the aid of steam rockets integrated in the vehicle, external transverse forces of up to 45 kN are applied to the rear of the vehicle for a duration of approximately 100 ms. This structure allows the effects of a side collision to the rear of the vehicle on vehicle motion and driving behaviour to be examined on a repeated basis without causing damage, and provides evidence for the effectiveness of functional prototypes.

In order to illustrate the benefits of SCM in a real driving test, the accident condi-

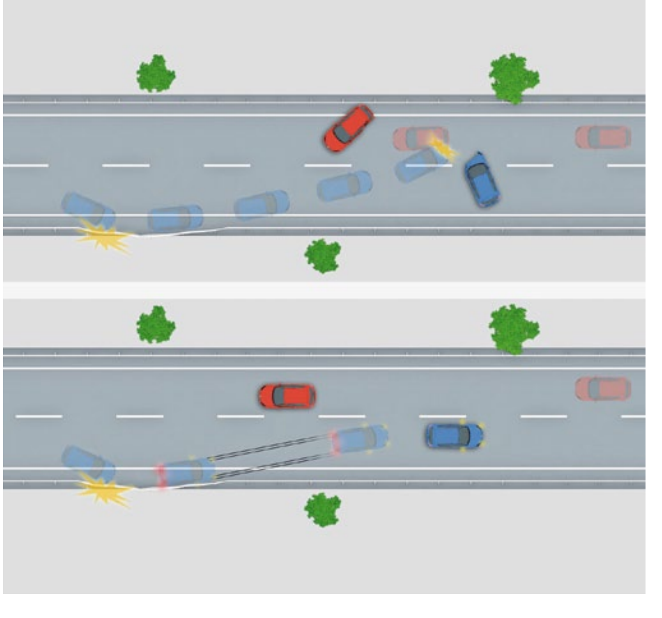

❹ After an accident the insufficient reaction of the driver is compensated by electronics (Figure © Volkswagen) tions of a specific intersection accident recorded in the Gidas database were reconstructed as an example. The vehicle, which was hit at the rear, began skidding in this accident, left the roadway, collided with a street light in the area of the driver door, and rolled over. The reconstruction of the accident in the simulation, as well as the trajectory of the vehicle without SCM in the driving test, in which the position of the street light has been marked with a pylon, are shown in ❸ (left).

The driving test clearly shows that even experienced and prepared drivers could not stabilise the induced lateral force by means of immediate, fast counter steering. In uncontrollable movement conditions such as this, it is particularly important to reduce kinetic energy in order to minimise the severity of potential secondary collisions. The course of movement of the vehicle equipped with SCM, depicted in ③ (right), clarifies that the secondary collision with the street light could have been avoided through the initiation of full deceleration – automatically and immediately after the initial collision. This means that the electronics of the SCM can compensate for the driver's insufficient reaction following an accident, ❹.

## SUMMARY AND OUTLOOK

Systematic accident data analysis shows that in many accidents there are multiple collisions, which means that it is possible to reduce the overall accident severity by specifically influencing vehicle motion after the initial collision. As the first application for this type of driving safety functions, the intelligent networking of the airbag and ESP systems in vehicles with Secondary Collision Mitigation (SCM) from Bosch enables automatic deceleration after the initial collision. Although it is not possible to avoid secondary collisions in all accident situations through use of this networking, the targeted speed reduction does generally reduce the risk of injury.

In addition, the extended time span between the initial and secondary collisions provides the driver with more opportunities to intervene. A benefit/risk estimation based on real accident data as well as functional validation in a simulation and driving test show the potential for reducing personal injury and property damage in road traffic. Additional driving safety functions that influence the course of movement between collisions by means of complex driving dynamic interventions have great potential and are currently being researched [3, 4].

### REFERENCES

**[1]** Georgi, A.; Brunner, H.; Scheunert, D.: Gidas – German In-Depth Accident Study, Fisita Congress 2004, Barcelona, Spain, 2004, www.gidas.org
**[2]** Stabrey, S.; Georgi, A.; Blank, L.; Marchthaler, R.: Minderung der Schwere von Unfällen mit Mehrfachkollisionen durch automatische Bremseingriffe. In: VDI-Bericht 2009: Autoreg 2008 Steuerung und Regelung von Fahrzeugen und Motoren, Baden-Baden. Düsseldorf: VDI Verlag, 2008
**[3]** Derong Yang: Post Impact Vehicle Path Control in Multiple Event Accidents. Technical Report, Department of Applied Mechanics, Chalmers University of Technology, Goteborg, Sweden, ISSN 1652-8565, 2011
**[4]** Salfeld, M.; Stabrey, S.; Trächtler, A.: Optimal Control Inputs to Affect Vehicle Dynamics in Various Driving States. In: IFAC Proceedings Volumes (IFAC Papers Online), pp. 151, 2007

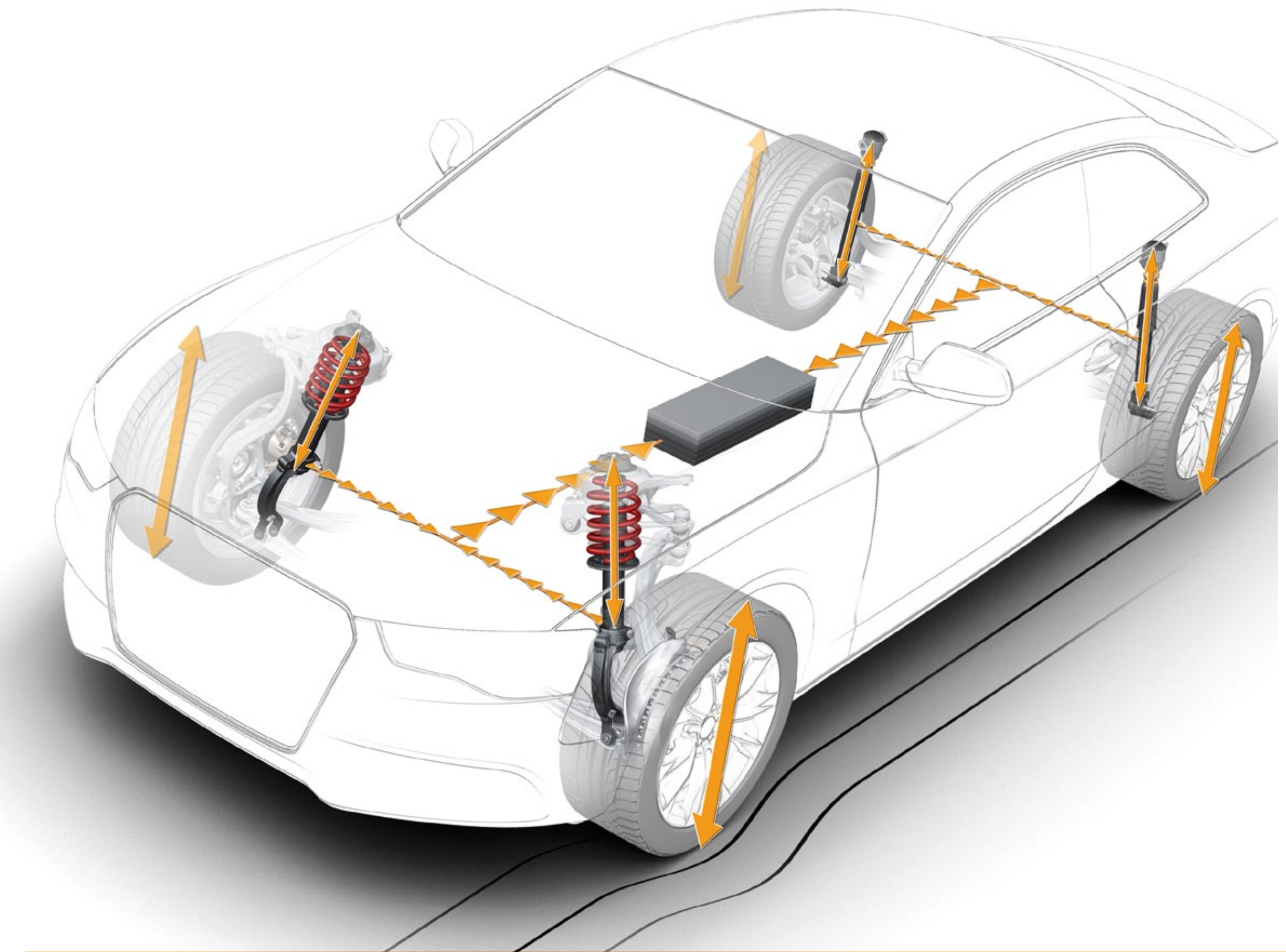



# ESTIMATION OF THE RECUPERATION POTENTIAL OF SHOCK ABSORBER ENERGY

Whereas braking energy recuperation is already an established component of efficient vehicle architectures, no use has yet been made of shock absorber energy. An estimation of its potential by Audi provides an insight into the amount of energy that is dissipated in a shock absorber and how much of it can potentially be recuperated. For this purpose, the shock absorber energy is numerically determined in a freely parameterisable quarter-vehicle simulation model.

AUTHOR

**DIPL.-ING. MARCO WILLEMS**
is Project Leader Controlled Damper Systems MLBevo at Audi AG in Ingolstadt (Germany).

## MOTIVATION

When pursuing the aim of reducing fuel consumption and $CO_2$ emissions, a distinction must be made between two approaches: the energy source and the energy consumer. Improvements in efficiency on the energy source side are aimed at optimising the conversion of primary into kinetic energy. Regardless of the propulsion concept, reducing fuel consumption makes a contribution towards increasing a vehicle's overall energy efficiency. Eq. 1 shows resistance to vehicle movement:

**EQ. 1**

$$F_{Total} = \underbrace{F_{Aerodynamic}}_{f(A,\,c_D)} + \underbrace{F_{Gradient} + F_{Acceleration} + F_{Rolling}}_{f(m,\Theta)}$$

The most prominent constituent in total resistance to movement is aerodynamic drag ($F_{Aerodynamic}$), comprising the influencing factors frontal area $A$ and drag coefficient $c_D$. Whereas resistance to gradients and acceleration ($F_{Gradient}$, $F_{Acceleration}$) are determined solely by the parameters of vehicle mass $m$ and inertia $\Theta$, rolling resistance has to be examined in a more differentiated manner. In addition to the tyre flexing converted into heat, rolling resistance includes the energy dissipated by the vehicle's shock absorbers.

Like braking energy, the energy converted in the shock absorbers is removed intentionally from the complete vehicle system. The value of the energy dissipated by a shock absorber, and whether its recuperation could be worthwhile, are discussed below.

The study was based on a quarter-vehicle model. In addition to the synthetic profiles specified in ISO 8608, the road excitation profiles also included measured profiles of real road surfaces. Finally, the influence of different vehicle parameters on the energy conversion in the shock absorbers was examined.

To simplify examination of the tyre-axle-body oscillating system, excitation is solely by way of road surface irregularities. Vertical excitation constituents caused by braking and acceleration have not been taken into account, but if the vehicle is driven in a sporty manner they may contribute a significant additional energy input to the tyre-axle-body system.

## GENERATING A SYNTHETIC ROAD EXCITATION PROFILE

An alternative to the measurement of actual road profiles is the synthetic generation of surface irregularity profiles from the power spectral density $\Phi(\Omega)$ specified in ISO 8608 [1]. Power spectral density $\Phi(\Omega)$ according to ISO 8608 is a function of the distance circle frequency $\Omega$ of road surface excitation.

**EQ. 2**

$$\Phi_h(\Omega) = \Phi(\Omega_0) \cdot \left[\frac{\Omega}{\Omega_0}\right]^{-w}$$

In this context, $\Omega_0$ stands for a reference circle frequency. Waviness $w$ describes the character of the road in terms of long- and short-wave excitation. The power spectral density of reference circle frequency $\Phi(\Omega_0)$ in Eq. 2 is a parameter for road surface irregularity [2].

**EQ. 3**

$$\Phi_h(\omega) = \frac{1}{v} \cdot \Phi_h(\Omega)$$

**EQ. 4**

$$\tilde{h}^2 = \int_0^\infty \lim_{T\to\infty} \frac{4 \cdot \pi}{T} \left[\hat{h}(\omega)\right]^2 d\omega = \int_0^\infty \Phi_h(\omega)\, d\omega$$

where

$$\Phi_h(\omega) = \lim_{T\to\infty} \frac{4 \cdot \pi}{T} \left[\hat{h}(\omega)\right]^2$$

By means of the vehicle speed $v$, the spectral density of the distance circle frequency $\Phi(\Omega_0)$ can be transferred to the spectral density $\Phi(\omega)$ as a function of the excitation circle frequency $\omega$, Eq. 3. $\Phi(\omega)$ in turn is by way of Eq. 4 in a direct relationship with the square of the mean value $\tilde{h}^2$ of the height of the road surface irregularity.

**EQ. 5**

$$\tilde{h}^2 \big|_m^n \approx \sum_{i=m}^{i=n} \Delta\omega \cdot \Phi(\omega_i)$$

**EQ. 6**

For

$m - n = \Delta\omega$

the following applies

$$\hat{h}(\omega_k) \approx \sqrt{\Delta\omega \cdot \Phi(\omega_k)}$$

By applying the mid-point rule to Eq. 4 as a numerical approximation procedure for integrations, we obtain the square of the mean value for the surface irregularity height $\tilde{h}^2 \big|_m^n$ at interval $\omega = m \ldots n$, Eq. 5. If a sufficiently small value of $\Delta\omega$ is chosen, Eq. 6 applies. From this, we can derive the mean surface irregularity

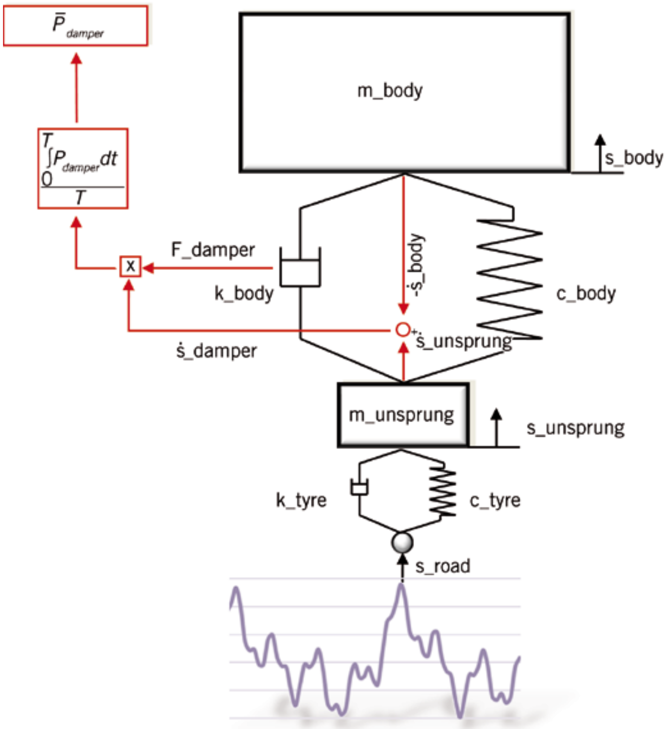


| Reference vehicle data | |
|---|---|
| Body/wheel m_body | 400 kg |
| Unsprung mass/wheel m_unsprung | 40 kg |
| Damping coeffizient body k_body | 1500 Ns/m |
| Damping coeffizient tyre k_tyre | 100 Ns/m |
| Spring stiffness body c_body | 2100 N/m |
| Spring stiffness tyre c_tyre | 150.000 N/m |

❶ Quarter-vehicle model for determining damping energy



height for the excitation frequency $h(\omega_k)$ as a discrete value for all $\omega_k$.

Assuming that the stochastically distributed road surface irregularities are derived from the sum of *z* different excitations, the road profile *h*(t) can be developed from a Fourier series.

**EQ. 7**

$$h(t) = \sum_{i=1}^{z} \hat{h}(\omega_i) \cdot \sin(\omega_i \cdot t + \beta_i)$$

To generate road profiles, Eq. 7 is formed in Matlab/Simulink. Information on road categories according to ISO 8608 contains no details of the phase position of the individual frequencies in the road surface irregularity. For this reason, the phase shift β is generated in the model used here by a uniformly distributed random number at interval [0; π/2] for the *i* calculated frequency bands. $\Delta\omega = 0.01\ \text{Hz}\cdot 2\pi$ was chosen as frequency bandwidth.

Allocation of road profiles by way of the characteristic values of $\Phi(\Omega_0)$ is taken from ISO 8608.

## VEHICLE SIMULATION MODEL

To investigate the damping power, the vehicle is simulated as a quarter-vehicle model, ❶. As implemented in Matlab/Simulink, the model represents the tyres in a simplified form as tyre spring and shock absorber in parallel, according to Voigt-Kelvin [3]. Damping is shown as a speed-related value *k*. To calculate the mean power, the integral of the damping force and damping velocity product is divided by the total time interval *T*. The value for the individual vehicle parameters can be taken from the reference vehicle shown in ①. As an excitation signal, the road surface irregularity profiles derived above are input to the model as a function of time.

## RESULTS OF SIMULATION WITH SYNTHETIC ROAD SURFACE IRREGULARITY PROFILES

The values based on spectral density and waviness are generated in the individual frequency bands with a stochastic phase shift. On account of the superimposition

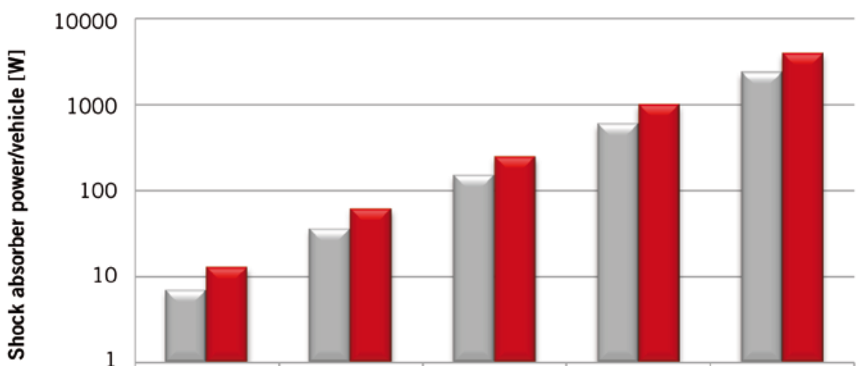


| | A "excellent" | B "good" | C "medium" | D "poor" | E "very poor" |
|---|---|---|---|---|---|
| 80 km/h | 7 | 36 | 152 | 600 | 2377 |
| 140 km/h | 13 | 62 | 250 | 1015 | 3991 |

❷ Mean power converted in the shock absorber, depending on the road category according to ISO 8608 and travel speed

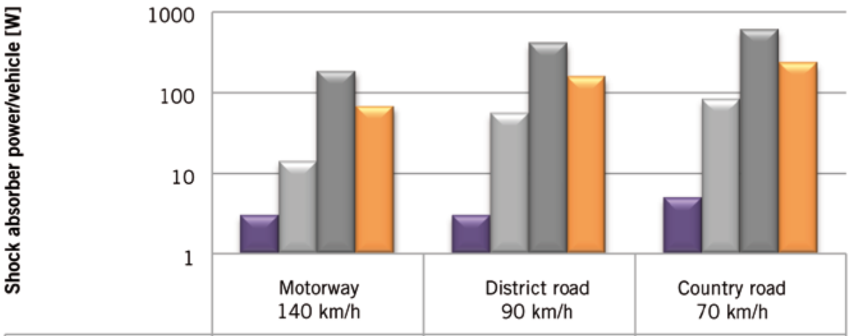


| | Motorway 140 km/h | District road 90 km/h | Country road 70 km/h |
|---|---|---|---|
| excellent | 3 | 3 | 5 |
| medium | 14 | 55 | 83 |
| poor | 184 | 411 | 613 |
| average | 67 | 156 | 234 |

❸ Measured spectral density and waviness of German roads [4] and mean shock absorber power conversion on different german roads

of the amplitudes of different frequency bands, the resulting amplitude $s_{road}(t)$ is subject to scatter. This scatter must also be expected from the amplitude patterns of actual road profile measurements that have a similar spectral density and waviness [4]. For the results described below, four road surface profiles were therefore generated for each spectral density and waviness, and investigated for shock absorber energy conversion on the vehicle. The results also described below are in each case the mean values from four investigations.

❷ shows the power converted in the vehicle's four shock absorbers for road categories A to E ("excellent" to "very poor"). Shock absorber power conversion on roads with an "excellent" surface according to ISO 8608 (A) is low, at 7 to 13 W according to travel speed. Roads in the "very poor" (E) category, however, result in an energy conversion in the shock absorber of approximately 4 kW per vehicle. In addition to road surface irregularities, the speed of the vehicle has a significant influence on the amount of power converted in the shock absorber. Since only power converted up to an excitation frequency of 20 Hz is examined in the calculations presented here, the higher shock absorber power conversion value at high speeds results solely from the increase in $\Phi(\omega)$.

The road categories stated in ISO 8608 were compiled from measured values collected all over the world. ISO 8608 therefore has to satisfy the demand for applicability in industrial countries, where the roads are in many cases "excellent", but also in threshold countries with some "very poor" roads. A large number of measurements were taken from the German road network. If the spectral densities and waviness values for German roads are imported into the procedure described above, the shock absorber power values per vehicle shown in ❸ are obtained. In view of the top speeds determined by road construction or laid down by law, different travel speeds were chosen for motorways, country roads and local roads.

It is evident that the power converted in the shock absorbers already differs significantly within any one road category. Whereas on a motorway with an "excellent" surface no more than 3 W per vehicle are converted in the shock absorber within the evaluated frequency range, the power conversion figure on a "poor" motorway is as high as 184 W per vehicle. The average amount dissipated in the shock absorber on motorways is 67 W per vehicle.

The increase in waviness and spectral density from one road category to the next leads to an increase in converted shock absorber energy to as much as 411 W per vehicle on country roads and 613 W per vehicle on local roads.

## SIMULATION WITH ACTUAL SURFACE WAVINESS PROFILES FROM SELECTED ROADS

Despite the categorisation of road quality into motorways, country roads and local roads, there are large differences in the bandwidth of energy dissipated in the shock absorber on "excellent" and "very poor" road surfaces. For a better understanding of the preceding simulation, shock absorber energy with actual road surface waviness profile measurements was therefore incorporated. By means of a low-pass filter, the excitation frequency of the input signal was limited to 20 Hz, as in the preceding simulations.

The Nürburgring Nordschleife racing circuit and a British motorway were chosen as road profiles. An average travel speed was used, as in the previous calculations. For the Nürburgring, average speeds of 120 and 150 km/h were adopted.

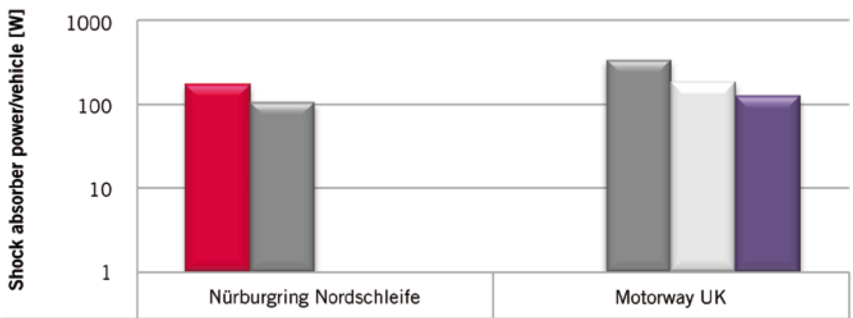


| | Nürburgring Nordschleife | Motorway UK |
|---|---|---|
| 150 km/h | 171 | |
| 120 km/h | 106 | 336 |
| 80 km/h | | 180 |
| 60 km/h | | 124 |

❹ Mean shock absorber power conversion results with actual measured road profiles

The power converted in the shock absorbers is in this case up to 171 W per vehicle, ❹. Compared with the familiar road categories in ③, this is equivalent to a “poor” motorway surface. At 336 W per vehicle, the British motorway is at the same level as a “poor” German country road according to ③.

### INFLUENCE OF VEHICLE PARAMETERS

As a further step, the influence of different vehicle parameters on shock absorber energy was examined by varying parameters in relation to the reference vehicle. The variable parameters were body and wheel mass, the degree of body damping, the body’s eigenfrequency and the firmness of the tyre carcass. The excitation signal for the quarter-vehicle model was in each case the surface irregularity profile of the Nürburgring.

❺ compares the results with different parameters. The greatest influence within the vehicle configuration that was investigated derives from tyre wall rigidity. If this results in a higher spring rate, more excitation is transmitted to the body mountings of the quarter vehicle as a two-mass oscillator, and the damping energy that has to be dissipated is correspondingly higher. A 50 % increase in body mass leads to 9 % higher damping energy. A 37.5 % increase in unsprung mass results in a 4 % increase in damping energy. The influence of increases in body damping mass or body eigenfrequency is at a comparable level.

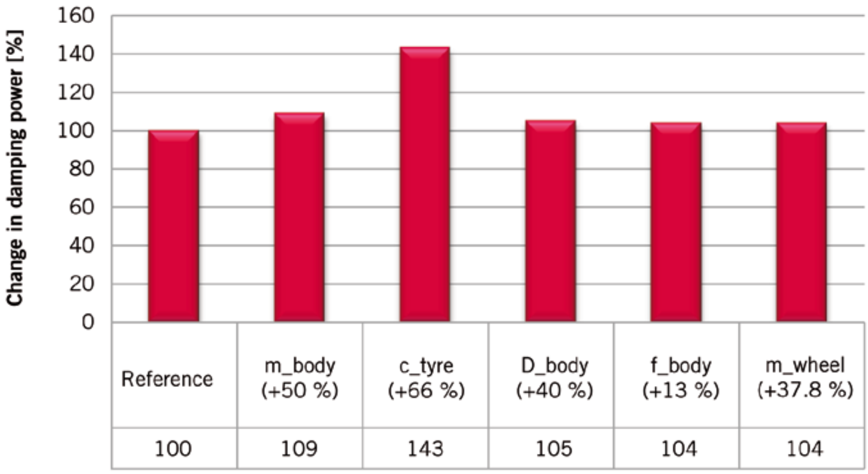


❺ Relative change in damping power when vehicle parameters are varied

### SUMMARY AND OUTLOOK

The investigation results presented here show the energy dissipated in the shock absorber. The influence of varying road quality in the mean shock absorber energy values can be clearly seen (67 W per vehicle to 234 W per vehicle). If published conversion figures for electrical energy saving in the vehicle are applied (1 A ~ 0.3 g $CO_2$/km) [5] the $CO_2$ potentials are as shown in ❻.

The values in ⑥ relate to the German road network and are based on 100 % recuperation of the energy dissipated. The degree of efficiency of technical solutions for recuperating systems will reduce these values. Nevertheless, with particular reference to growing markets in countries with a less well developed road network, shock absorber energy could be an interesting means of reducing $CO_2$ emissions.

In addition to the actual recuperation itself, shock absorber functionality and characteristics will be a key challenge in the design of a technical solution.


#### REFERENCES

**[1]** ISO 8608: Mechanical vibration – Road surface profiles. Reporting of measured data, International Organisation for Standardization, Schweiz, 1995
**[2]** Mitschke, M.; Wallentowitz, H.: Dynamik der Kraftfahrzeuge, 4. Auflage. Springer-Verlag, Berlin/Heidelberg, 2004
**[3]** Wallentowitz, H.: Vertikal-/Querdynamik von Kraftfahrzeugen. Schriftenreihe Automobiltechnik, 7. Auflage. ika, Aachen, 2005
**[4]** Braun, H.; Hellenbroich, T.: Messergebnisse von Straßenunebenheiten. In: VDI-Bericht 877, VDI-Verlag, Düsseldorf, 1991
**[5]** Goede, M.: Karosserieleichtbau als Baustein einer $CO_2$-Reduzierungsstrategie. 16. Aachener Kolloquium Fahrzeug- und Motorentechnik 2007, Aachen, 2007


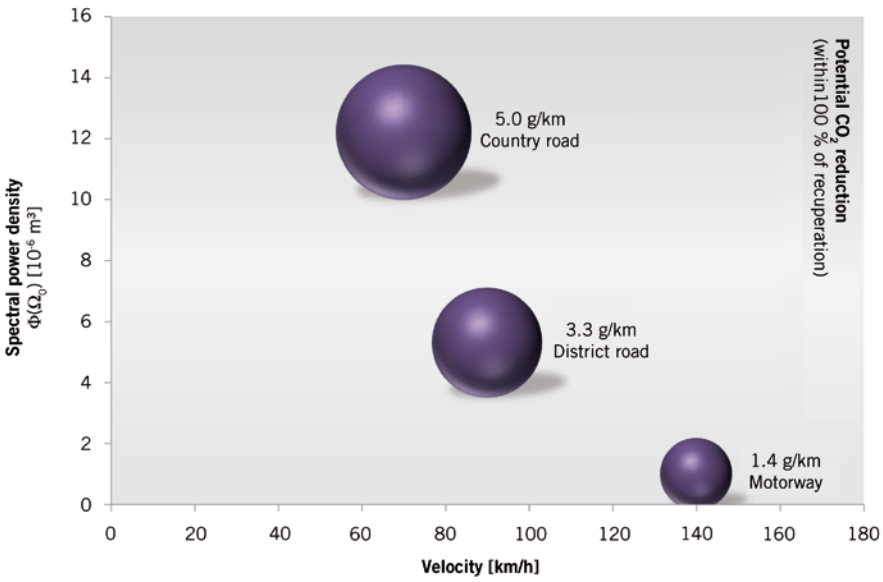


❻ $CO_2$ saving potential for 100 % recuperation of the dissipated damping power

SPRINGER-VIEWEG.DE

# Including more than 160,000 technical terms for handling construction projects abroad




Klaus Lange

## Elektronisches Wörterbuch Auslandsprojekte Deutsch-Englisch, Englisch-Deutsch; Electronic Dictionary of Projects Abroad English-German, German-English

Vertrag, Planung und Ausführung; Contracting, Planning, Design and Execution

**2010. EUR 169,95**
**ISBN 978-3-8348-0883-7**

The electronic technical dictionary „Projects Abroad“ is indispensable for all those communicating and negotiating with contractors, clients or engineers in English in the context of construction projects abroad.

With some 84,000 English-German and 76,000 German-English entries it is one of the most comprehensive reference works on the market, covering engineering, operations and legislation in the construction sector - a reliable companion to help you successfully handle construction projects abroad.

The UniLex Pro user interface includes many search features including a pop-up search option that automatically displays translations in a pop-up window - regardless of the program being used at the time.

System requirements:

- Windows 7, XP
- Available hard disk space: min. 200 MB
- Core memory: min. 512 MB
- CD-ROM drive

### About the Author

He has worked together with international partners to offer numerous seminars preparing students for construction projects abroad.

### Yes, please send me

___ Copies
**Elektronisches Wörterbuch Auslandsprojekte Deutsch-Englisch, Englisch-Deutsch; Electronic Dictionary of Projects Abroad English-German, German-English**
ISBN 978-3-8348-0883-7
EUR 169.95

### Fax +49(0)6221 / 345 – 4229

Company | Surname, First Name

Department

Street (no P.O. boxes, please) | Postal Code | City

Date | Signature



Springer Vieweg

**Ordering is easy at: SpringerDE-service@springer.com Phone +49(0)6221 / 345 – 4301**

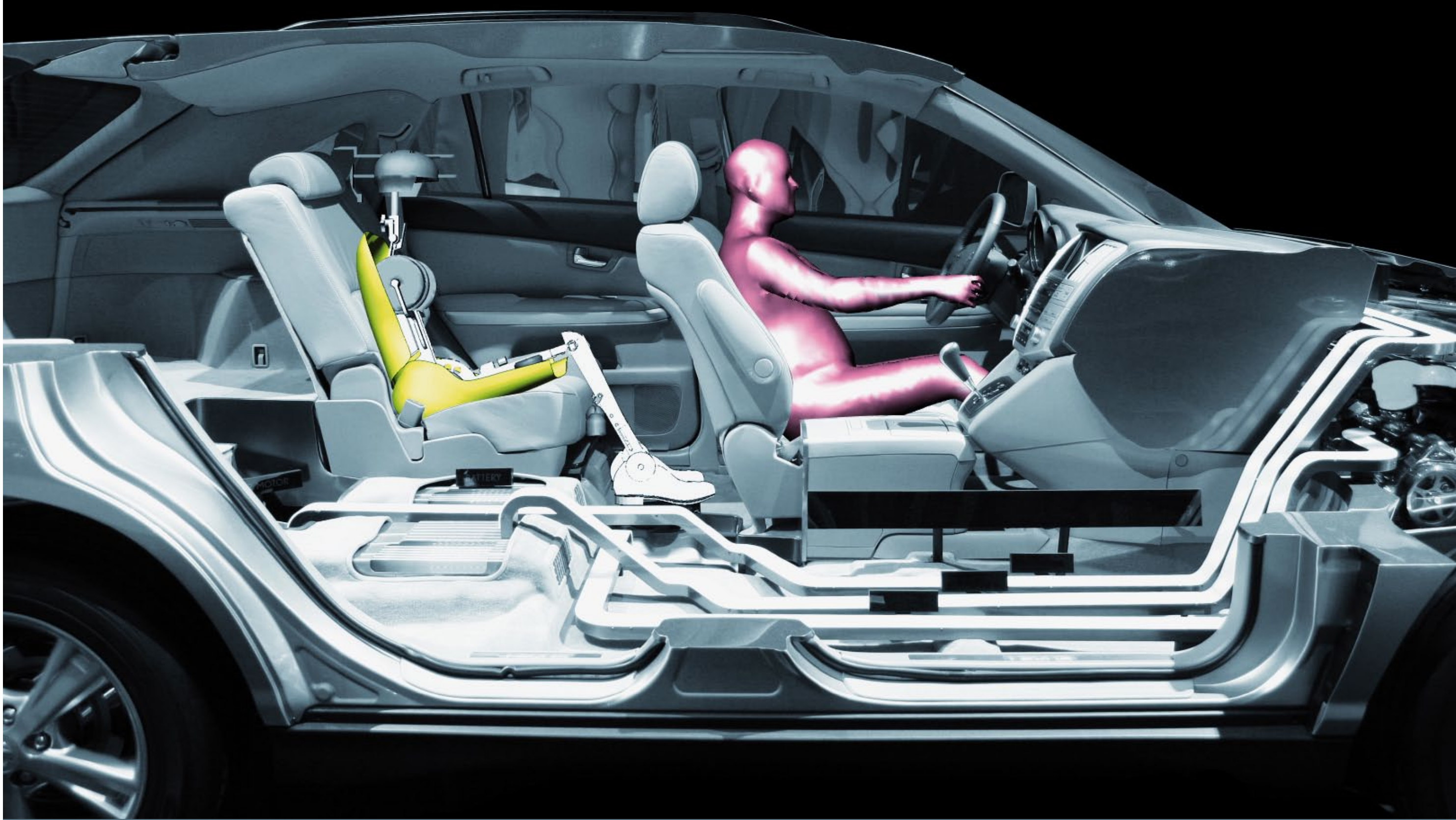



# COMPUTER-BASED OPTIMISATION OF SEATS FOR A COMFORTABLE AND SAFE RIDE

Increasingly rising costs, shorter development times and continuously rising safety requirements are reasons for the fact that car manufacturers and seat suppliers are increasingly looking for the evaluation and implementation of simulation-based virtual prototyping solutions. The simulation specialist ESI points out, how the developers can work on comfort-relevant tasks for “soft” seat elements and human models with the multidisciplinary simulation solution Pam-Comfort. With resilient model elements for body parts and seat cushions it is possible to map reality far better, there are even advantages regarding the strong crash test dummies, well known from experimental investigations.

AUTHORS

**JÜRGEN RÜCKERT**
is Support and Project Engineer for the units Pam-Crash/Safe and Pam-Comfort at ESI GmbH in Eschborn (Germany).

**MANFRED R. MÜLLER**
is Account and Business Development Manager at ESI GmbH in Eschborn (Germany).

## SEAT AS AN INTERFACE

The seat is an important interface between vehicle and passenger and coins considerably the passenger's comfort perception. Car manufacturers and seat suppliers expend a great deal of effort to secure that this feeling remains not only in the showroom, but also on a ten-hour trip to the Lake Garda – for an entire vehicle lifetime and for passengers with different physiognomies.

In the past decades the seat development was mainly based on physical prototypes, which were evaluated and optimised during an iterative process. In the past a majority of the work was completed on the basis of these physical prototypes which are expensive to manufacture and need complex measuring techniques. Today it shows up that this procedure is less and less compatible with the demands after a higher cost efficiency as well as the realisation of innovative solutions for weight reduction, the use of recyclable materials and the increase of occupant safety.

Therefore OEMs as for example Ford, General Motors, Hyundai or Renault increasingly use global numeric simulation methods for the seat development. Together with software providers such as ESI they elaborate solutions for an industrial use and investigate in the context of extensive studies and pilot projects, how processes must be defined, which simulation tools are to be used, and how high the agreement of the simulation results with the reality is.

## NEW APPROACHES FOR THE SIMULATION IN SEAT DEVELOPMENT

The consistent pursuit of this objective is the base for a paradigm shift which not only enables the reduction of the number of prototypes but which increases the innovative ability of an enterprise and its development efficiency. Simulation programmes are already used in the seat development for many years, but mainly they deal with structure mechanical analysis of the seat frame or with safety-related investigations of the overall system.

By contrast, investigations of the comfort and safety-relevant tasks within the range of the soft components of a seat like cushions, seat covers etc. represent rather the exception, although these topics have a central meaning for the behaviour and the function of the overall system. In reality a comfort-oriented simulation is linked with some technical and organisational expenditure. Reasons for this are on the one hand complex simulation scenarios with numerous from each other dependent process steps, on the other hand the high requirements on the assigned simulation software, since transient effects, nonlinearities, contacts and friction have to be considered.

## VIRTUAL PROTOTYPING APPROACH

The punctual use of simulation programmes enables local improvements, but usually they do not affect the quality of the overall system significantly, and physical prototypes remain still necessary. Only if in the context of a virtual prototyping approach all development and product-related aspects can be covered on the basis of only one digital data model, the advantages of simulation can be used in its entirety and physical models can be diminished, ❶.

Usually, virtual prototyping approaches require the employment of different simulation programmes, in order to illustrate the effects of physical phenomena close-to-reality. In industrial practice such multidisciplinary approaches at a justifiable expenditure are only realisable with solutions, which are based on a common data model and which offer a uniform user environment, which makes the change between different applications either not noticeable or drastically simplified.

With Pam-Comfort ESI offer a solution, which contains all necessary simulation tools and solvers under one uniform user interface, adapted to the specific needs. All applications access a common database and by that significantly simplify multidisciplinary applications. A comprehensive library for dummies (HPM1, HRMD, HPM2, Hybrid 3 and BioRID) and human models (5 %, 50 %, 95 % models of female and male anthropometries) is available as well, ❷. The simulation programme is a component of the ESI virtual performance solution and thus fully compatibly to other ESI products such as Pam-Crash and Pam-Safe. Due to the use of a single core model, ①, the data of a simulation step can be used as initial values for subsequently following simulation at small expenditure.

In the context of the accomplished projects already impressing successes could

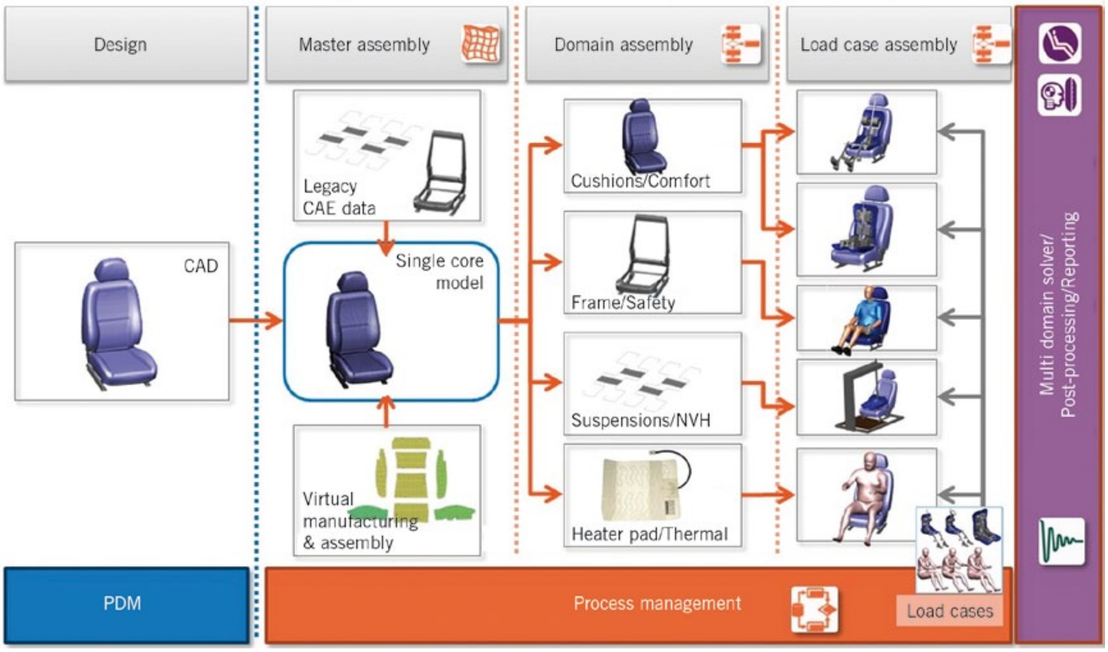


❶ With virtual prototyping the development tasks on a component as well as on system level can be processed on basis of a single core model (master model)

be achieved and the suitability for an industrial employment has been proven. Nevertheless the industrial use of the virtual prototyping technology still is in its starting phase. That is why ESI closely cooperates with car manufacturers, in order to learn from first hand, what is expected by the simulation tools in industrial practice. In order to obtain certainty if the used simulation tools generate results, that meet reality as good as possible, the automakers expend a great deal of effort in tests or pilot projects, with which among other things simulation results are compared with experimental data.

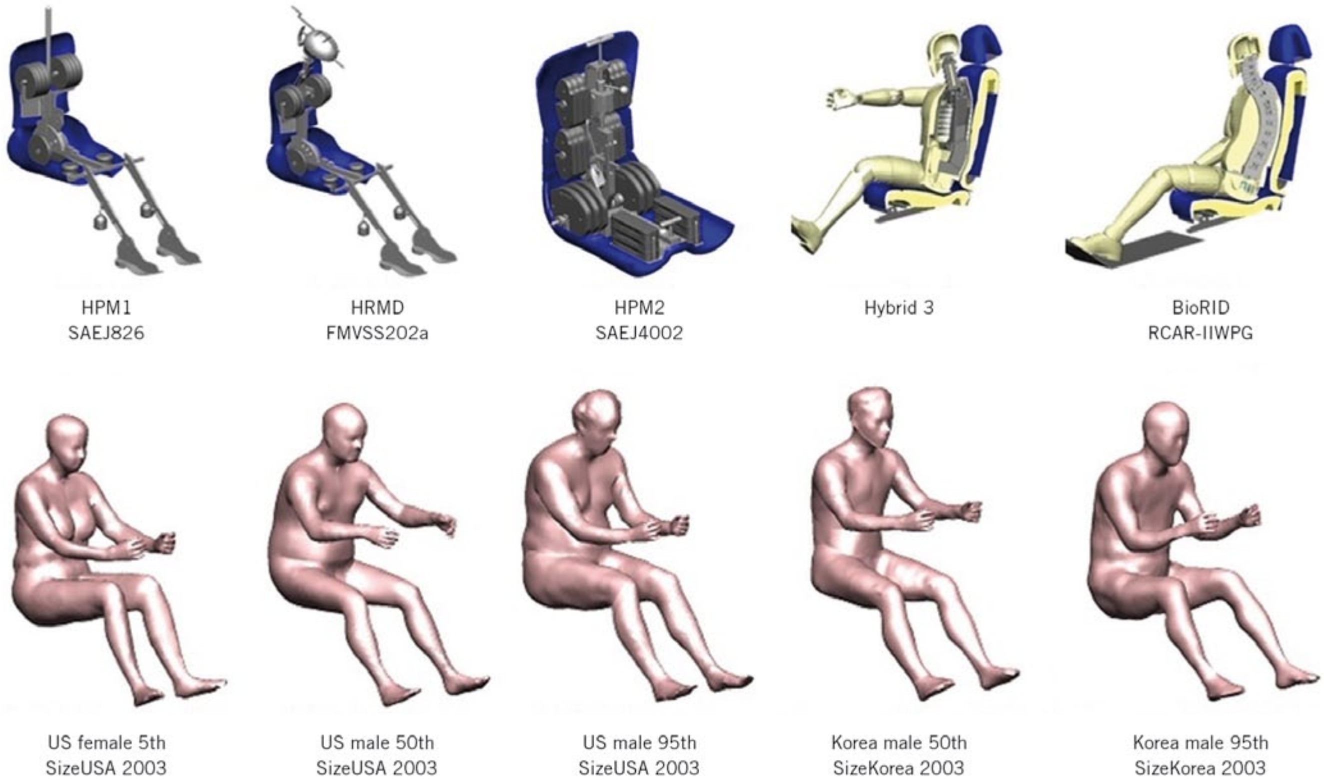


❷ The simulation library contains a vast number of validated dummies models (upper row) and human models (lower row)

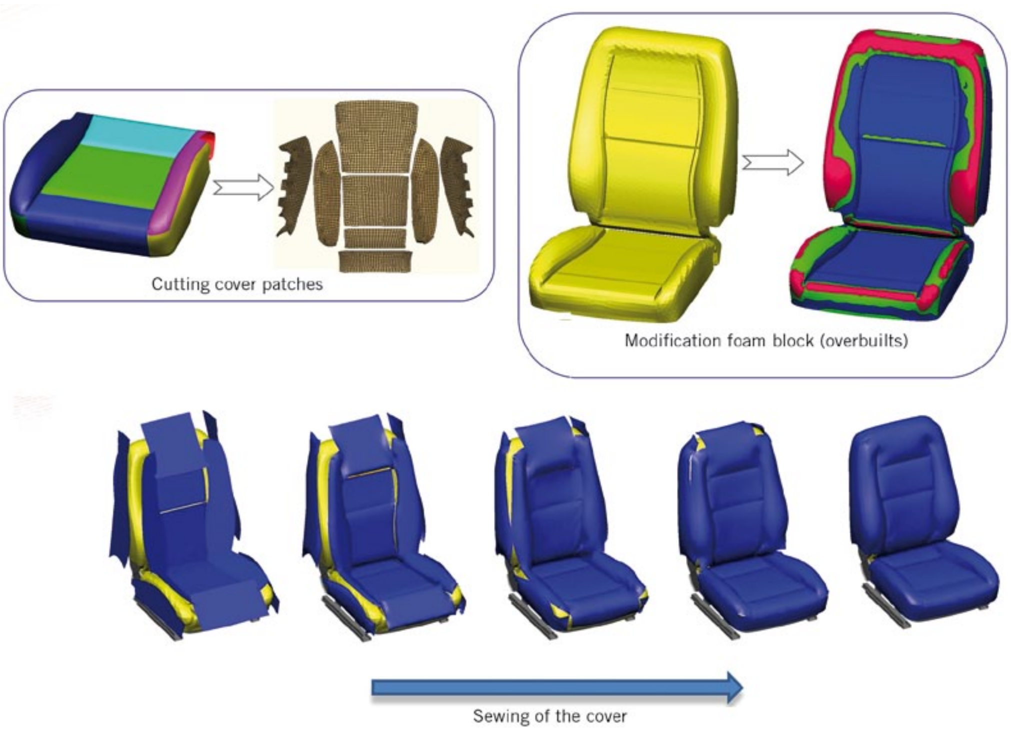


❸ The cutting and sewing of the seat cover as well as the wrapping of the foam block can be simulated with the software Pam-Comfort. By an inverse manufacturing simulation the foam blocks and covers can be optimised to avoid wrinkling and to meet the designed Class-A shape.



## VIRTUAL SEAT DEVELOPMENT

The evaluation of the comfort behaviour is not only important for the passenger comfort itself. Beyond that the addressed tasks have also a central importance for occupant safety and the product quality, since realistic statements about characteristics and behaviour of a seat can only be met if for example the behaviour of foam materials and coverings is considered.

## COMFORT SIMULATION IS A MULTI-STAGE PROCESS

Although not explicitly treated in this paper, the simulation and optimisation of the structural components such as seat frames etc. is part of the overall seat development process and the preliminary stage of the process steps described in this paper. Concentrating on the comfort investigations with all necessary manufacturing simulations and virtual tests, a multi-level process chain is required, in which the start conditions of the individual process steps result from the preceding process steps.

The seating position of a dummy respectively passenger can only be determined accurately and close-to-reality, if the stresses induced by the seat cover and the wrapping process are considered. Therefore preliminary simulations of the manufacturing of the foam blocks as well as the sewing and wrapping of the seat covers are mandatory for realistic statements. In principle the virtual prototyping process consists of the following process steps developing one on the other:

- manufacturing simulation (foam blocks, seat covers)
- occupant positioning
- occupant safety
- mechanical and thermal comfort
- durability.

## MANUFACTURING SIMULATION OF FOAM BLOCKS AND SEAT COVERS

The manufacturing and/or modification of the foam blocks are the first stages in the process chain but no integral part of Pam-Comfort. The injection process of foam blocks into their moulds is simulated and optimised with ESI ProCast and the Viewer Visual-Cast; the results can be transferred to Pam-Comfort without any problems.

A seat cover free from wrinkles, the minimisation of bridging gaps between cover and foam block as well as the prestress of the cover induced by the wrapping process are substantial quality and comfort criteria. With Pam-Comfort the cutting of the fabric patches and the sewing of the seat cover but also the wrapping around the foam block can be simulated, ❸. This is done under consideration of both experimentally determined material properties of foam and fabrics and the friction between cover and foam block.

In high agreement with reality the formation of wrinkles can be determined as well as the pre-stresses and deflections in the cover and the foam blocks of cushion and backrest. Likewise it is possible to derive the shape of the seat cover patches and/or to modify the foam blocks (overbuilts, ③) by an inverse simulation on the basis of the designed class-A surfaces of a seat design.

## POSITIONING OF THE H-POINT

The determination of the correct seating position is the basis for most of the following comfort evaluations and safety assessments, ❹. The correct prediction of the H-point (hip-point), the angle of the torso as well as the backset value (the distance between head and headrest) can be made in accordance to the procedures described in SAEJ826 and/or FMVSS 202a and with test dummies from the comprehensive ESI library. It was shown that the correlation between the measuring data and the values which were predicted by

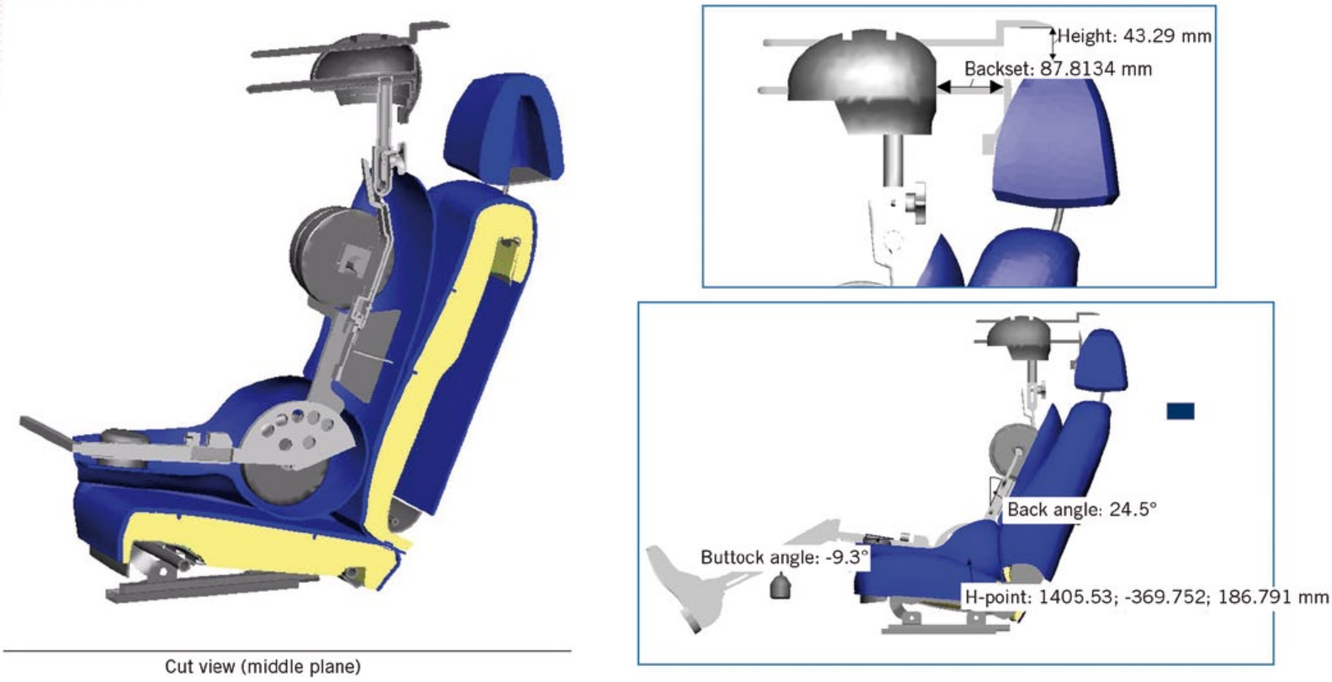


❹ The accurate evaluation of the H-point and backset values according to the SAEJ826 and FMVSS 202a procedures for the correct positioning at the following comfort- and safety-related simulations

simulation under consideration of the pre-stress of the seat cover were much better than without this consideration, ❺.

## COMFORT

Beyond the prediction of the accurate seating position the high variability and interoperability of Pam-Comfort enables different comfort-related investigations. For example it is possible to analyse the seat pressure distribution, ❻, or to perform evaluations of the transmissibility for the analysis of the dynamic comfort behaviour under the influence of external vibrations. For this purposes validated human models from the ESI library can be used which enable more detailed statements than test dummies [4].

With the virtual performance solution, part of which is Pam-Comfort, it is also possible to process evaluations of the thermal comfort (seat ventilation, effect of seat heating) or however NVH inves-

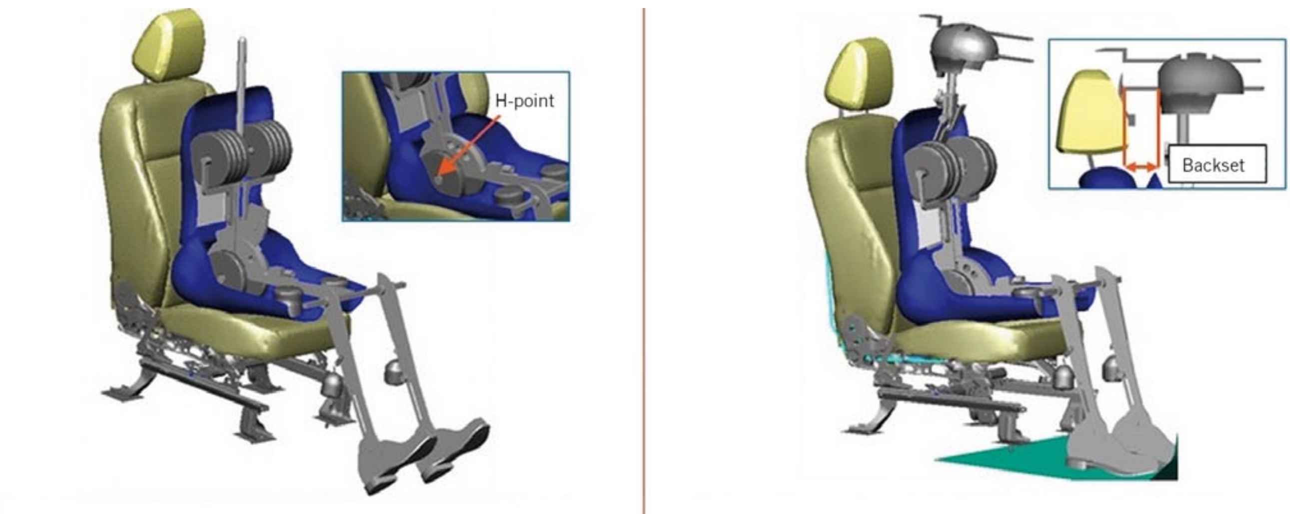


| | H-point X [mm] | H-point Z [mm] | Back [°] |
|---|---|---|---|
| Delta/Experiment | -3.1 | +1.3 | +1.7 |

| H-point X [mm] | H-point Z [mm] | Back [°] | Backset [°] |
|---|---|---|---|
| +0.2 | -1.3 | +0.5 | +4.2 |

❺ The consideration of the preliminary simulations (pre-stress of the seat cover, etc.) enables a significantly more accurate prediction of the H-point and backset values

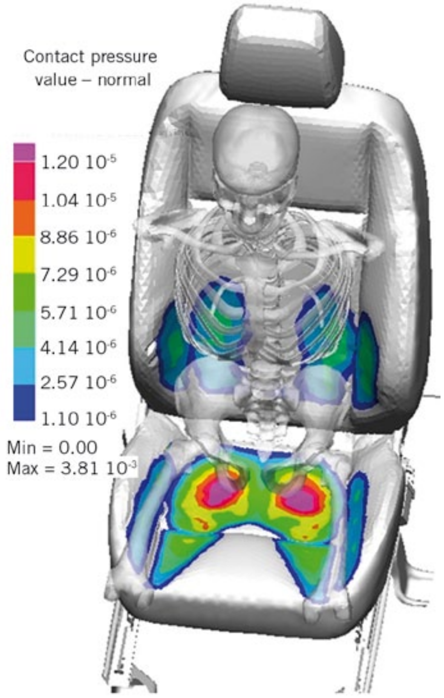


❻ The use of human models from the library enables a realistic prediction of the pressure distribution on cushion and at backrest of the seat

tigations (noise, vibration, harshness). The additionally needed programmes access the same data model and require the practically same input model.

## OCCUPANT SAFETY

In Pam-Comfort an extremely detailed and realistic seat model is generated. By its belonging to the simulation environment this model can be directly handed over to the programmes Pam-Crash (crash, impact), Pam-Safe (airbag deployment, seat belts) or Pam-NVH (vibrations, etc.) for further simulations. In particular by the computer-aided determination of the H-point the test dummies can be positioned correctly according to the guidelines before sled-tests are performed in Pam-Safe.

## WEAR AND DURABILITY

The programme Pam-Comfort offers furthermore the possibility for detailed investigations regarding wear, durability and aging of the "soft" components of a seat. By the execution of predefined load cycles the aging of the foam material and the seat covers can be analysed. Furthermore passenger ingress/egress simulations can be performed for the analysis of the losses of pre-stress in foam blocks and seat covers or the changed position of the H-point. The load path for simulations accomplished with a so-called butt-dummy affects the creation of wrinkles substantially, as well as the friction between cover and dummy represents a substantial factor of influence.

## CONCLUSION

Today, the virtual prototyping of seats is no longer a vision, but lived reality. This development process is increasingly used by the OEMs, in order to replace the traditional trial-and-error procedures on basis of physical prototypes. Objective is not only a cost reduction, but also an increase of product quality, occupant safety and innovative ability. The achieved successes with Pam-Comfort, since 2012 component of the virtual performance solution by ESI, clearly visualise the contained potential. The enterprises assess this approach accordingly positive and promote its further realisation with emphasis.


**REFERENCES**

**[1]** Montmayeur, N.; Marca, C.; Dwarampudi, R.; Kolich, M.; Nunez, S.: Virtual Seat Manufacturing and Testing for FMVSS 202a Backset Prediction. In: Digital Human Modeling Conference, June 2007, Seattle, WA, USA, 2007

**[2]** Montmayeur, N.; Marca, C.; Cabane, C.; Dwarampudi, R.; Kolich, M.; Nunez, S.: Virtual Seat Comfort Engineering through Hardness and Initial Softness Prediction. In: Digital Human Modeling Conference, June 2007, Seattle, WA, USA, 2007

**[3]** Montmayeur, N.; Marca, C.; Cabane, C.; Dwarampudi, R.; Kolich, M.; Nunez, S.: Virtual Seat Comfort Assessment through Effective Fore-aft Lumbar Travel Prediction with a HPM-II Dummy Model. In: Digital Human Modeling Conference, June 2007, Seattle, WA, USA, 2007

**[4]** Choi, H. Y.; Sah, S.; Na, S.; Montmayeur, N.; Marca, C.: Human Body Modeling for Virtual Seat Comfort Testing. In: 2006 Digital Human Modeling for Design and Engineering Conference, July 2006



## THANKS

This paper was created in collaboration with several experts at ESI Group in Aix-en-Provence (France). For their help the authors give a reward for: Nicole Montmayeur, Product Line Manager of the Virtual Prototyping Solutions, and Christian Marca, Product Manager of the Virtual Prototyping Solution for Seats.




AUTHORS

**DR.-ING. HENNING HOLZMANN**
is Director Vehicle CAE at Adam Opel AG in Rüsselsheim (Germany).

**DIPL.-ING. (FH) KARL MICHAEL HAHN**
is head of the Chassis Controls group within the Driving Performance CAE unit at Adam Opel AG in Rüsselsheim (Germany).

**JONATHAN WEBB MEng.**
is Product Manager Chassis Development at Applus Idiada in Santa Oliva (Spain).

**DIPL.-ING. (FH) OLIVER MIES**
is Application Engineer at IPG Automotive in Karlsruhe (Germany).

## NUMBER OF VARIANTS IS INCREASING

Electronic stability control (ESC) makes a valuable contribution to active driving safety [1, 2]. Therefore ESC has become mandatory in many markets globally as an original equipment of new vehicles. As a consequence the type approval of a new model requires proof of an effective ESC system. To date this is done via physical ESC homologation test driving. For that purpose the vehicle is equipped with a steering robot to go through the so-called sine-with-dwell manoeuvre. This requires a considerable amount of time and effort as the test takes at least a day per vehicle for preparation and carrying out. Also the test is subject to weather conditions.

At the same time the number of variants of global vehicle projects in particular has increased dramatically. An example from Opel highlights this: While the Corsa (model year 2005) was available in roughly 70 variants, the same figure totals at around 150 for the Insignia (model year 2008), while the Astra/Zafira (model year 2009) can be ordered in roughly 400 variants. Without a powerful simulation environment this would result in a clash between the number of variants and economic constraints.

However, the ECE-R 13H regulation offers a solution for braking systems. The regulation permits a combination of real-world testing and simulation-based methods. Opel has taken this path and has demonstrated to the industry for the first time that simulation-based passenger car ESC homologation with CarMaker/HiL by IPG Automotive is ready for use [3]. The same had already been proven for heavy commercial vehicles by a brake system supplier [4]. Opel wants to use this strategy to speed up the time-to-market of new vehicles, and to lower the development cost by reduced use of hardware and prototypes.

## SIMULATION-BASED ESC HOMOLOGATION

The European regulation ECE-R 13 H says that simulation-based methods may be used for the ESC homologation of vehicle variants. However, this still requires a driving test with a real vehicle first. Based on the results from the real vehicle, a vehicle simulation environment using the IPG Automotive CarMaker tool was parameterised and thoroughly validated during virtual test driving. The correlation between the simulation results and the measurements collected in a reference vehicle soon reached the level of matching which is required by the technical service and the type approval authorities.

The pilot application to the Opel Meriva, portrayed here, laid the foundation to present simulation results to the type approval authorities in order to receive the homologation for all vehicle configurations on the basis of a single vehicle tested in the real world. This approach fits seamlessly into Opel's existing "Road to Lab to Math" strategy (RLM) [5]. It

# SIMULATION-BASED ESC HOMOLOGATION FOR PASSENGER CARS

As of 2012 the type approval of a new passenger car in the EU requires proof of an effective ESC. To increase the efficiency of vehicle variant ESC homologation for vehicle variants, Adam Opel AG has applied its dynamics simulation environment, which very much relies on CarMaker/HiL, to the minivan Meriva. The results of simulation and real-world driving tests on the proving ground of Idiada match so well that a simulation-based ESC homologation according to ECE-R 13H is reliably feasible.



aims to support real-world testing on the track by a combination of simulation and Hardware-in-the-Loop (HiL) testing, and ultimately by purely mathematical simulation (Software-the-Loop, SiL).

## SINE-WITH-DWELL DRIVING MANOEUVRE

The sine-with-dwell test with the ECE-R 13H is a dynamic driving manoeuvre which standardises an abrupt evasive action in front of an obstacle. Basically the test follows the NHTSA Federal Motor Vehicle Safety Standard, FMVSS No. 126 [6]. The sine-with-dwell test consists of a pre-test and the actual driving manoeuvre. The pre-test serves to measure the steering angle amplitude $A$ that is needed at a steering speed of 13.5°/s to generate a lateral acceleration of 0.3 $g$ while the vehicle travels on a circular path at a steady speed of 80 km/h (required steering angle).

At the beginning of the actual test manoeuvre the vehicle coasts without steering or braking action in the highest gear at 80 km/h ± 2 km/h. The test starts with a steering angle of 1.5 × $A$. During each test run the steering angle is increased by 0.5 × $A$ up to a maximum steering angle of 270°. The test runs with increasing steering angle levels are run in a right-left and left-right sequence each. The applied sine steering with 0.7 Hz provokes a massive yaw reaction while the 500 ms dwell time represents the reaction time of an average driver. In total the manoeuvre is a reproducible version of a critical double lane change situation. ❶ shows the steering angle curve during the manoeuvre plus an exemplary vehicle reaction with and without ESC action.

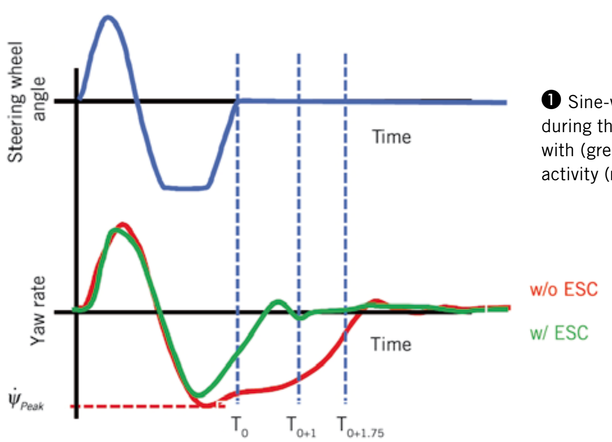


❶ Sine-with-dwell test: Steering angle during the manoeuvre plus yaw rate curve with (green curve) and without ESC activity (red curve)

The sine-with-dwell test is assessed against three criteria of vehicle stability. The crucial element is to check how fast the ESC reacts and how fast the vehicle is brought back to a stable state by reducing the yaw rate. For that purpose the yaw rate and vehicle position are measured at three points in time. To get the homologation the yaw rate has to be ≤35 % of the maximum yaw rate 1 s after the end of the steering action ($T_0$+1 s). At $T_0$+1.75 s the yaw rate must not be higher than ≤20 % of the maximum yaw rate.

In addition there is a vehicle reaction criterion which assesses the vehicle's capability for sideways displacement to avoid an obstacle (minimum requirement is 1.83 m or 6 ft for a vehicle with under 3.5 t of overall weight). Within the limits of meeting the before mentioned three criteria of stability, the vehicle manufacturer has the freedom to choose a more conventional or a more sporty ESC setting, depending on the brand philosophy.

## DATA ACQUISITION WITH THE REFERENCE VEHICLE

During this pilot project the validation scope was purposely expanded far beyond what is required for the actual homologation. With a view to future projects this was done firstly to gain fundamental insight into the validation quality of subsystems, and secondly to completely understand the interdependencies within the chain of effects. For the measurement of the objective vehicle behaviour Adam

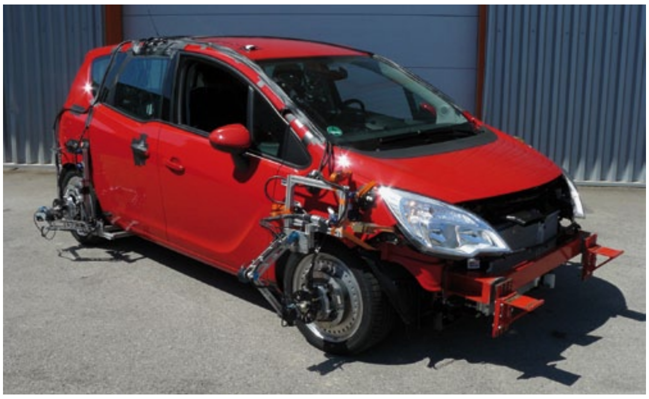

❷ The Opel Meriva reference vehicle with Idiada instrumentation for dynamic driving tests


❸ Visualisation of the CarMaker vehicle model used for ESC homologation

Opel AG cooperated with Idiada, where a Meriva was equipped with a very comprehensive set of sensors. Static measurement of fundamental parameters of the reference vehicle's wheel suspension was carried out for the front and rear axle on a kinematics & compliance rig (K&C rig).

The comprehensive tests delivered detailed data on the geometric position of the suspension and its joints, plus data about the controlled movement of the wheel within the suspension during load influence like on the road. The following dynamic measurements carried out with and without steering robot, provided data about the real vehicle behaviour on the test track. ❷ depicts the reference vehicle as instrumented by Idiada. This was used to analyse dynamic details such as effective forces, wheel centre positions, slip angles, toe and camber, a beginning wheel spin, and the resulting vehicle reaction (centre of gravity acceleration, speed, inclination etc.).

## VEHICLE SIMULATION MODEL AND VIRTUAL DRIVE TEST

Adam Opel AG uses an integrated software tool chain to simulate driving dynamics with optimum precision [7]. A multi-body simulation (MBS) is the starting point. Within the MKS the vehicle is generated and parameterised. As this MBS is not a real time tool, however, the model is subsequently transferred to the test and development environment CarMaker/HiL. The hardware used is a dSpace HiL hardware platform which is controlled from the CarMaker simulation environment, and which interacts with the CarMaker vehicle model, ❸. The HiL simulation environment which is used by Opel and which was applied for the simulation-based pilot project of Opel Meriva ESC homologation is shown in ❹.

A proprietary Opel test automation of the drive manoeuvre catalogues ensures that the HiL systems can be used around the clock. The automation contains features for a remote configuration of the CarMaker environment (vehicle, driver, road parameters) as well as automated execution and evaluation of a large set of

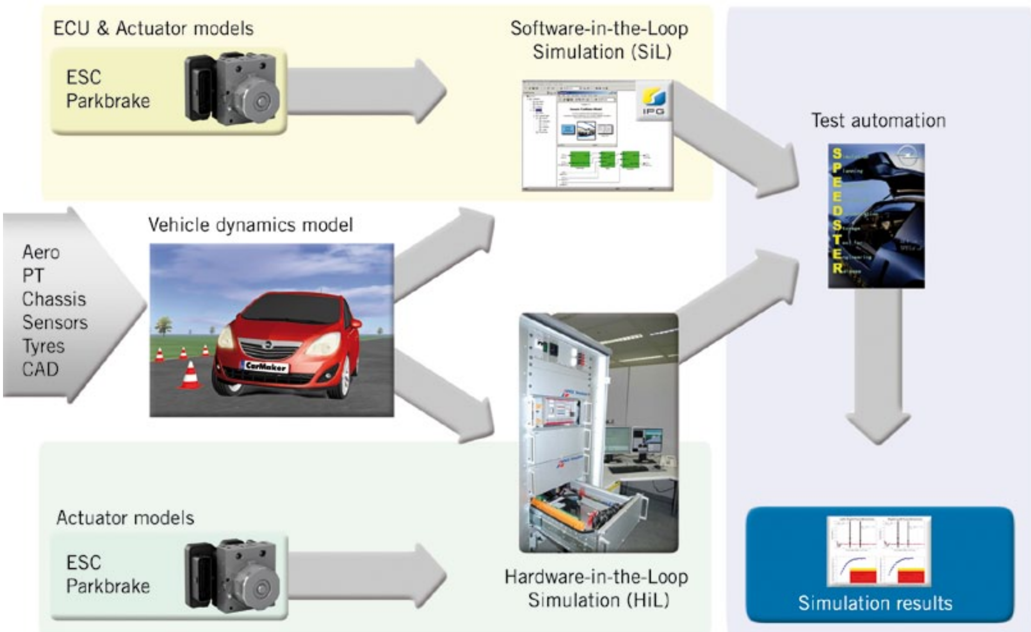


❹ HiL simulation environment that was used

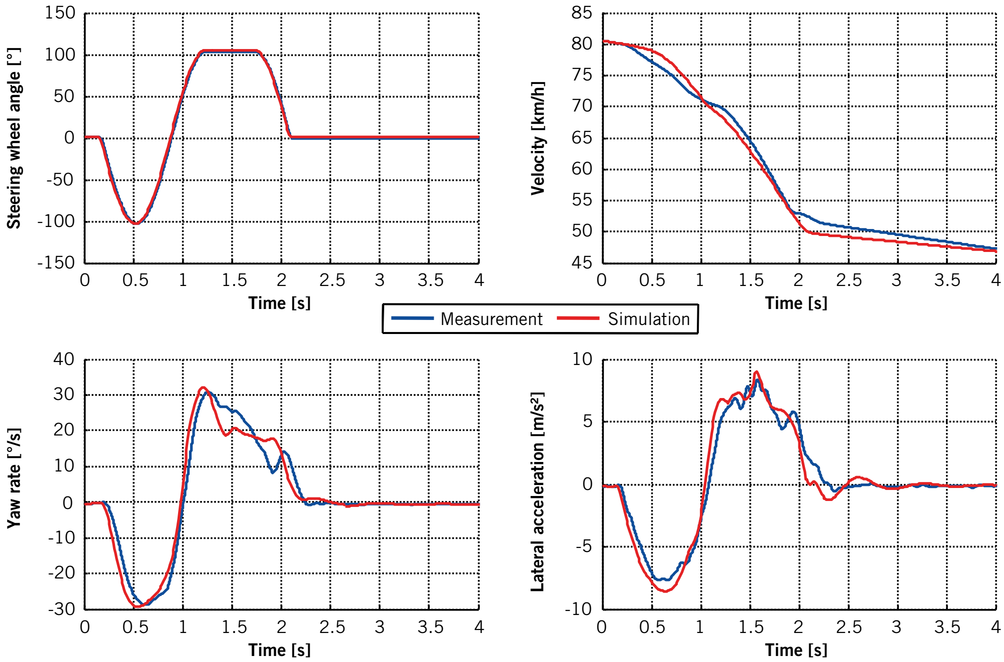


❺ Good correlation between measurements, gained in the reference vehicle (blue curves), and results of the simulated sine-with-dwell test (red curves)



virtual driving manoeuvres. In addition the test automation generates an automated test report.

## VALIDATION RESULTS

Prior to the simulated homologation test, the complete simulation environment was intensely validated. Beginning with simple driving manoeuvres the model was tested with increasingly complex manoeuvres. Finally the sine-with-dwell test according to ECE-R 13H was carried out. During the validation of the vehicle model the main focus was on the model representing the brake hydraulics. Input parameters were the brake pedal force, valve actuation and pump actuation. The wheel brake pressure and wheel brake torque served as outputs. The complexity of simulated manoeuvres was increased from a simple straight line braking procedure through an ABS stop and on to the highly dynamic wheel-individual modulation of brake pressure during ESC activity.

❺ depicts the ultimately achieved excellent match of the simulation carried out on the HiL simulator with the real-world measurements gained via the instrumented reference vehicle. The results shown come from a manoeuvre with around 100° of steering angle and a right-left sequence. Both, the gradients and the maximum values of yaw rate and lateral acceleration show a very good match. This indicates that the simulation environment used reproduces the relevant parameters of dynamics with the precision required by the regulation ECE-R 13H.

## SUMMARY AND OUTLOOK

Within a pilot project Opel has analysed together with Idiada and IPG Automotive whether and how a simulation-based ESC homologation according to ECE-R 13H is possible. The use of an integrated tool chain which includes the driving dynamics development and testing environment CarMaker has demonstrated that this kind of valid homologation testing in a HiL environment is feasible. The preconditions include a stable process, a precise vehicle dynamics model, and a sophisticated integration solution to facilitate model expansions and hardware coupling.

Validation of the simulation environment based on static and dynamic measurements confirms an excellent level of correlation. This is also confirmed by the simulated sine-with-dwell test which delivers results that are very close to the real-world measurements. Hence the simulation solution used has reached the required precision for ESC homologation.

What is more, the development and optimisation process from the real-world measurements to the simulation and on to homologation is fully transparent and well documented. As a conclusion it can be said that the number of real-world vehicle tests during ESC homologation can indeed be considerably reduced by the method of simulation.

### REFERENCES

**[1]** Langwieder, K.; Gwehenberger, J.; Hummel, T.; Bende, J.: Benefit Potential of ESP in Real Accident Situations Involving Cars and Trucks. ESV paper No.150, 18th ESV Conference, Nagoya, Japan, 2003
**[2]** Hummel, T.; Kühn, M.: An Investigation into the Availability of ESP in Cars in 2009. http://www.udv.de/uploads/tx_udvpublications/Web_komp__E_Nr.16_UDV_Kompakt_ESP2009_01.pdf
**[3]** Holzmann, H.; Hahn, K. M.; Weyer, F.; Römer, M.; Webb, J.; Boltshauser, S.; Tosolin, G.; Bu, Q.: Simulation-based Homologation of ESC Systems According to ECE-R 13-H. Stuttgarter Symposium Automobil- und Motorentechnik. 13 – 14 March 2012
**[4]** Wurster, U.; Ortlechner, M.; Schick, B.; Drenth, E.; Crawley, J.: First ECE 13/11 Homologation of Electronic Stability Control (ESC) by Vehicle Dynamics Simulation – Challenges, Innovations and Benefits. Proceedings, chassis.techplus 2010, Munich, 7 – 8 June 2010
**[5]** Kochem, M.; Holzmann, H.: Einsatz der Road-Lab-Math Strategie bei der simulationsbasierten Entwicklung von Fahrwerkregelsystemen. Vortrag, VDI-Tagung Autoreg, Wiesloch, 7. und 8. März 2006
**[6]** NHTSA National Highway Traffic Safety Administration: Final Regulatory Impact Analysis http://www.nhtsa.gov/DOT/NHTSA/Rulemaking/Rules/Associated%20Files/ESC_FRIA_%2003_2007.pdf
**[7]** Holzmann, H.; Halfmann, C.; Hahn, K. M.; Kochem, M.: Virtual Development and Application of Chassis Components and Chassis Controls at GM Europe. SAE Paper 2007-01-0813, 2007

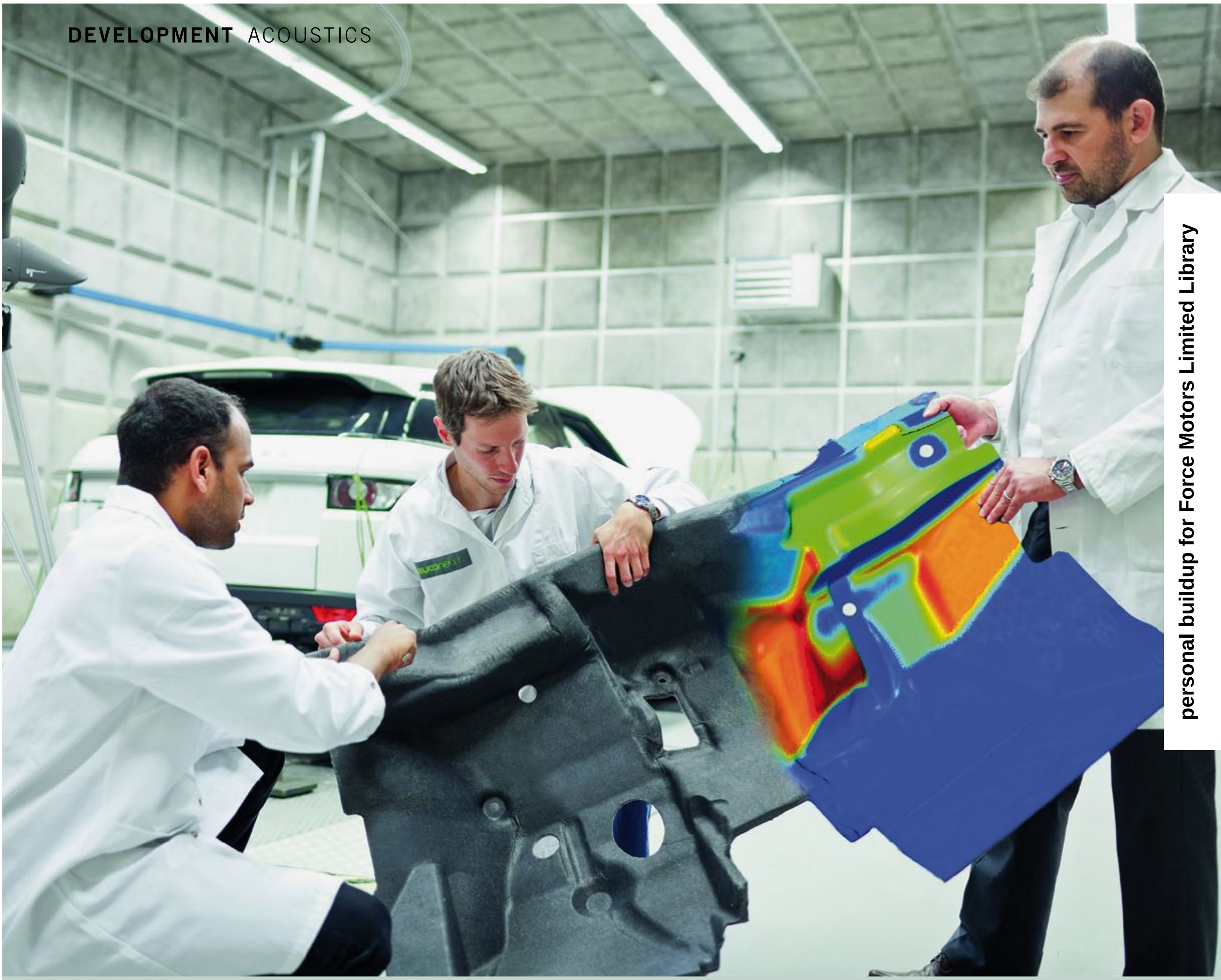



# OPTIMISATION OF A HYBRID SOUND PACKAGE WITH STATISTICAL ENERGY ANALYSIS

In acoustics development, more and more cutting-edge simulation tools such as 3D calculation and statistical energy analysis (SEA) are used in order to reduce the weight of the sound insulation packages in the vehicles. Therefore, Autoneum developed a hybrid solution of insulating and absorbing materials as an alternative to conventional insulative heavy layer-foam constructions that, despite its lightweight character, provides a high acoustic performance regarding insulation and absorption.

AUTHORS

**MARCO SEPPI**
is Head Acoustic Concepts and Products at Autoneum Management AG in Winterthur (Switzerland).

**CLAUDIO CASTAGNETTI**
is Global Product Manager at Autoneum Management AG in Winterthur (Switzerland).

**VIJAY RAVINATH**
is Scientific Manager for High Frequency Methods in the Simulation Team at Autoneum Management AG in Winterthur (Switzerland).

## CHANGE IN TRENDS IN ACOUSTIC INSULATION

In the past years, two main types of acoustic concepts have been largely used to design noise control treatments: either insulative or absorptive packages. Insulation is traditionally obtained by means of a mass-spring barrier system, where the mass element is formed by a layer of high-density impervious material (heavy layer) and the spring element is formed by a layer of low-density material like a non-compressed felt or foam. Insulative parts of mass-spring type are characterised by a high insertion loss (IL), but provide practically no absorption. On the other hand, absorptive parts follow an insulation slope that increases only with 6 dB/octave in insertion loss, while the ideal slope of 12 dB/octave is typical of mass-spring systems.

A benchmarking study based on 80 European vehicles shows that the insulating mass-spring systems have become less with time. Absorbing packages and generally lightweight hybrid solutions have increased their market share, ❶. It is a common practice of benchmarking experts to define as hybrid the parts that combine absorption and insulation functions within the same multilayer construction.

In addition, there is a current design trend to use a more refined subdivision of the acoustical functions on the local areas of an acoustical part. As an example, an inner dash treatment can be split in two main areas, one providing high absorption and the other providing high insulation. Generally, the lower part of the dash is more suitable for insulation because the noise coming from the engine and the front wheels through this lower area is more relevant, while the upper part of the inner dash is more suitable for absorption because some insulation is already provided by other elements of the car, for instance by the instrument panel.

## DESIGN AND SIMULATION OF A HYBRID SOUND PACKAGE

Autoneum designed an optimal hybrid inner dash using a specific acoustic principle to increase the insulation of lightweight parts and therefore tuning the balance between absorption and insulation in an optimal way. With the concept of dynamic stiffness control, it is possible to move out of the frequency range of interest the negative radiation effects of the porous top felt, an unwanted noise radiation that would otherwise reduce the insertion loss of the part [1].

Benchmarking study data coming from market observation and from the acoustical experimental analysis of parts and vehicles have been used as a base for product development together with specifications of the OEMs and from the patents search, ❷. The first step in the creation of the product consisted in a large

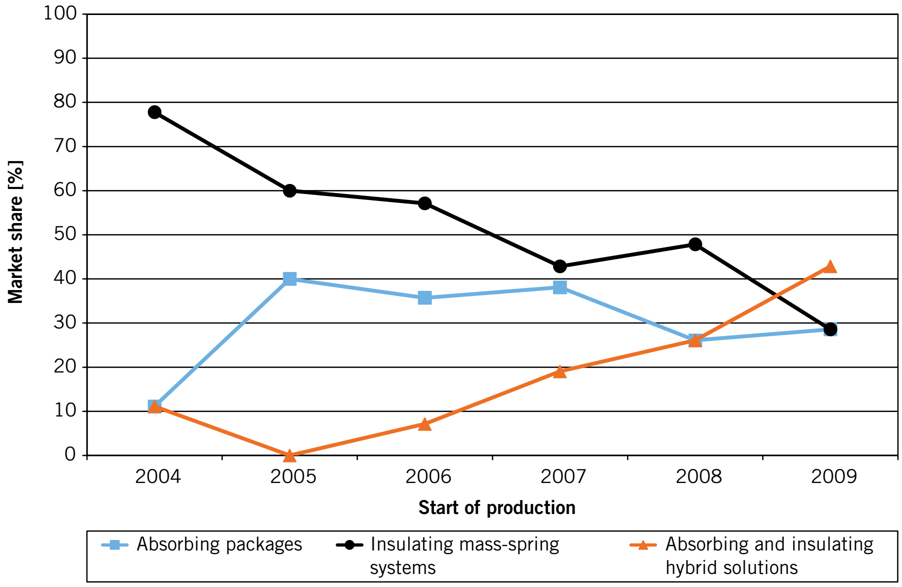


❶ Evolution of the acoustic concept of inner dashes in Europe (as an example of a benchmarking study based on 80 European vehicles)

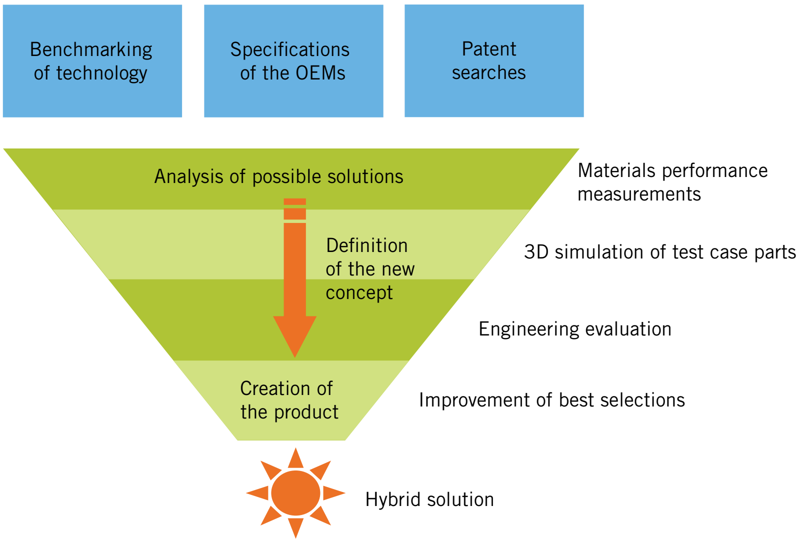


❷ Steps in the innovation design process for hybrid packages

screening of the possible solutions accompanied by intensive acoustic material measurements. Subsequently and already at the initial stages of the project, a transfer matrix method (TMM) based software [2], has been used to simulate the 3D acoustic performance of various solutions. The next engineering step consisted in the selection of a multilayer with clear advantages in terms of insulation performance (IL rate of 12 dB/octave) and local tuning of insulation and absorption properties. The final hybrid construction consists of three layers:

: a porous top felt layer, characterised by a high dynamic stiffness
: a thin and air impervious plastic film layer
: a standard porous decoupling layer (made of foam or felt).

This hybrid material behaves as a lightweight mass-spring insulator where the mass effect is provided by the weight of the top layer, ❸, and the barrier effect is given by the impervious film. One can therefore observe the typical mass-spring resonance frequency after which the insertion loss grows at a rate of 12 dB/octave. The top layer, in this case porous, keeps a non-negligible absorption different from standard pure insulators. For the described multilayer, if the porous felt layer was not characterised by a controlled and high dynamic stiffness, the insulation would be affected by a resonance effect, ③.

## OPTIMISATION WITH TMM AND SEA TOOLS

Cutting edge CAE proprietary tools, namely VisualSisab, [2], based on the transfer matrix method (TMM), and Revamp, [4], based on the statistical energy analysis (SEA), are intensively used to optimise the design of the hybrid material with controlled dynamic stiffness. The typical steps to simulate the impact of a 3D inner dash part on the vehicle acoustic performance are:

: analysis of the available packaging space and subdivision of the part surface based on vehicle SEA panels – TMM
: 3D calculation of the local acoustic performance (insulation and absorption), based on measured material models including stiffness measurements [3] – TMM
: transfer of the insulation/absorption simulated data subdivided by panels to the high frequency acoustic model of the car compartment and calculation of the sound pressure level (SPL) at the driver's ear position – SEA.

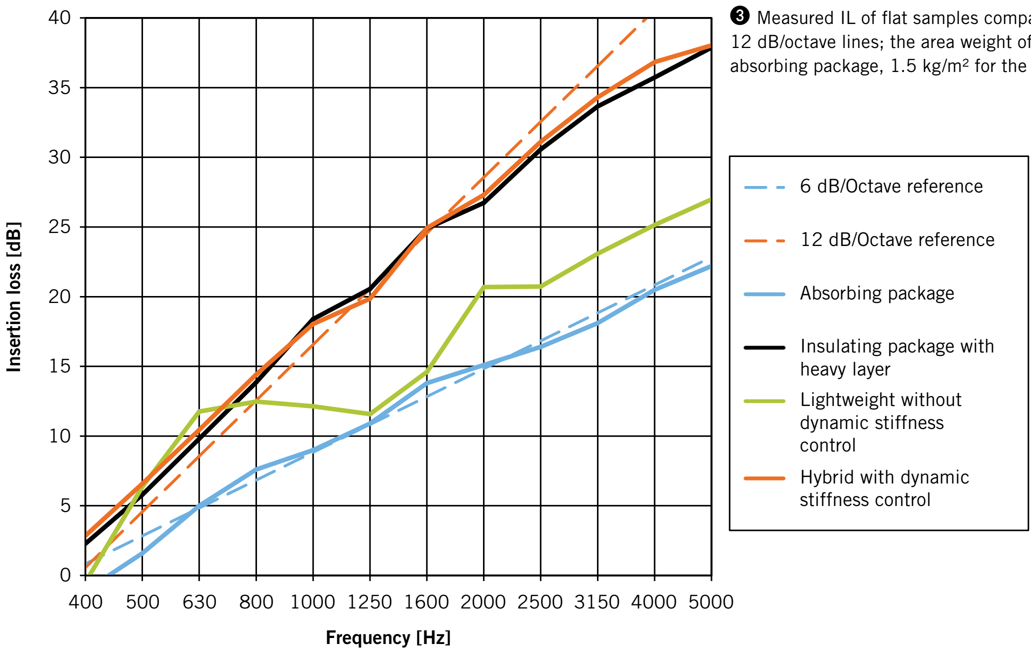


❸ Measured IL of flat samples compared to reference 6 dB/octave and 12 dB/octave lines; the area weight of the top layer is 1.2 kg/m² for the absorbing package, 1.5 kg/m² for the other three packages

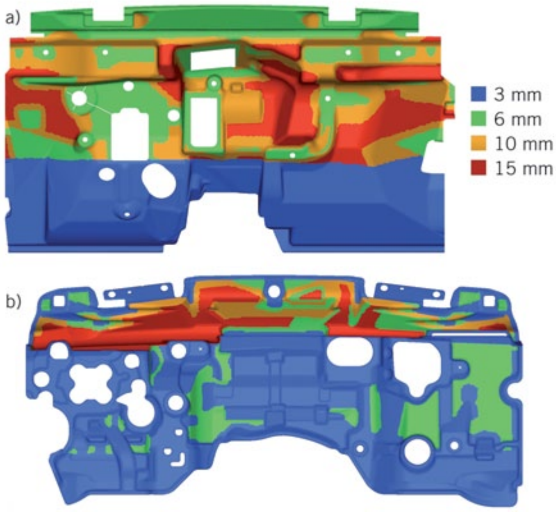


❹ Thickness distribution of the top felt layer for the two application cases: C-segment vehicle (a) and D-segment vehicle (b)

The top layer thickness is the main parameter to optimise the design of the part. Low values of the thickness (3 mm) are linked to high stiffness and high insulation performance while higher values of the thickness provide good absorption properties. The top layer thickness can assume different values in every area of the part, provided that the total packaging space (that is also spatially variable) is not exceeded. For example, if the available thickness is 15 mm in a certain small area, the top layer thickness can be set at 3, 7, 10 or 12 mm while the rest of the space is filled by a film and by a bottom decoupling layer.

In another area, the available thickness can be, for example, 10 mm. As a consequence, the possible top felt layer thicknesses are reduced to 7 and 3 mm. The best configuration defines the optimum top layer thickness of the part for each area. It is obtained through the calculation of all the possible variants and the selection through a Pareto analysis [5].

## CUSTOMISED DESIGN

Since a validated SEA model is used, the optimised thickness distribution of the top layer does not only take into account the material characteristics that determine the performance of the part but also the acoustic properties of the car compartment. The design is linked to the acoustic characteristics of the specific car and to the available packaging space: it is a customised design.

Two application cases are considered: an inner dash of a C-segment vehicle that was developed in cooperation with an OEM [5], and an inner dash of a D-segment vehicle. For both cases, the same bill of material and the same area weight of the top layer (1500 g/m²) have been used.

❹ (a) shows the result of the optimisation process in the C-segment vehicle: the final design for the top layer thickness is represented in a scale of colours, each colour being associated to a different thickness class (blue for 3 mm, red for 15 mm). Lower thickness values are chosen as optimal for the lower part of the dash and partly for certain areas of the upper part (in particular on the left side), while high values of thickness are dominating on the upper part of the dash. As a consequence, high insulation is privileged in the lower dash and high absorption in the area behind the instrument panel. This gives a reason for the general trend towards hybrid solutions that was mentioned before.

A similar behaviour is observed also for the D-segment vehicle, ④ (b). In this case, the subdivision between insulative and absorptive areas is even more evident, with a clear split between higher and lower part of the dash. The design is linked to characteristics of the instrument panel and to the fact that in the lower area, for the specific case, the available packaging space was rather limited.

For both application cases, simulations and measurements (based on the acoustic transfer function, ATF) have been run to compare the SPL of the hybrid solution to those of a standard acoustic package, ❺. In the case of the C-segment vehicle, the values for the hybrid package are compared to a standard insulative heavy layer-foam solution, having the same foam material as decoupling layer and a barrier layer of 6 kg/m² (heavier by 5.5 kg at part level).

The standard insulative solution is performing up to 1250 Hz better, because of the weight advantage at frequencies for which insulation is clearly relevant. However, the difference is kept low because the hybrid package uses the prop-

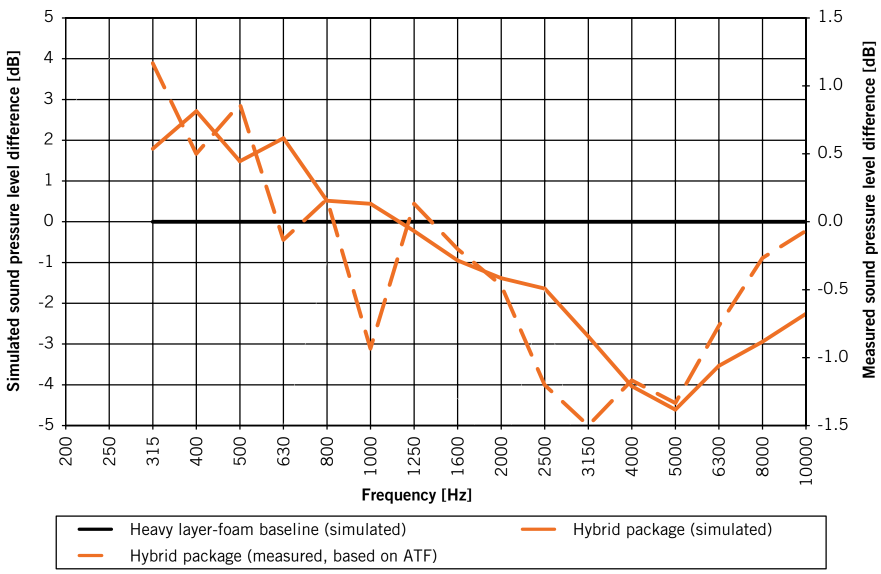


❺ On the C-segment vehicle, comparison between the hybrid solution and a standard mass-spring solution as baseline: simulated SPL difference (left scale) and measurement SPL difference, generated from the acoustic transfer function, ATF (right scale)

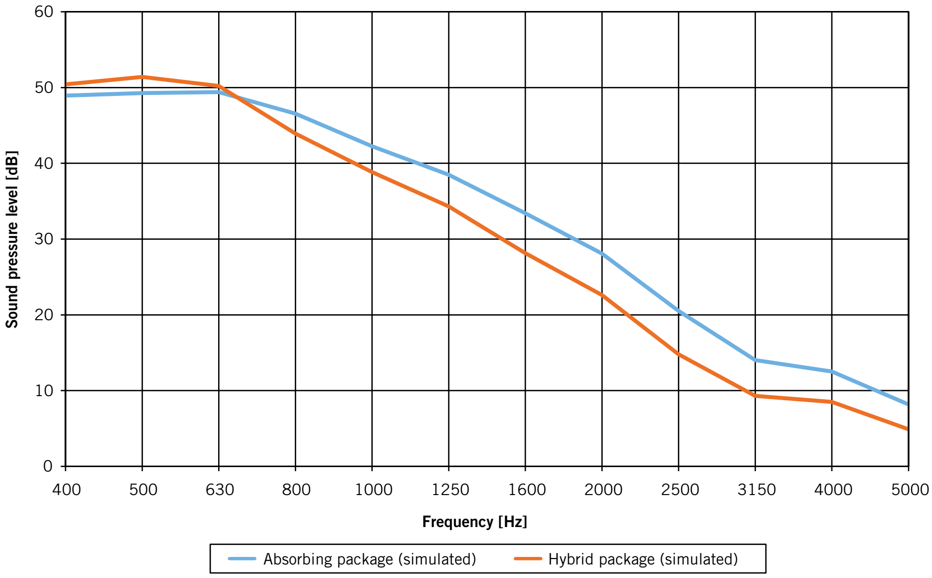


❻ SPL comparison between the hybrid solution and a standard absorbing solution, both simulated at driver's ear position

erty of high dynamic stiffness to produce a fairly good insertion loss. Above 1250 Hz, the advantage of the absorption and of the optimal balance between absorption and insulation is in favour of the hybrid package. Overall, on the whole frequency range, the two solutions are not very different in terms of calculated SPL and, when measured in the vehicle, performed in a very similar way [5]. The ATF measurements in the vehicle confirmed a very similar trend as the simulated SPL, ⑤. Compared to the heavy insulative solution, the hybrid package allows a substantial weight reduction – while keeping an equivalent acoustic performance at vehicle level.

In the case of the D-segment vehicle, ❻, the hybrid solution is compared to a lightweight absorbing package formed by two felt layers without barrier, the top felt layer being compressed to increase the AFR. The two solutions have an equivalent weight of around 2.3 kg. A very similar calculated SPL is obtained at low frequency, while the hybrid package allows a reduction of the SPL in the medium-high frequency. Only at a very high frequency, absorption has the main impact on SPL and the performance of the two solutions is again more similar.

All the data presented are valid for airborne excitations and under the hypothesis that the structure-borne noise is negligible. This hypothesis is valid for a medium-high frequency (normally for frequencies above 500 Hz); however, at a lower frequency, the structure-borne noise is dominant. Road measurements of the hybrid part mounted on a vehicle have not shown any specific deterioration of the performance for structure-borne noise [5]. Future simulations at part level based on finite element calculations with simulation tools like Treasuri2FE [6] will be implemented to confirm the first experimental observations.

**REFERENCES**


**[1]** Seppi, M.; Bertolini, C.; Castagnetti, C.: Analytical Prediction of Resonance Effects for Lightweight Acoustic Packages with Increased Insulation. Proceedings, Internoise 2012, August 19 – 22, New York City, USA

**[2]** Bertolo, P.; Caprioli, D.: VisualSisab: A Visual Tool for a Quick and Accurate Assessment of the Acoustic Properties of Car Parts. Proceedings, RAC Rieter Automotive Conference 2007, Winterthur, Switzerland, A4, pp. 1 – 23

**[3]** Bertolini, C.; et al.: Transfer Function Based Method to Identify Frequency Dependent Young Modulus, Poisson Ratio and Loss Factor of Poroelastic Materials. Proceedings, Sapem 2008, December 2008, University of Bradford, Bradford (UK)

**[4]** Bertolini, C.; Gigante, L.: An SEA-Based Procedure for the Definition of Sound Package Component Targets Starting From Global Vehicle Targets. Proceedings, VibroAcoustics Users' Conference Europe, Leuven, Belgium, 2003

**[5]** Negro, E.; et al.: Optimization of a Dash "Hybrid" Insulator Absorber Based on Pareto Analysis of SEA Simulation Results. Proceedings, Automotive Acoustics Conference 2011, Zurich, Switzerland, 7 and 8 July 2011

**[6]** Bertolini, C.; et al.: Treasuri2FE: A Tool for the FE Simulation of Sound Package Parts Fully Integrated in Nastran. Proceedings, SAE 2009 Noise and Vibration Conference and Exhibition, May 2009, St. Charles, IL, USA

# OPTIMISED SOLAR CONTROL GLAZING FOR IMPROVED COMFORT AND FUEL EFFICIENCY

A recent study by Saint-Gobain Sekurit demonstrates how fuel consumption caused by the air conditioning system can be reduced by equipping the car with optimised solar control glazing. By using a heat management glazing package consisting of an SGS CoolCoat and dark tinted glazing, a saving of 30 % is possible compared to standard green tinted glazing.

AUTHORS

**DR. VOLKMAR OFFERMANN**
is Marketing Director at Saint-Gobain Sekurit International in Herzogenrath (Germany).

**DR.-ING. ANN-KATRIN GLÜSING**
is Communications Manager at Saint-Gobain Sekurit International in Herzogenrath (Germany).


## MOTIVATION

Sustainable mobility is one of the urgent challenges for the automotive industry. Glazing can provide various solutions that allow OEMs to achieve their targets. One of these solutions is optimised solar control glazing, which can not only improve comfort inside a vehicle, but can also reduce the additional fuel consumption caused by the air conditioning system.

In this context, it is important to note that legislation in Europe and the US will pay much more attention in the future to off-cycle fuel consumption, and other regions of the world are likely to follow. Air conditioning system fuel consumption is a key element in this discussion. Therefore, any support for the vehicle's heat management by using advanced glazing is becoming increasingly important.

## GLAZING TO REDUCE THE HEAT LOAD AND FUEL CONSUMPTION

Today, most cars on the market are equipped with green glazing. Improved solar protection, for example with reduced heat input, can be achieved by so-called heat-reflecting technologies, which are already available today as optional equipment on many cars. In this product family, Saint-Gobain Sekurit has recently developed a new windshield technology called SGS CoolCoat, which is approximately twice as efficient as today's heat-reflecting products.

The technology is based on a multilayer coating on the inner glass layer of the glass sandwich, as shown in ❶. The main component of the invisible coating is thin silver layers. These layers act like a mirror for infrared rays, and reflect the heat of the sun directly to the outside.

❷ shows that the amount of heat entering a car with green tinted standard glazing is 65 %, whereas with CoolCoat only 40 % enters the vehicle. Consequently, the interior of the vehicle stays cooler, the air conditioning runs less and comfortable temperatures can be reached faster than with standard glazing. As a result, the use of the air conditioning system can be reduced and fuel consumption can be lowered.

Behind the B-pillar, it is also possible to equip the car with dark tinted glazing for the side and rear windows. This is a simple way to avoid excessive heating-up of the interior. This benefit is, however, limited by the fact that the glass bulk itself is heated up under intense solar radiation, and the hot glass re-radiates additional heat into the interior. With the most advanced dark glass type called VG10, the heat entering the car can be reduced to 37 %.

## MEASUREMENTS ON A CAR

Even though it is well known that windows have a high influence on heating up a car, very few measurements are available regarding the real benefit in terms of fuel consumption reduction. Hence, a quantitative measurement in a climate wind tunnel with solar simulation [1] was performed. Two glazing car sets were compared:

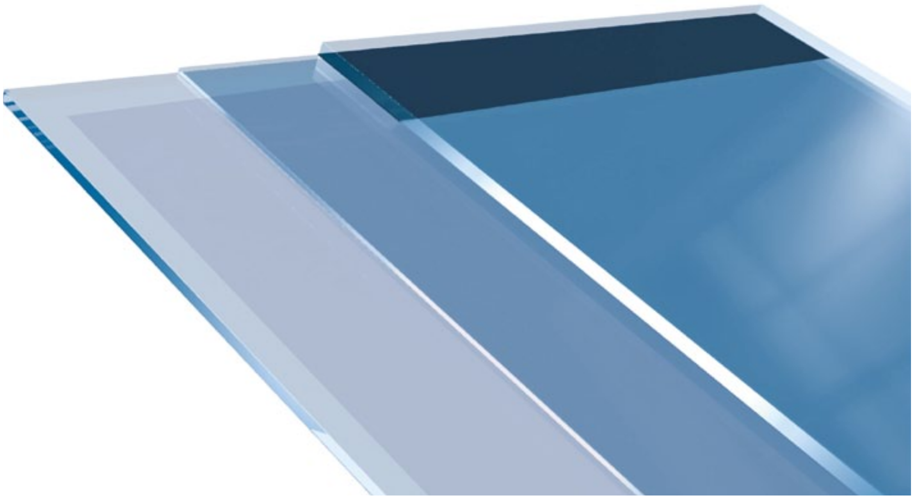

❶ Schematic representation of the laminated coated windshield SGS CoolCoat (from left: inner glass sheet, CoolCoat coating, PVB foil, black print and outer glass sheet)

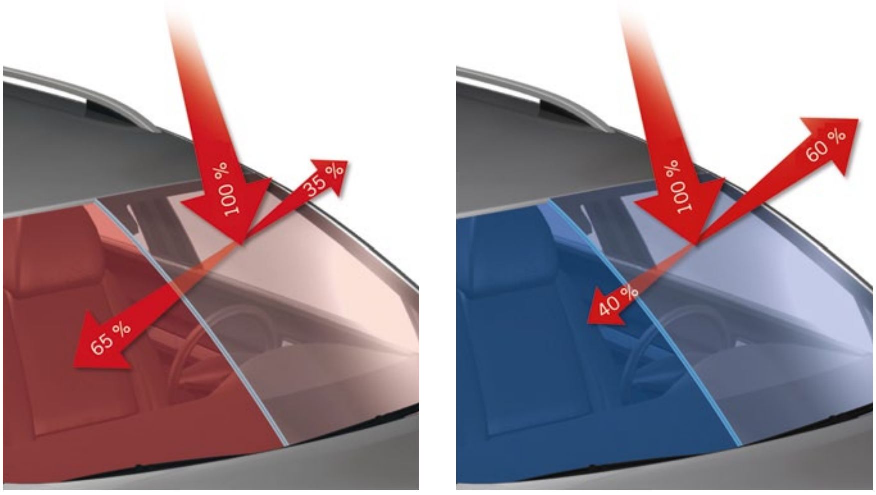


❷ SGS CoolCoat provides better comfort and less heating up than green glass, since only 40 % of the heat from the sun enters the car instead of 65 %

: standard green tinted glass all round and
: a CoolCoat windshield, green glass front door glazing, dark grey glass behind the B-pillar.

Both car sets were tested with and without the air conditioning running (automatic mode, 21 °C target temperature). In all cases, the solar load simulated a sunny summer day with 1000 W/m² radiation. In order to obtain a realistic representation of real situations in Europe, rows of illumination lamps were positioned at 60° and 90°, as shown in ❸. The boundary conditions of the test chamber were a temperature of 35 °C and a relative humidity of 40 %. The driving cycle employed for the tests was a combination of a pre-conditioning phase, a heating up phase, the NEDC as the currently valid cycle for emissions legislation and a final stationary cycle. The vehicle used for the tests is described in ❹.

During the test, temperatures were recorded at various positions inside the cabin. The fuel consumption was determined with an external fuel tank on a set of scales, as shown in ❺.

## TEST RESULTS AND DISCUSSION

The NEDC driving cycle was performed three times with each glass configuration with the air conditioning system switched on (set to 21 °C target temperature), and three times with the air conditioning system switched off. The fuel consumption was determined in each case. ❻ shows the average fuel consumptions obtained for the four different configurations.

The results clearly show that the use of the air conditioning system can be noticeably reduced if a CoolCoat windshield in combination with dark tinted glazing behind the B-pillar is used. In the test conditions employed, the air conditioning system fuel consumption can be reduced by 30 % due to the glazing, which means, for example, a saving of 1.3 l/100 km for urban driving. For the


❸ Test car in the climate wind tunnel with solar simulation

| CAR CHARACTERISTICS | FORD KUGA TDCI 2X4 TITANIUM |
|---|---|
| Specials | No sun roof, automatic climate control |
| Fuel consumption combined [l/100 km] | 5.9 |
| Fuel consumption city [l/100 km] | 7.5 |
| Fuel consumption highway [l/100 km] | 5.0 |
| $CO_2$ emission combined [g $CO_2$/km] | 154.0 |
| Colour | White |
| Displacement [cm³] | 1997 |
| Number of doors | 4/5 |
| Emission standard, emission certification | Euro 5, 4 (green) |

❹ Description of test vehicle with a mileage of 6300 km [2]

NEDC cycle, a saving of 0.7 l/100 km was measured, which is equivalent to 19.1 g $CO_2$/km. Finally, the average benefit of such glazing in Europe over a full year was calculated by modelling, taking into account European weather data [3].

The calculations reveal that, for an annual EU average, the advanced glazing car set provides a reduction in the vehicle's $CO_2$ emission by 3.8 g $CO_2$/km. For the specific car geometry used, 1.6 g $CO_2$/km of this reduction can be attributed to the SGS CoolCoat windscreen.

It is worth mentioning that less heating up of the cabin also results in improved comfort compared to a standard glazing. ❼ shows the temperature on the instrument panel while being measured during the tests. CoolCoat can reduce the instrument panel temperature during the heat-up phase by 15 °C, which has a very positive impact on the subjective comfort perception. In addition, direct sun radiation on the driver's arms and legs is strongly reduced.

## FURTHER GLAZING TECHNOLOGIES

SGS CoolCoat is the latest anti-heat innovation. A similar anti-heat performance can be achieved with another innovative product recently brought to the market, SGS ClimaCoat. In SGS ClimaCoat, the coating is so conductive that it can even be heated by applying an electric voltage to the coating. Hence, SGS ClimaCoat incorporates two key benefits in one windscreen: heatable in the winter and heat reflecting in the summer.

The system operates with a standard 14-V power supply. This simplifies its implementation, unlike the previous solution with 42 V, and reduces system complexity. With a heating power of between 400 and 500 W, it rapidly defrosts and demists the windscreen. Strenuous ice scraping is no longer necessary. The driver simply pushes a button to activate the SGS ClimaCoat to achieve a clear view and improved safety in less than 2 min, ❽.

Since April 2011, the heatable windshield has been available on the new VW Passat B7. Further models will be introduced in the near future.

## OUTLOOK FOR ELECTROMOBILITY

Good vision for the driver is an essential safety requirement for all vehicles, no matter whether they are electric or have a conventional internal combustion engine. The major difference, however, is that, in a conventional vehicle, the engine generates heat, and this can be

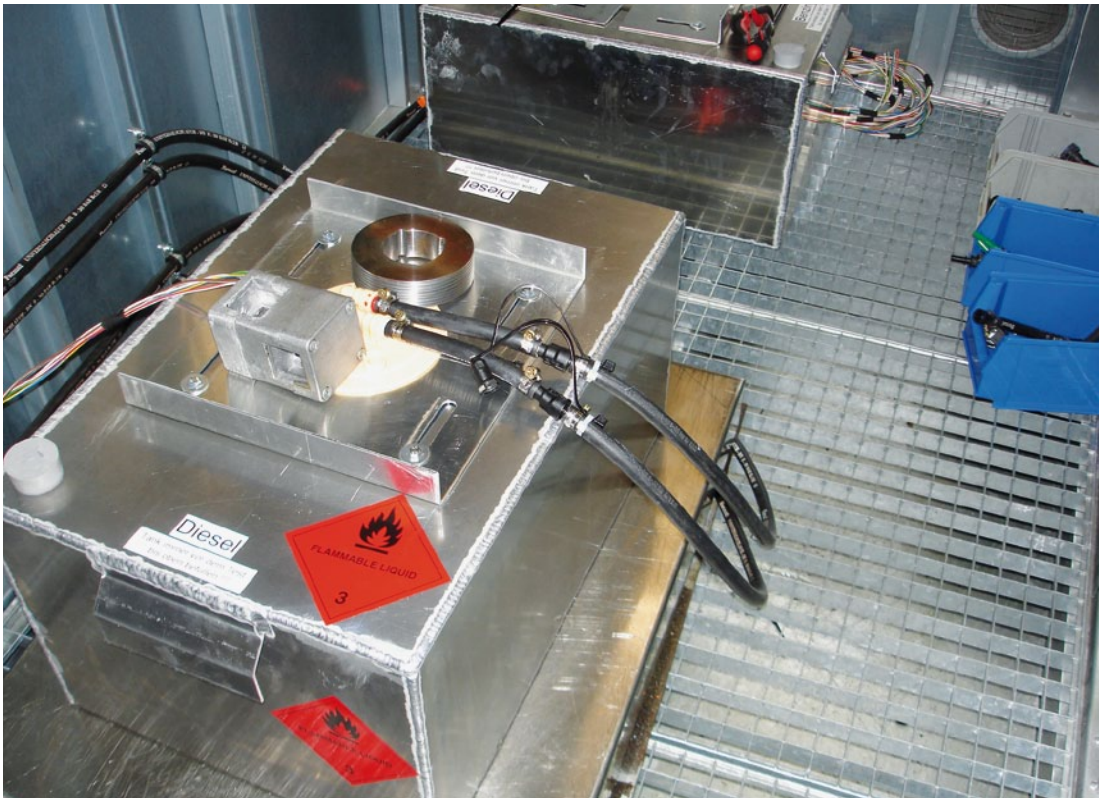


❺ Fuel scales for measuring the fuel consumption at the external fuel tank

| CONSUMPTION [l/100 km] | | | | | Δ | CONSUMPTION [g $CO_2$/km] | | | | Δ |
|---|---|---|---|---|---|---|---|---|---|---|
| Cycle | Green tinted glass | | Anti heat glass package (CoolCoat + dark grey glass) | | CoolCoat + dark grey glass vs. green tinted glass (w. AC) | Green tinted glass | | Anti heat glass package (CoolCoat + dark grey glass) | | CoolCoat + dark grey glass vs. green tinted glass (w. AC) |
| | w/o. AC | **w. AC** | w/o. AC | **w. AC** | | w/o. AC | **w. AC** | w/o. AC | **w. AC** | |
| City | 8.0 | **12.3** | 7.7 | **11.0** | -1.3 | 210.0 | **322.9** | 201.7 | **288.1** | -34.8 |
| Highway | 6.8 | **8.4** | 6.7 | **8.0** | -0.4 | 178.9 | **220.4** | 175.4 | **210.0** | -10.4 |
| NEDC | 7.3 | **9.9** | 7.1 | **9.2** | -0.7 | 190.3 | **259.6** | 185.1 | **240.6** | -19.1 |

❻ Overview of the fuel consumption results with solar control glazing (with and without air conditioning, AC)

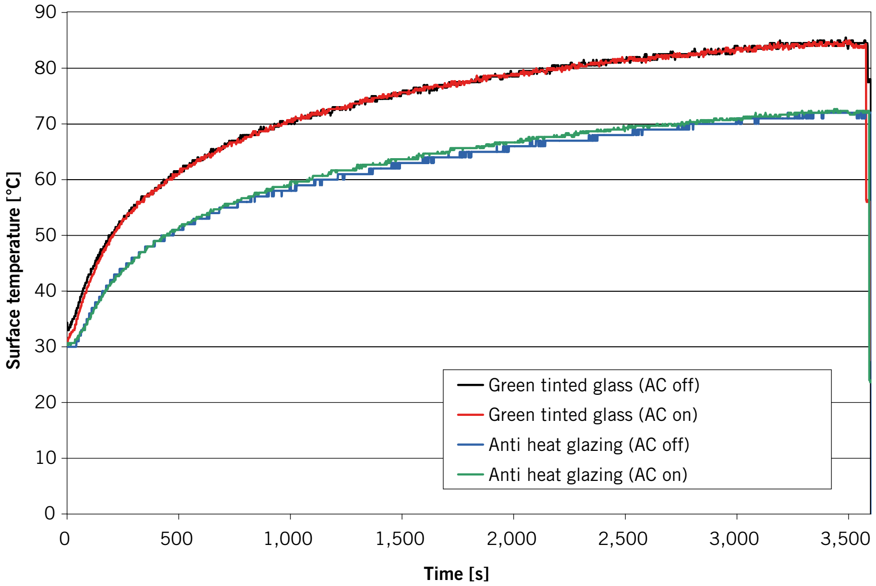


❼ Lower surface temperature in the cabin with solar control glazing

used to generate hot air which is then blown against the windscreen to defog it. In an electric vehicle the situation is different, since the engine remains cold. Tests reveal that for such a vehicle it is far more efficient to remove the fog from the windscreen by heating the glazing itself than by generating hot air in a heater and blowing this against the glazing. Therefore, the heated windscreen helps to save energy, and consequently the driving range of the EV is extended.

## SUMMARY AND CONCLUSION

The results of this study clearly show the benefits of anti-heat glazing in sustainable vehicle development. With anti-heat glazing, the air conditioning system needs to cool less, and hence fuel consumption is reduced. The tests show that, for a car with a SGS CoolCoat windshield and dark tinted glazing, a saving of approximately 30 % can be achieved, which results in a reduction in $CO_2$ emission by 3.8 g $CO_2$/km on the European annual average. It can be concluded that advanced glazing is an efficient means of helping car manufacturers to achieve future goals of reducing the energy consumption of their vehicles.

### REFERENCES


**[1]** Visteon Innovation & Technology GmbH, Kerpen, 2012

**[2]** Ford Werke GmbH, Ford Kuga Broschüre, MY 2012

**[3]** Strupp, N. C.; Lemke, N.: Klimatische Daten und Pkw-Nutzung – Klimadaten und Nutzungsverhalten zu Auslegung, Versuch und Simulation an Kraftfahrzeug-Kälte-/Heizanlagen in Europa, USA, China und Indien. FAT-Schriftenreihe 224, Frankfurt am Main, 2009


❽ De-icing test of a SGS ClimaCoat windshield compared to a standard windshield

# We make connections – worldwide.





4 issues per year
Print version one year subscription:
94,00 EUR (plus postage)

4 issues per year
e-magazine one year subscription:
103,00 EUR

**The trade journal for adhesives and sealing technologies.**
**More information:**

**www.adhaesion.com**

adhesion ADHESIVES & SEALANTS
A SELECTION OF ARTICLES FROM ADHÄSION KLEBEN & DICHTEN + NEW FEATURES

# IMPRINT

ATZ WORLDWIDE

www.ATZonline.com

Founded 1898 as „Der Motorwagen“

Organ of the VDI-Gesellschaft Fahrzeug- und Verkehrstechnik (FVT)
Organ of the Forschungsvereinigung Automobiltechnik e. V. (FAT) and of the Normenausschuss Automobiltechnik (NAAutomobil), formerly known as FAKRA, in the DIN Deutsches Institut für Normung e. V.
Organ of the Wissenschaftliche Gesellschaft für Kraftfahrzeug- und Motorentechnik e. V. (WKM)

09 I 2012 _ September 2012 _ Volume 114
**Springer Vieweg I Springer Fachmedien Wiesbaden GmbH**
P. O. Box 15 46 · 65173 Wiesbaden · Germany I Abraham-Lincoln-Straße 46 · 65189 Wiesbaden · Germany
Amtsgericht Wiesbaden, HRB 9754, USt-IdNr. DE811148419

**Managing Directors** Dr. Ralf Birkelbach (Chairman), Armin Gross, Albrecht Schirmacher I **Director Corporate Publishing, Corporate Content & Ad Sales** Armin Gross
**Director Marketing & Direct Sales** Rolf-Günther Hobbeling I **Director Production** Christian Staral





**EDITORS IN CHARGE**
Dr. Johannes Liebl, Wolfgang Siebenpfeiffer

**EDITOR IN CHIEF**
Dr. Alexander Heintzel
phone +49 611 7878-342 · fax +49 611 7878-462
alexander.heintzel@springer.com

**VICE-EDITOR IN CHIEF**
Dipl.-Ing. Michael Reichenbach
phone +49 611 7878-341 · fax +49 611 7878-462
michael.reichenbach@springer.com

**MANAGING EDITOR**
Kirsten Beckmann M. A.
phone +49 611 7878-343 · fax +49 611 7878-462
kirsten.beckmann@springer.com

**EDITORIAL STAFF**
Dipl.-Ing. (FH) Richard Backhaus
phone +49 611 5045-982 · fax +49 611 5045-983
richard.backhaus@rb-communications.de
Dipl.-Ing. (FH) Andreas Fuchs
phone +49 6146 837-056 · fax +49 6146 837-058
fuchs@fachjournalist-fuchs.de
Dipl.-Ing. Ulrich Knorra
phone +49 611 7878-314 · fax +49 611 7878-462
ulrich.knorra@springer.com
Roland Schedel
phone +49 6128 853-758 · fax +49 6128 853-759
ATZautotechnology@text-com.de
Stefan Schlott
phone +49 8726 967-572
redaktion_schlott@gmx.net
Markus Schöttle
phone +49 611 7878-257 · fax +49 611 7878-462
markus.schoettle@springer.com
Martina Schraad
phone +49 611 7878-276 · fax +49 611 7878-462
martina.schraad@springer.com

**PERMANENT CONTRIBUTORS**
Andreas Burkert, Prof. Dr.-Ing. Stefan Breuer, Harmut Hammer, Prof. Dr.-Ing. Fred Schäfer

**ENGLISH LANGUAGE CONSULTANT**
Paul Willin

**ONLINE I ELECTRONIC MEDIA**
*Portal Manager Automotive*
Christiane Brünglinghaus
phone +49 611 7878-136 · fax +49 611 7878-462
christiane.bruenglinghaus@springer.com
*Editorial Staff*
Katrin Pudenz M. A.
phone +49 6172 301-288 · fax +49 6172 301-299
redaktion@kpz-publishing.com

**SPECIAL PROJECTS**
*Managing Editorial Journalist*
Markus Bereszewski
phone +49 611 7878-122 · fax +49 611 7878-462
markus.bereszewski@springer.com

**ASSISTANCE**
Christiane Imhof
phone +49 611 7878-154 · fax +49 611 7878-462
christiane.imhof@springer.com
Marlena Strugala
phone +49 611 7878-180 · fax +49 611 7878-462
marlena.strugala@springer.com

**ADDRESS**
Abraham-Lincoln-Straße 46 · 65189 Wiesbaden
P. O. Box 1546 · 65173 Wiesbaden, Germany
redaktion@ATZonline.de

**ADVERTISING**

**HEAD OF KEY ACCOUNT MANAGEMENT**
Tanja Pfisterer

**HEAD OF SALES MANAGEMENT**
Britta Dolch

**SALES MANAGEMENT**
Volker Hesedenz
phone +49 611 7878-269 · fax +49 611 7878-78269
volker.hesedenz@best-ad-media.de

**KEY ACCOUNT MANAGEMENT**
Rouwen Bastian
phone +49 611 7878-399 · fax +49 611 7878-78399
rouwen.bastian@best-ad-media.de

**DISPLAY AD MANAGER**
Susanne Bretschneider
phone +49 611 7878-153 · fax +49 611 7878-443
susanne.bretschneider@best-ad-media.de

**AD PRICES**
Advertising ratecard from October 2011

**MARKETING I OFFPRINTS**

**PRODUCT MANAGEMENT AUTOMOTIVE MEDIA**
Sabrina Brokopp
phone +49 611 7878-192 · fax +49 611 7878-407
sabrina.brokopp@springer.com

**OFFPRINTS**
Martin Leopold
phone +49 2642 907-596 · fax +49 2642 907-597
leopold@medien-kontor.de

**PRODUCTION I LAYOUT**
Kerstin Brüderlin
phone +49 611 7878-173 · fax +49 611 7878-78173
kerstin.bruederlin@springer.com

**SUBSCRIPTIONS**
Springer Customer Service Center GmbH
Haberstraße 7 · 69126 Heidelberg, Germany
phone +49 6221 3454-303 · fax +49 6221 3454-229
Monday to Friday, 8 a.m. to 6 p.m.
springervieweg-service@springer.com


**SUBSCRIPTION CONDITIONS**
The eMagazine appears 11 times a year at an annual subscription rate 199 € for private persons and 299 € for companies. Special rate for students on proof of status in the form of current registration certificate 98 €. Special rate for VDI/ÖVK members on proof of status in the form of current member certificate 172 €. Special rate for studying VDI members on proof of status in the form of current registration and member certificate 71 €. Annual subscription rate for combination ATZworldwide (eMagazine) and ATZ (print) 398 €. All prices include VAT at 7%. Every subscription comes with access to the ATZonline archive. However, access is only available for the individual subscription holder. To obtain access for your entire company/library/organisation, please contact Rüdiger Schwenk (ruediger.schwenk@springer.com or phone +49 611 7878-357). The subscription can be cancelled in written form at any time with effect from the next available issue.

**HINTS FOR AUTHORS**
All manuscripts should be sent directly to the editors. By submitting photographs and drawings the sender releases the publishers from claims by third parties. Only works not yet published in Germany or abroad can generally be accepted for publication. The manuscripts must not be offered for publication to other journals simultaneously. In accepting the manuscript the publisher acquires the right to produce royalty-free offprints. The journal and all articles and figures are protected by copyright. Any utilisation beyond the strict limits of the copyright law without permission of the publisher is illegal. This applies particularly to duplications, translations, microfilming and storage and processing in electronic systems.

**YOUR HOTLINE TO ATZ**

Editorial Staff
☎ +49 611 7878-341
Customer Service
☎ +49 6221 3454-303
Advertising
☎ +49 611 7878-269

**PEER REVIEW**

# PEER REVIEW PROCESS FOR RESEARCH ARTICLES IN ATZ, MTZ AND ATZ ELEKTRONIK



Scientific articles of universities in ATZ Automobiltechnische Zeitschrift, MTZ Motortechnische Zeitschrift and ATZelektronik are subject to a proofing method, the so-called peer review process. Articles accepted by the editors are reviewed by experts from research and industry before publication. For the reader, the peer review process further enhances the quality of the magazines‘ content on a national and international level. For authors in the institutes, it provides a scientifically recognised publication platform.

In the Peer Review Process, once the editors has received an article, it is reviewed by two experts from the Advisory Board. If these experts do not reach a unanimous agreement, a member of the Steering Committee acts as an arbitrator. Following the experts’ recommended corrections and subsequent editing by the author, the article is accepted.

In 2008, the peer review process utilised by ATZ and MTZ was presented by the WKM (Wissenschaftliche Gesellschaft für Kraftfahrzeug- und Motorentechnik e. V./ German Professional Association for Automotive and Motor Engineering) to the DFG (Deutsche Forschungsgemeinschaft/German Research Foundation) for official recognition. ATZelektronik participates in the Peer Review since 2011.

AUTHORS

**DIPL.-ING. (FH) KATHARINA HAGEN**
is Research Associate at the Chair of Traffic and Transportation Psychology at TU Dresden (Germany).

**DIPL.-ING. DIPL.-PSYCH. CHRISTOPH SCHULZE**
is Senior Research Associate at the Chair of Traffic and Transportation Psychology at TU Dresden (Germany).

**PROF. DR. BERNHARD SCHLAG**
is Head of the Chair of Traffic and Transportation Psychology at TU Dresden (Germany).

# INTERACTIONS BETWEEN VEHICLES AND PEDESTRIANS

In future, vehicles with alternative powertrains, including those with electric or hybrid electric drive systems, will be a familiar sight on our roads. Compared to vehicles with a petrol or diesel engine, they produce a different type of exterior noise, primarily at low speeds. This raises issues of acoustic perceptibility. As part of a BASt and FAT project, the Chair of Traffic and Transport Psychology at the TU Dresden has therefore examined the effects of a change in acoustic perceptibility on pedestrians.

THE SEAL OF APPROVAL FOR SCIENTIFIC ARTICLES IN ATZ.
ATZ PEER REVIEW
RECEIVED 2012-02-10
REVIEWED 2012-05-31
ACCEPTED 2012-06-05
REVIEWED BY EXPERTS FROM RESEARCH AND INDUSTRY.

## 1 INTRODUCTION

Interactions between vehicles and pedestrians are a determining factor in road traffic safety. Safe interpretations require an adequate mutual information basis. Against the background of alternative propulsion concepts, the change in vehicle information provided by external noise, and pedestrian information needs are considered. The latter can be achieved by immediate or technically conveyed sensory perceptibility. Visual and auditory sensory channels shall be primarily considered (long distance senses).

## 2 NOISE EMISSIONS OF ALTERNATIVE PROPULSION VEHICLES

Tests available in international literature on exterior noises in alternative propulsion vehicles usually compare the noises with those generated by similarly constructed vehicles with internal combustion engines. Measurements or perception statements of test persons acoustically detecting approaching vehicles are used for this purpose. The test results lead to the conclusion that noise emission is mainly influenced by the driving speed, ❶.

At constant speed up to approximately $v=20$ km/h, alternative propulsion vehicles emit lower noise levels than comparable vehicles with internal combustion engine. In this driving situation, test persons will not – or at a very low distance – detect that vehicle by noise. Above this speed, the dominant tyre and wind noise will compensate those of vehicles with conventional engines. However, tests also show that even alternative propulsion vehicles will produce relevant qualitative and vehicle specific acoustic characteristics [6]. Neither general statements concerning noise quantity nor statements based on propulsion technology may comprehensively describe the individual case.

Not many speed modulating driving situations exist and the findings are in general insufficient. Individual results show for moderately accelerating alternative propulsion vehicles in the speed range up to $v=30$ km/h compared to internal combustion engines lower noise emissions. Tests on braking actions in the speed range of $v \leq 20$ km/h show no perceptibility variations compared to conventional vehicles. Test results on high rates of acceleration and acceleration at typical urban driving speeds up to $v=50$ km/h are still not available. In addition, there are no findings reported in literature on vehicles that are about to set off.

## 3 INFORMATION REQUIREMENTS AND SITUATION OF PEDESTRIANS

The relevant information situation comprises information which a pedestrian has access to, irrelevant of a certain sense modality. Modifications of this information situation due to changing ambient noises emitted by vehicles may develop from already perceived noise sources. Therefore, only these sources are considered. However, this does not imply any restrictions on possible measures influencing the information situation.

### 3.1 INFORMATION REQUIREMENTS

Visual and acoustic information of pedestrians on approaching vehicles is dependent on the interaction constellation and is influenced by a multitude of situational and personal as well as physiological and psychological factors. Besides the habitual and situational sensory ability, personal factors also comprise cognitive information processing, motivation as well as mental and physical aspects of performing an action [7].

The evaluation of relevant pedestrian information needs requires interactions with primary reaction request directed to the pedestrian are important. This comprises all situations in which the pedestrian is given no preference to vehicle traffic. Gidas (German In-Depth Accident Study) accident data evaluations show that these situations comprise the most imminent problems in traffic safety. The most frequent accident constellation amongst all vehicle accidents with the participation of a pedestrian is crossing of a single lane double marked road at a distance of intersections. Depending on the sensory restrictions of the participating pedestrians, intersections gain importance in accident scenarios [8].

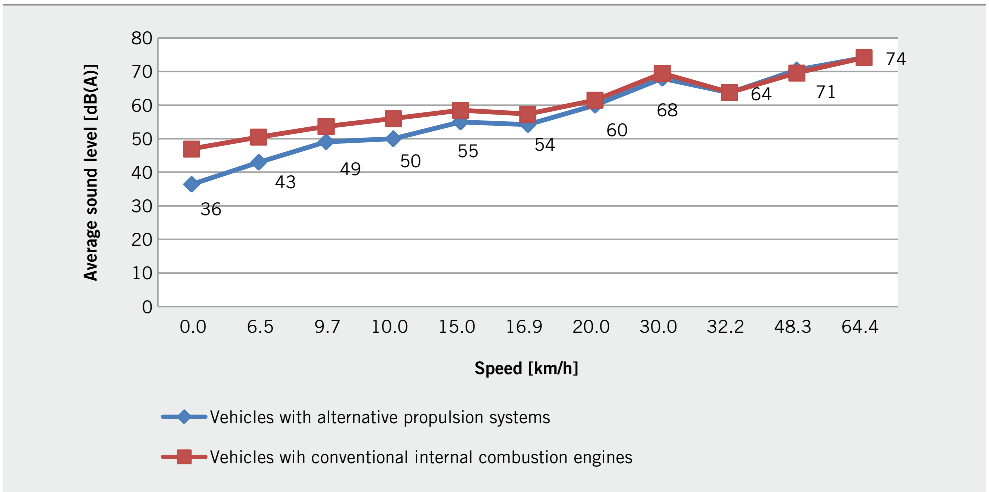


❶ Mean noise level against speed (results of five comparative empirical studies [1, 2, 3, 4, 5])

Hazard cognition is a central aspect of traffic safety. High dynamics of road traffic requires proactive behaviour. Hazard cognition comprises mental anticipation of potentially dangerous situations and adjustment of the attitude to the anticipated sequence [9]. An adequate information basis is required for hazard cognition. However, situations must also be considered in which mutual attention or pedestrian right of way applies. For this case the pedestrian needs information for reassurance and danger avoidance if he is not granted right of way by a vehicle. Focus group interviews with pedestrians show that these situations occur frequently at intersections [8].

Pedestrians receive information on the movement of vehicles beyond the relevant viewing direction primarily acoustic in interactions with typical vehicles. This for instance comprises information on presence, distance, speed and direction of the vehicles. Besides hazard cognition, this information is also important for retrospective evaluation one's behaviour in order to avoid future potentially dangerous situations. Portions of acoustically realised distance estimation [10] are also important. When visually focusing on distant vehicles, close vehicles may be acoustically detected at the same time [11]. Accelerating and ready to set off vehicles with internal combustion engine usually create characteristic noises, but no distinctive visual impressions. These pieces of information are behaviour and safety relevant in many situations. Therefore, they may be considered as information relevant.

### 3.2 INFORMATION SITUATION

According to the described considerations, several situations may result in information variations. Initially, the pedestrian will have to estimate the area of his immediate next steps. This projection is performed at regular intervals in the range of 3 to 5 s (movement space). Therefore the movement relevant space of a pedestrian may be defined as within a radius of 5 m. Considering the acoustic information source of alternative propulsion vehicles, this distance range has to consider information on vehicles with driving speeds of approximately up to $v = 20$ km/h and vehicles ready to set off. Second, the proximate range around the pedestrian must be considered. Vehicles, which will reach the movement space within 5 s, should be able to be considered in the hazard estimation. The relevant driving speeds of $v \leq 20$ km/h considered here results in the proximate range of $d < 30$ m. Information on rapidly accelerating vehicles should be able to be considered in a similar time-related but due to higher movement dynamics ($v \leq 50$ km/h) extended distance range ($d > 30$ m). The recognition of rapidly accelerating vehicles could gain importance because of the high torque of electric powertrains available at start-off [12].

The background noise plays an important role. It can be assumed that pedestrians have acoustic access to the above pertained information for typical internal combustion engines at moderate background noise. It may approximately assumed that the background noise is at a moderate level if individual vehicles are in an audible distance [2, 4, 13].

### 3.3 DISCUSSION OF VISUAL COMPENSATION POTENTIAL

Acoustic perception differences may only rule the information situation if no sensory alternatives exist. The primary sensory channel is vision. This alternative can be largely ruled out for vision impaired pedestrians (visually handicapped and blind persons according to Social Security Code). Visually handicapped and blind persons already use information sources like memory, acoustic and tactile perceptions as well as technical means for navigation to compensate impaired visual perception. Only adapted technical devices have compensation potential. In order to determine compensation of the information situation, also with view to ergonomic design and practicability, empirical studies need to be performed.

For pedestrians without significant visual handicap, visual compensation should be considered. Perception of vehicles includes

| AREA OF MEASURES | MA | MEASURES |
|---|---|---|
| **INFORMATION AND KNOWLEDGE-ORIENTED MEASURES** | 01 | Motorists should be frequently reminded that pedestrians and cyclists are vulnerable road users and that they should pay more attention to them |
| | 02 | Sensitize all pedestrian to particularly quiet vehicles |
| | 03 | Sensitize particularly affected people (visually impaired, blind, children) to particularly quiet vehicles |
| | 04 | Pedestrians should always wear conspicuous clothing in traffic |
| **INFRASTRUCTURE MEASURES** | 05 | Built more pedestrian crossings and pedestrian refuge islands |
| | 06 | Equip more intersections with traffic lights |
| | 07 | Additional elements should be applied to the roadway at intersections without traffic lights in order to facilitate the hearing of an approaching vehicle |
| | 08 | The pedestrians should give a signal indicating their presence to the infrastructure (such as traffic lights) |
| **ONBOARD (ACOUSTIC) MEASURES** | 09 | Particularly quiet vehicles should always emit a well audible perception signal in urban areas |
| | 10 | Particularly quite vehicle should emit a well audible perception signal only while reversing |
| | 11 | Particularly quiet vehicles should emit a specificnoise level only for dogs (guide dogs) |
| **MEASURES OF VEHICLE-PEDESTRIAN COMMUNICATION** | 12 | Particularly quiet vehicles should give the pedestrian a signal of their presence (such as via radio an acoustic or vibration signal to a device worn by pedestrian) |
| | 13 | Pedestrians should give particularly quiet vehicle, a signal of their presence (such as wireless) |
| **ONBOARD (AUTOMATIC) MEASURES** | 14 | Particularly quiet vehicles should automatically detect pedestrians and warn the driver |
| | 15 | Particularly quiet vehicles should automatically detect pedestrians, warn the driver and brake automatically if necessary |

❷ Analysed measures [8]


❸ Means of the measure evaluation by pedestrians without sensory impairment and with visual impairment (five-point scale from 1 (not helpful at all) to 5 (very helpful) for pedestrian interaction with particularly quiet vehicles)



constellations like movement of vehicles located on the side or behind the pedestrian. A modified gaze behaviour may offer a compensation in a predictable sequence, however, unexpected vehicles cannot be detected this way. A second drawback is the motion of the pedestrian. A visual search directed in several directions is easier to perform when the person is standing still. Thus, visual tracking of peripheral vehicle movements while walking respectively crossing is impeded.

A differentiation between vehicles at standstill and ready to set off positions by means of visual perception may possibly be effected by means of eye contact with the driver. This is conditional upon mutual recognition. This applies to some but not all situations. Vehicles in rapid acceleration may be recognised merely visually only by means of permanent gaze direction. Since for pedestrians at least when crossing the requirement of observing several directions exists, gaze diversions occur at regular intervals and rapidly accelerating vehicles cannot be perceived as such by vision only.

It can be concluded that the mere adaption of the gaze behaviour may not provide an information situation to the pedestrian, which is equivalent to seeing and hearing of regular conventional vehicles. Furthermore, it can be assumed that the portion of pedestrians with lower compensation potential due to physical and sensory handicaps will increase in the course of demographic transition [7].

## 4 SUBJECTIVE ASSESSMENT OF EXEMPLARY MEASURES

The success of many possible measures for influencing the described pedestrian information situation is also dependent on acceptance by pedestrians and drivers. In order to provide statements, a total of 15 exemplary measures have been evaluated, ❷. A central dimension for evaluating the acceptance in the context of traffic influencing measures is the efficiency evaluation by traffic participants [14, 15]. Amongst pedestrians the visually handicapped are of special importance, while amongst the drivers, the alternative propulsion vehicle drivers are of special interest.

In the period from November 2010 until May 2011, a total of 603 pedestrians participated in an online survey [8]. The survey included persons without and with visual and hearing impairment. Visually impaired persons assess – more than pedestrians

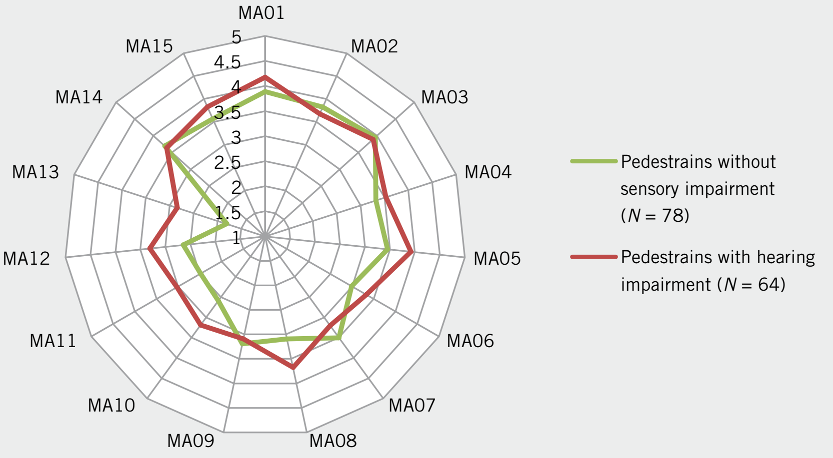


❹ Means of the measure evaluation by pedestrians without sensory impairment and with hearing impairment (five-point scale from 1 (not helpful at all) to 5 (very helpful) for the interaction of pedestrians with particularly quiet vehicles)

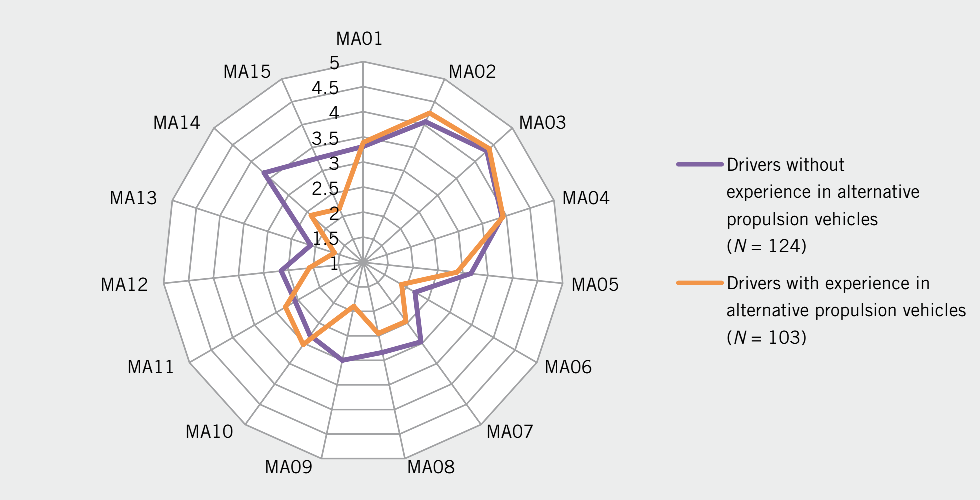


❺ Means of the measure evaluation by drivers with and without driving experience in alternative propulsion vehicles (five-point scale from 1 (not helpful at all) to 5 (very helpful) for pedestrian interaction with particularly quiet vehicles)

without sensory impairment – various infrastructural measures, automatic devices in the vehicle as well as perceptibility signal as helpful, ❸.

Persons without impairments as well as hearing impaired persons evaluate besides infrastructural measures and perceptibility signal also information oriented measures as helpful. Hearing impaired persons additionally evaluate measures for compensation of their perceptibility deficit by means of technical communication between vehicle and pedestrian as positive, ❹. By means of vehicle based automatic pedestrian recognition with warning respectively emergency braking the interviewed pedestrians hope for a technical emergency backup, which is not available in today's interactions with vehicles.

A total of 227 active drivers participated in a further online survey in the same period, 45 % of which had alternative propulsion vehicle driving experience. Of the surveyed drivers, all presented measures were rated as less helpful, except for the informing measures, ❺.

Drivers with alternative propulsion vehicle driving experience assess infrastructural and vehicle based measures as less helpful compared to drivers without alternative propulsion vehicle experience and pedestrians. The most significant assessment differences can be found between "vision impaired pedestrians" and "drivers with alternative propulsion vehicle driving experience", ❻. Both groups show a contrasting response behaviour with significant assessment differences in most measure areas.

The assessed measures differentiate in their efficiency potential concerning the pedestrian information situation. Infrastructural measures (such as elements in the road creating a noise at tyre contact) and vehicle-pedestrian communication (such as vehicle transmits information to a device worn by pedestrian) may influence the pedestrian information situation. A vehicle based perception signal may also serve this purpose, for instance as in "noise on demand". Information oriented measures and vehicle based automatic pedestrian recognition influence traffic safety, however, not the direct pedestrian information situation. Assessments of vision impaired pedestrians seem to have a closer relation to objectively assessable efficiency than the assessments of drivers familiar with alternative drive train technology.

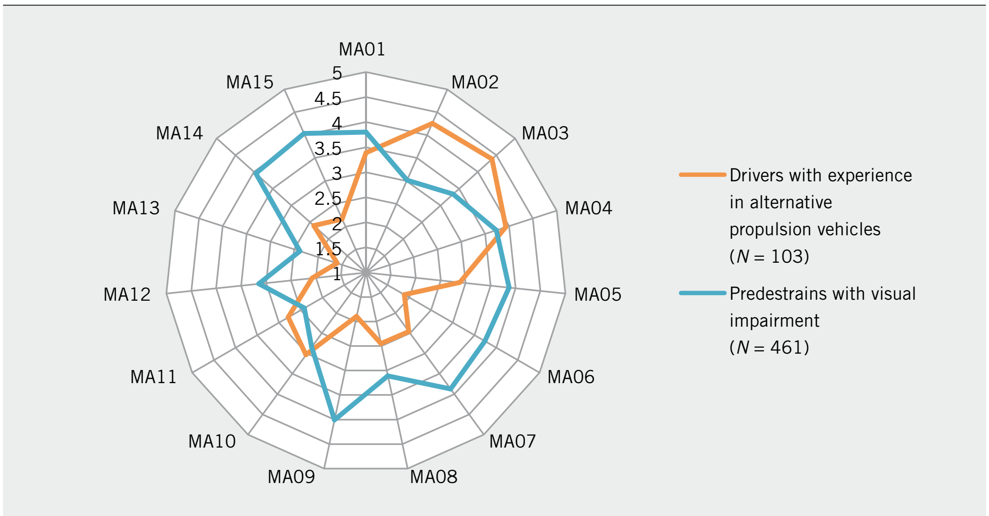


❻ Means of the measure evaluation by drivers with alternative propulsion vehicle experience and vision impaired pedestrians (five-point scale from 1 (not helpful at all) to 5 (very helpful) for pedestrian interaction with particularly quiet vehicles)

## 5 SUMMARY AND OUTLOOK

Vehicles with alternative propulsion systems may emit different exterior noises than vehicles with internal combustion engines. This article discusses scenarios between vehicles and pedestrians, which may lead to deficits in the pedestrians' information situation. So far findings of the acoustic perceptibility for a number of potentially affected driving conditions are still missing, such as during high rates of acceleration or for standing vehicles that are about to set off. In addition to the literature-based considerations 603 pedestrians and 227 drivers evaluated various measures that could potentially influence this problematic. The results clearly show group-specific preferences, for example regarding onboard measures. Some measures, however, were rated equally helpful, such as additional elements applied to the roadway at intersections, which induce noise at tyre contact. Until now, consolidated findings are still lacking in their perceptual effects.

### REFERENCES

**[1]** Garay-Vega, L.; et al.: Quieter Cars and the Safety of the Blind Pedestrian: Phase I. NHTSA, DOT HS 811 304. Washington DC, USA, 2010
**[2]** Goodes, P.; Bai, Y. B.; Meyer, E.: Investigation into the Detection of Quiet Vehicle by the Blind Community and the Application of an External Noise Emitting System. In: SAE Technical Paper (2009), 2009-01-2189
**[3]** N. N.: Jasic – A Study on Approach Warning System for Hybrid Vehicle in Motor Mode. 49th World Forum for Harmonization of Vehicle Regulation (WP.29), Working Party on Noise (GRB), Feb. 16 – 18, 2009, Informal Document No. GRB-49-10, 2009
**[4]** Rosenblum, L.: Sound Measurement and Mobility. Transcript of the Quiet Cars Public Meeting on June 23, 2008, Docket-ID: NHTSA-2008-0108-0023, pp. 53 – 65
**[5]** Wiener, W.; et al.: The Impact of Hybrid Vehicle on Street Crossing. In: RE:view: Rehabilitation Education for Blindness and Visual Impairement (2006), 38 (2), pp. 65 – 78
**[6]** Wall Emerson, R,; et al.: A Pilot Study of Pedestrian with Visual Impairment Detecting Traffic Gaps and Surges Containing Hybrid Vehicles. In: Transportation Research (2011), Part F. 14, pp. 117 – 127
**[7]** Schlag, B. (Hrsg.): Leistungsfähigkeit und Mobilität im Alter. Köln: Eugen-Otto-Butz-Stifung, 2008
**[8]** Hagen, K.; Schulze, C.; Schlag, B.: Verkehrssicherheit von äußeren Verkehrsteilnehmern im Zusammenhang mit dem geringen Geräuschniveau von alternativen Antrieben. Schlussbericht, TU Dresden, 2011
**[9]** Schlag, B.; et al.: Mehr Licht – mehr Sicht – mehr Sicherheit. Wiesbaden: VS Verlag für Sozialwissenschaften, 2009
**[10]** Schiff, W.; Oldak, R.: Accuracy of Judging Time to Arrival: Effects of Modality, Trajectory, and Gender. In: Journal of Experimental Psychology: Human Perception and Performance (1990), 16(2), pp. 303 – 316
**[11]** Grosse, K.: Audio-Visual Perception in Interactive Virtual Environments. TU Wien, Institut für Computergraphik und Algorithmen, 2009
**[12]** N. N.: Potenziale von Elektro-Mobilität. Wien: VCÖ-Schriftreihe Mobilität mit Zukunft, 2009
**[13]** Kerber, S.: Wahrnehmbarkeit von Fahrzeugaußengeräuschen in Hintergrundgeräuschen: Psychoakustische Beurteilung und modellbasierte Prognosen. München: Dr.-Hut-Verlag, 2008
**[14]** Schade, J.; Schlag, B.: Acceptability of Transport Pricing Strategies. Oxford: Elsevier, 2003
**[15]** Schade, J.: Akzeptanz von Straßenbenutzungsgebühren: Entwicklung und Überprüfung eines Modells. Lengerich: Pabst Science Publishers, 2005

## THANKS

This research has been funded by the cooperation of the Bundesanstalt für Straßenwesen (BASt) and the Forschungsvereinigung Automobiltechnik e. V. (FAT) under the title „Verkehrssicherheit von äußeren Verkehrsteilnehmern im Zusammenhang mit dem geringen Geräuschniveau von alternativen Antrieben" [8]. This report includes parts of a research work on behalf of the Federal Ministry of Transport, Building and Housing, represented by the BASt, under the title „Verkehrssicherheit für schwächere Verkehrsteilnehmer im Zusammenhang mit dem geringen Geräuschniveau von Fahrzeugen mit alternativen Antrieben (Nichtgeräusch)" (FE-No. 82.0379/2010). Finally, the authors would like to thank the various associations for visual and hearing-impaired people and the participants who took part in the study. Without all the great support and participation, the study would have been impossible. Furthermore, we are pleased to record thanks the working group members for their constrictive discussions during the whole project.

# INTERACTION BETWEEN CHASSIS DAMPER AND ELASTOMER-MOUNT

Chassis dampers from ZF Friedrichshafen are designed in a way that the damping provides the required input to the driving impression. For conventional passenger cars, the damper is linked to the car body by an elastomer-mount. The investigation of the interaction between these two parts, which was developed as external dissertation at the Technical University of Darmstadt, delivers scientific findings of the vibration behaviour of this subsystem.

THE SEAL OF APPROVAL FOR SCIENTIFIC ARTICLES IN ATZ.
ATZ
PEER REVIEW
RECEIVED 2012-01-27
REVIEWED 2012-05-16
ACCEPTED 2012-06-05
REVIEWED BY EXPERTS FROM RESEARCH AND INDUSTRY.

AUTHORS

**DIPL.-ING. ANJA STRETZ**
is a Staff Member in the Chassis Development at ZF Friedrichshafen AG in Schweinfurt (Germany).

**PROF. DR. RER. NAT. HERMANN WINNER**
is Head of the Department of Automotive Engineering at the Technical University of Darmstadt (Germany).

## 1 INTRODUCTION

The subjective driving impression of a car passenger is largely influenced by disturbances such as the generation of noise in the passenger compartment, vibrations, impacts and movements of the car body. The more the passengers experience these vibrations, the worse the driving comfort is evaluated. Dampers are used in the chassis to reduce the vibrations of the car body and the wheels within their natural frequencies. For conventional passenger cars, the damper is linked to the car body by an elastomer-mount. The elasticity of these mounts delivers the isolation of vibrations and with it the driving comfort. The damper and the upper elastomer-mount (which is referred to as top-mount within this work) are connected over the piston rod of the damper. Within this frequency response system the damper as well as the top-mount shows elastic and damping properties. The translational degree of freedom of the piston rod allows this mass to vibrate between damper and top-mount. With the combination of these parts together, new vibration characteristics of the suspension appear. The interaction between the damper and the top-mount complicates the achievement of the desired characteristics of damping and compliance for the whole vehicle, when developing these parts separately.

## 2 SUBSYSTEM DAMPER AND TOP-MOUNT

The registration and evaluation of driving comfort is based on mechanical vibrations, which are transferred to the passengers as structure borne noise, and acoustic vibrations, in terms of noise in the vehicle interior. The requirement for the vibration behaviour of the chassis is: No noise and no vibration in the vehicle interior [1]. Concerning this matter the damper module, which is reduced here to the subsystem of damper and top-mount, ❶, is analysed within this work. To investigate the interaction between damper and top-mount two key aspects were derived [2]. It is differed between the damper as transfer element of road induced vibrations and the damper module as source of vibrations.

The transfer of vibrations through the damper module is defined by the transfer properties of damper and topmount. The properties of damper and topmount change with increasing frequency. Elastomer-mounts are characterised by their dynamic stiffness. Up to now the dynamic stiffness is also used to differ the dynamic properties of the damper and accordingly of the damper module from the static properties [3, 4, 5, 6, 7, 8, 9, 10]. The frequency-related ratio of the complex damping force to the input-side complex vibration amplitude during simple harmonic vibrations is termed dynamic stiffness [4].

Additionally to the frequencies of the excitation, there can be frequencies measured at the piston rod which are not present in the excitation. Consequently, the damper module must be seen as a source of vibrations. These vibrations reach the car passengers as structure borne noise. A certain noise which appears is called chuckle noise [11]. At the same time high accelerations are measured at the strut rod top, the noise in the passenger compartment generates customer complaints [12]. Up to now the reason of the vibrations which can be measured at the piston rod of the damper and which differ significantly from the excitation are searched inside the damper. The following causes for this noise are mentioned in state-of-the-art literature:
: non-linear damping characteristic [11, 12]
: opening and closing mechanism of the valves [11, 13, 14, 15]
: friction [13, 15, 16].
It is concluded, that the piston rod transmits the vibrations that are going to excite the vehicle carbody [13].

## 3 DAMPER AS TRANSFER ELEMENT OF VIBRATIONS

As the damper has damping and elastic properties, the physical schematic is a Maxwell model meaning a series connection of the inner damper elasticity $c_D$ and the damping $d_D$, ❷. To detect the elastic properties of the damper, the spring power is established. That number is the surface integral of the damping force over the excitation velocity for one cycle with the period $T$. Assuming linear characteristics of the Maxwell model and harmonic excitation in Eq. 1, the spring power can be calculated analytically with Eq. 2. Explanation of used formula symbols see ❸.

EQ. 1

$$x_0(t) = \hat{x}_0 \sin(\omega t)$$


❶ Damper module consisting of damper and top-mount [17]

| | |
|---|---|
| **EQ. 2** | $P_{\mathrm{F}} = \int_0^{\mathrm{T}} F \mathrm{d}v = \frac{1}{2} T \hat{x}_0{}^2 \omega^2 c_{\mathrm{dyn,D}} \cos\varphi$ |

Additionally the well-known number of the damping work is used, which is the surface integral of the damping force over the excitation for one cycle:

| | |
|---|---|
| **EQ. 3** | $W_{\mathrm{D}} = \int_0^{\mathrm{T}} F \mathrm{d}x = \frac{1}{2} T \hat{x}_0{}^2 \omega c_{\mathrm{dyn,D}} \sin\varphi$ |

To calculate the integrals the phase angle $\varphi$ and the dynamic stiffness $c_{\mathrm{dyn,\,D}}$ of the Maxwell model are necessary:

| | |
|---|---|
| **EQ. 4** | $\tan\varphi(\omega) = \frac{c_{\mathrm{D}}}{\omega d_{\mathrm{D}}}$ |

| | |
|---|---|
| **EQ. 5** | $c_{\mathrm{dyn,\,D}}(\omega) = \frac{\omega d_{\mathrm{D}} c_{\mathrm{D}}}{\sqrt{c_{\mathrm{D}}^2 + \omega^2 d_{\mathrm{D}}^2}}$ |

The quotient of the spring power and the damping work according to Eq. 6 leads to the ratio of damping constant and spring stiffness weighted with $\omega^2$:

| | |
|---|---|
| **EQ. 6** | $\frac{P_{\mathrm{F}}}{W_{\mathrm{D}}} = \frac{\omega^2 d_{\mathrm{D}}}{c_{\mathrm{D}}}$ |

However the damping element and the spring stiffness cannot be described as constant linear elements. With the quotient of the surface integrals (left side of Eq. 6) and the division by $\omega^2$ the mentioned ratio can now be used for any characteristics. Eq. 7 gives an effective ratio of damping constant and spring stiffness. This ratio is established as effective damper-stiffness ratio. It is a reference for different dampers to quantify the spring properties relatively to the damping. Resulting from Eq. 7, high spring stiffness or low spring power leads to a small value of the effective damper-stiffness ratio:

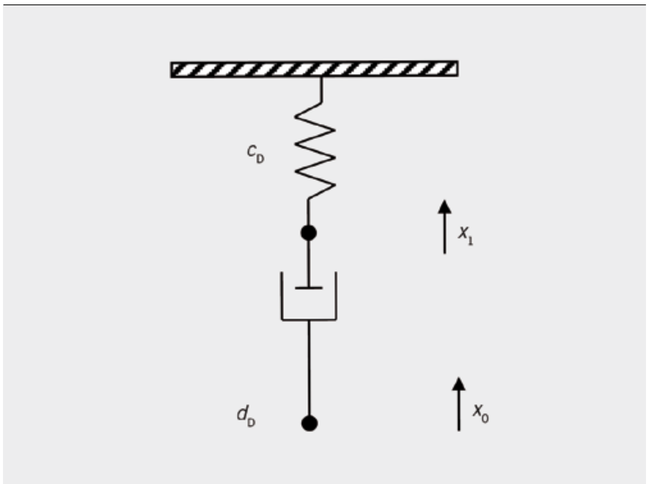


❷ Physical schematic of a damper

| | |
|---|---|
| **EQ. 7** | $\tau_{\mathrm{D,\,eff}}(\omega) = \frac{P_{\mathrm{F}}}{W_{\mathrm{D}} \omega^2} = \left(\frac{d_{\mathrm{D}}}{c_{\mathrm{D}}}\right)_{\mathrm{eff}}$ |

The reciprocal of $\tau_{\mathrm{D,\,eff}}(\omega)$ equates to the cut-off frequency of the Maxwell model. For an ideal Maxwell model with linear characteristics $\tau_{\mathrm{D,\,eff}}(\omega)$ is independent of $\omega$, so that a measure of the deviation from this ideal model is the dependency of $\omega$.

A simulation model of a quarter car, ❹, is used to show the effect of the damper-stiffness ratio. Two dampers with the same damping work but different spring powers are applied to the model ($P_{\mathrm{F,\,damper1}} > P_{\mathrm{F,\,damper2}}$).

The differences of the vehicle vibration behaviour due to the properties of the dampers are evaluated with the vehicle body acceleration. The frequency spectra of this signal are compared for the model with a sinusoidal sweep excitation with increasing frequency and constant velocity amplitude. ❺ shows that damper 1 leads to higher amplitudes within the wheel resonance and to lower amplitudes outside this resonance. Achieving the same damping work, the spring power reduces the damping with the same consequence like a lowering of the damping characteristic of ideal damping elements.

## 4 DAMPER MODULE AS SOURCE OF VIBRATIONS

To analyse the emergence mechanism of module-induced vibrations, the components are simulated each without hysteresis. In

| FORMULA SYMBOLS | UNIT | EXPLANATION |
|---|---|---|
| $c_{\mathrm{D}}$ | N/m | Explanation |
| $c_{\mathrm{dyn,\,D}}$ | N/m | Spring stiffness of the damper |
| $c_{\mathrm{TM}}$ | N/m | Dynamic stiffness of the damper |
| $d_{\mathrm{D}}$ | Ns/m | Spring stiffness of the top-mount |
| $d_{\mathrm{rel}}$ | – | Damping constant of the damper |
| $d_{\mathrm{eff,\,D}}$ | Ns/m | Relative damping |
| $d_{\mathrm{eff,\,module}}$ | Ns/m | Effective damping of the damper |
| $d_{\mathrm{eff,\,total}}$ | Ns/m | Effective damping of the module (without hysteresis of the single components) |
| $F$ | N | Effective damping of the module (with top-mount spring stiffness and inner elasticity of the damper) |
| $m_{\mathrm{Kst}}$ | kg | Force |
| $P_{\mathrm{F}}$ | Nm/s | Piston rod mass |
| $T$ | s | Spring power |
| $v$ | m/s | Speed |
| $W_{\mathrm{D}}$ | Nm | Damping work |
| $x$ | m | Displacement |
| $\varphi$ | ° | Phase angle |
| $\omega$ | $s^{-1}$ | Frequency of the excitation |
| $\omega_{\mathrm{0Kst}}$ | $s^{-1}$ | Natural frequency of the piston rod mass |
| $\tau_{\mathrm{D,\,eff}}$ | s | Effective damper-stiffness ratio |
| $\tau_{\mathrm{module}}$ | s | Module-stiffness ratio |
| $\tau_{\mathrm{total}}$ | s | Stiffness ratio of the module (with top-mount spring stiffness and inner elasticity of the damper) |
| $\eta$ | – | Frequency ratio |

❸ Used formula symbols and their meaning

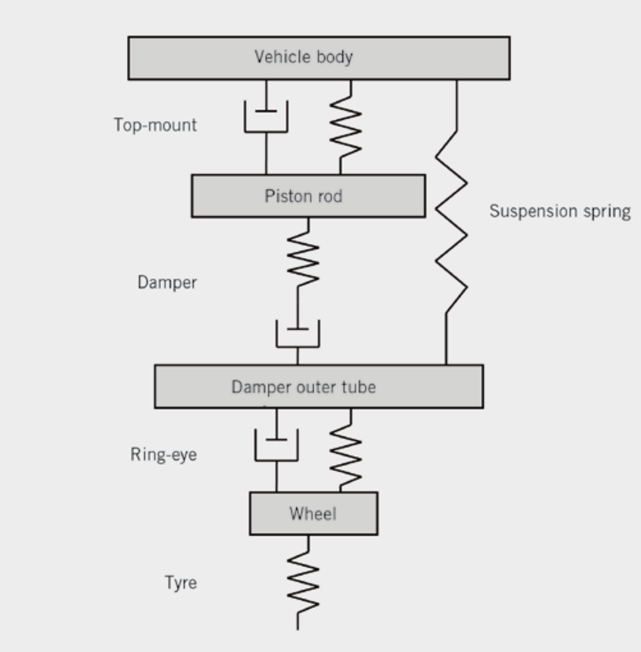


❹ Simulation of a quarter car

this case the topmount is simplified as spring with stiffness $c_{TM}$ and the damper as pure damping element with the damping constant $d_D$, ❻. The equation of motion for the piston rod mass $m_{Rod}$ in this configuration of frequency response system can be solved analytically for linear characteristics and harmonic excitations:

**EQ. 8**
$$m_{Kst}\ddot{x}_{Kst} + d_D\dot{x}_{Kst} + c_{TM}x_{Kst} = d_D\dot{x}_0$$

The module-stiffness ratio is established as quotient of damping constant and top-mount stiffness:

**EQ. 9**
$$\tau_{module} = \frac{d_D}{c_{TM}}$$

The result of the equation of motion can be converted to Eq. 13, when using the equations for the natural frequency of the piston rod (Eq. 10), the frequency ratio of excitation frequency and natural frequency (Eq. 11) and the phase angle between the excitation and the force (Eq. 12):

**EQ. 10**
$$\omega_{0Kst}^2 = \frac{c_{TM}}{m_{Kst}}$$

**EQ. 11**
$$\eta = \frac{\omega}{\omega_{0Kst}}$$

**EQ. 12**
$$\tan\varphi = \frac{\omega\tau_{module}}{1-\eta^2}$$

**EQ. 13**
$$x_{Kst} = \hat{x}_0 \frac{\omega\tau_{module}}{\sqrt{(1-\eta^2)^2 + (\omega\tau_{module})^2}} \cos(\omega t - \varphi)$$

A change of the damping constant or the differential damping during one excitation cycle, as it is the case for common nonlinear damping characteristics, causes a change of the module-stiffness ratio $\tau_{module}$ in time. This change leads to a difference in the result of the equation of motion, by what the piston rod is initiated to vibrate. For that reasons it is suggested in [18, 19] to adapt the

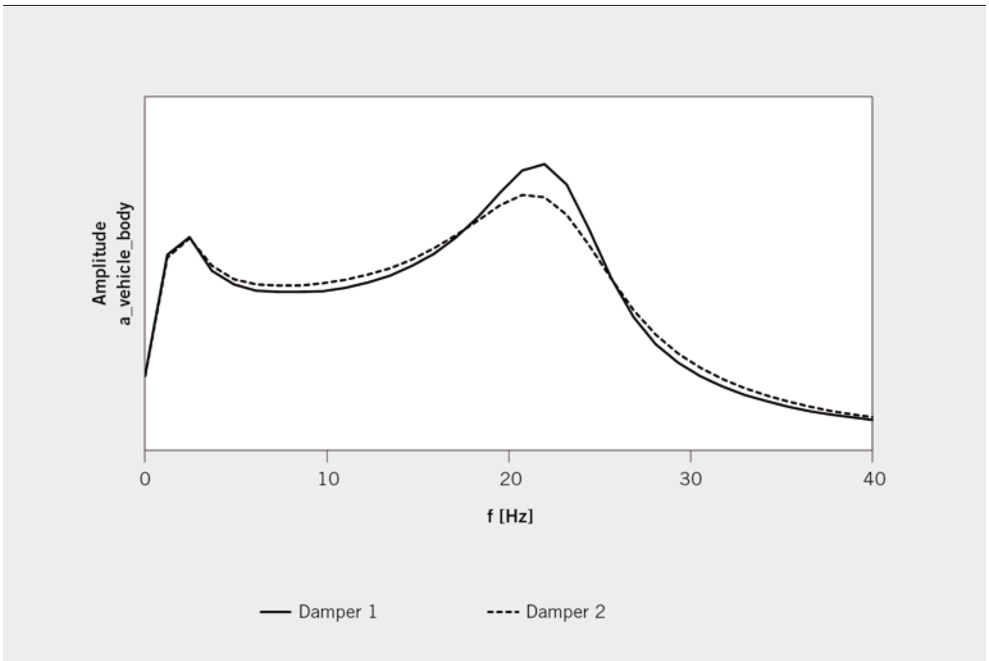


❺ Frequency spectra of the vehicle body acceleration for damper 1 and damper 2 top-mount characteristic to the damping characteristic in a way that there occurs no change of the stiffness ratio.

The above mentioned model of the damper module is simulated with a linear top-mount characteristic and a common non-linear damper characteristic, ❼, in which both parts have no hysteresis. ❽ shows the time response of the following quantities of this model: damper force, second derivative of the damper force with respect to time and acceleration of the piston rod. It can be seen, that the vibration of the piston rod starts when the value of the derivative is high. That derivative can be formulated in Eq. 16 with the equation for the excitation (Eq. 14) and the differential damping (Eq. 15):

**EQ. 14**

$$\mathrm{d}v = a \cdot \mathrm{d}t$$

**EQ. 15**

$$d_D = \frac{\mathrm{d}F}{\mathrm{d}v}$$

**EQ. 16**

$$\frac{\mathrm{d}^2F}{\mathrm{d}t^2} = a^2\,\frac{\mathrm{d}^2F}{\mathrm{d}v^2}$$

The value of the second derivative of force with respect to time gets higher with increasing curvature of the damper characteristic of force over velocity and with increasing acceleration in that curvature.

## 5 EFFECTIVE DAMPING

If a frequency response system consists of at least one damping element and one spring element, the resulting force is partly 0° and partly 90° shifted in phase regarding the excitation. The dynamic stiffness, which is calculated from the quotient of force amplitude to excitation amplitude for elastomer-mounts and dampers, can be separated in real and imaginary part using the phase angle. That algorithm is valid for linear characteristics and harmonic excitations. As real characteristics of dampers and top-mounts are nearly constant area by area, the analytical calculation has to be used for certain characteristic areas. The relative damping according to Eq. 17 is established as quotient of imaginary part of the dynamic stiffness and magnitude of the dynamic stiffness:

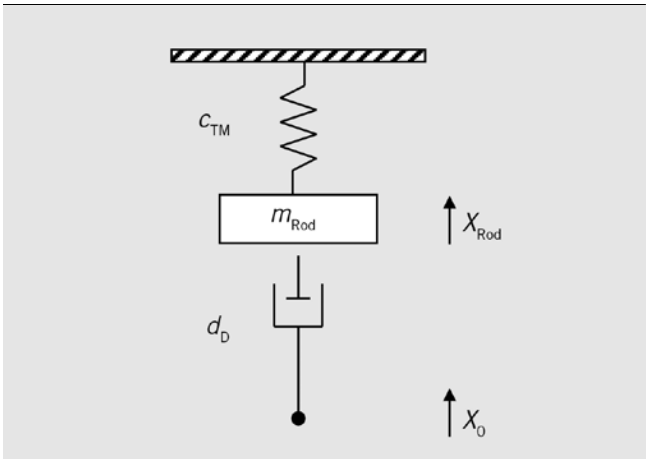


❻ Damper module without hysteresis of the single components

**EQ. 17**

$$d_\mathrm{rel} = \frac{\mathrm{Im}(c_\mathrm{dyn})}{|c_\mathrm{dyn}|}$$

The effective damping is the product of damping constant and relative damping. The effective damping of the damper, which can be simplified as Maxwell model, results from Eq. 18. The spring property can only be neglected for frequencies considerably lower than the cut-off frequency $\tau_{\mathrm{D,\,eff}}^{-1} = c_\mathrm{D}/d_\mathrm{D}$. According to that the damping of a damper with small cut-off frequency decreases with increasing frequency:

**EQ. 18**

$$d_\mathrm{eff,\,D} = d_\mathrm{D} \cdot d_\mathrm{rel,\,D} = d_\mathrm{D} \cdot \frac{c_\mathrm{D}}{\sqrt{c_\mathrm{D}^2 + (\omega d_\mathrm{D})^2}} = d_\mathrm{D} \cdot \frac{1}{\sqrt{1 + (\omega\tau_\mathrm{D})^2}}$$

The effective damping can be calculated for the damper module, ⑥, with Eq. 19. Therefore the mass of the piston rod has been neglected, as it is in usual configurations just effective above 100 Hz and that is why $\eta \ll 1$ is assumed according to Eq. 11:

**EQ. 19**

$$d_\mathrm{eff,\,module} = d_\mathrm{D} \cdot d_\mathrm{rel,\,module} = d_\mathrm{D} \cdot \frac{c_\mathrm{TM}}{\sqrt{c_\mathrm{TM}^2 + (\omega d_\mathrm{D})^2}} = d_\mathrm{D} \cdot \frac{1}{\sqrt{1 + (\omega\tau_\mathrm{module})^2}}$$

The comparison of Eq. 18 and Eq. 19 shows, that the top-mount spring operates like the inner spring of the damper. For this reason the effective damping of the damper module including a top-mount spring and a damper with inner elasticity can be calculated with the sum $\tau_\mathrm{total} = \tau_\mathrm{D} + \tau_\mathrm{module} = \mathrm{d}D/c_\mathrm{D} + d_\mathrm{D}/c_\mathrm{TM}$ as per Eq. 20:

**EQ. 20**

$$d_\mathrm{eff,\,total} = d_\mathrm{D} \cdot d_\mathrm{rel,\,total} = d_\mathrm{D} \cdot \frac{1}{\sqrt{1 + (\omega\tau_\mathrm{total})^2}}$$

## 6 SUMMARY

The driving comfort of a vehicle gets a positive evaluation, as long as there are no disturbing vibrations reaching the driver. Within this research work only the damper module consisting of the damper and the top-mount was investigated. For this reason two key aspects were analysed. One was the transfer of road induced vibrations through the damper module, and the other one was the emergence mechanism of vibrations in the damper module.

Additionally to the damping work the spring power is used to characterise the spring properties of the damper. Moreover the effective damper-stiffness ratio was established to be able to compare the dynamic properties of different dampers. The advantage of the established integral numbers is the usability for parts with nonlinear characteristics.

The change of the module-stiffness ratio, which was introduced as ratio between damping constant and top-mount elasticity, could be identified as reason for the module induced vibrations. This change leads to high values of the second derivative of force with respect to time whereby the piston rod itself is stimulated to vibrate.

For both, damper and damper module the relative damping as quotient of imaginary part and magnitude of the dynamic stiffness is used to quantify the ratio of the damping to the magnitude of the dynamic stiffness. The effective damping of the suspension

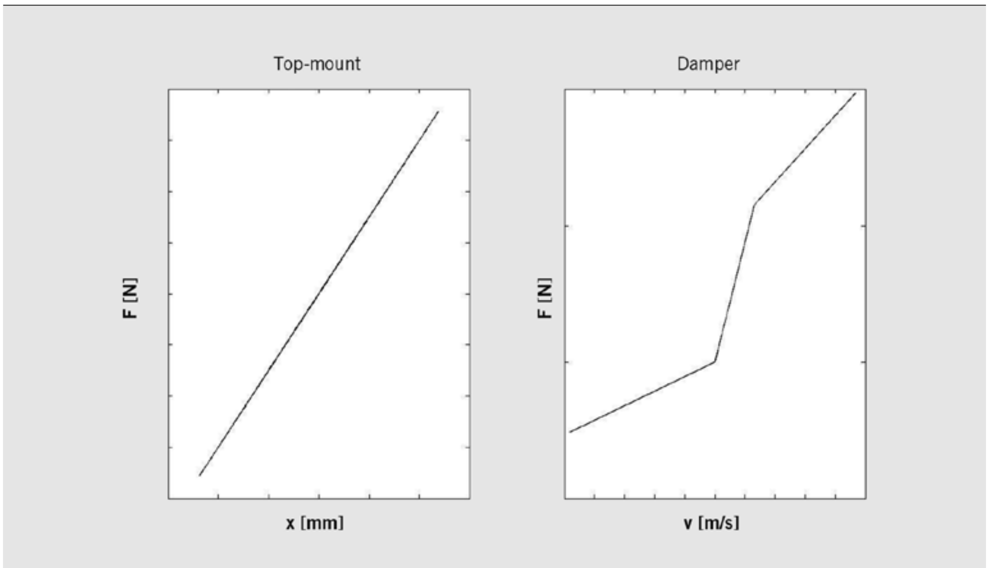


❼ Characteristics for the simplified damper module



results from the product of this number with the damping constant of the damper.

In the future the characteristics of damper and top-mount can be better tuned on each other based on these findings to reduce module induced vibrations and to find the optimum compromise between the effectiveness of damping and the isolation of vibrations.

**REFERENCES**

**[1]** Kudritzki, D.: Integrierte Analyse des Fahrkomforts durch Betrachtung des Systems Fahrwerk in Versuch und Simulation. VDI-Berichte No. 1335, 1997, pp. 407 – 428
**[2]** Stretz, A.; Sonnenburg, R.; Winner, H.: Komfortrelevante Untersuchung des dynamischen Schwingungsverhaltens von Dämpfermodulen in Kraftfahrzeugen. In: Subjektive Fahreindrücke sichtbar machen IV, 2010, pp. 76 – 94, ISBN 978-3-8169-2936-9
**[3]** Ammon, D.: Was macht der Stoßdämpfer mit dem Abrollkomfort?, VDI Berichte No. 1350, 1997, pp. 123 – 133
**[4]** Eickhoff, M.; et al.: Dynamische Eigenschaften eines Stoßdämpfermoduls. In: ATZ 111 (2009), No. 5, pp. 359 – 366
**[5]** Füllbier, K.-P.: Systemansatz zur Untersuchung und Beurteilung des Abrollkomforts von Kraftfahrzeugen bei der Überfahrt von Einzelhindernissen. Aachen, Technische Hochschule, Dissertation, 2001
**[6]** Kolm, H.; Kudritzki, D.; Wachinger, M.: Optimierung des Fahrkomforts durch Betrachtung der Dämpfungseigenschaften der Radaufhängung. VDI Berichte No. 1494, 1997, pp. 101 – 121
**[7]** Lasai, S.; et al.: Schwingungsanalyse von Subsystemen mit Hilfe der Simulation. In: ATZ 102 (2000), No. 4, pp. 266 – 272
**[8]** Seemann, M.: Identifikation und Optimierung des Fahrzeugschwingungskomforts unter Berücksichtigung nichtlinearer Fahrwerkseigenschaften. Aachen, Technische Hochschule, Dissertation, 2001
**[9]** Shaw, M. A.; Darling, J.: Development of hydro-elastic strut mountings for vehicle secondary ride enhancement: from concept to prototype evaluation. IMechE, 1998, No. C521/008, pp. 129 – 138
**[10]** Troulis, M.: Übertragungsverhalten von Radaufhängungen für Personenwagen im komfortrelevanten Frequenzbereich. Karlsruhe, Technische Hochschule, Dissertation, 2002
**[11]** Haver, J. Van: Practical Techniques for Evaluation of Structure-borne and Air-borne noise of shock absorbers. Proceedings ISMA19 – Tools for Noise and Vibration Analysis, 12 – 14 September 1994, pp. 65 – 77
**[12]** Amman, S.; Greenberg, J.: Subjective evaluation and objective quantification of automobile Strut noise. Institute of Noise Control Engineering, 1999, pp. 17 – 27
**[13]** Alberdi, M.; Carnicero, R.; Biera, J.: Shock absorber‘s knocking noise, 2002, Proceedings of ISMA, Volume V, pp. 1897 – 1902
**[14]** Kruse, A.; Schreiber, R.: Einfluss des dynamischen Druckaufbaus im Stoßdämpfer auf Fahrwerksgeräusche. VDI-Berichte No. 2003, 2007, pp. 437 – 448
**[15]** Sacramento, G.; Biera, J.: Simulation tool for shock absorber noise prediction in time and frequency domains. J. Vehicle Noise and Vibration, 2007, pp. 217 – 229
**[16]** Kruse, A.; Zimmermann, G.: Einfluss der Reibung auf das hochfrequente Schwingungsverhalten von Stoßdämpfern. VDI-Berichte No. 1736, 2002, pp. 47 – 58
**[17]** ZF Friedrichshafen AG: internes Dokument
**[18]** Eickhoff, M.; Sonnenburg, R.; Stretz, A.: Kolbenstangenschwingungen in Dämpfermodulen, Ursachen und Abstellmaßnahmen. In: ATZ 112 (2010), No. 1, pp. 34 – 39
**[19]** Sonnenburg, R.; Stretz, A.: Damper modules with adapted stiffness ratio. Archive of Applied Mechanics 81 (2011), No. 7, pp. 853 – 862, ISBN DOI 10.1007/s00419-010-0455-2

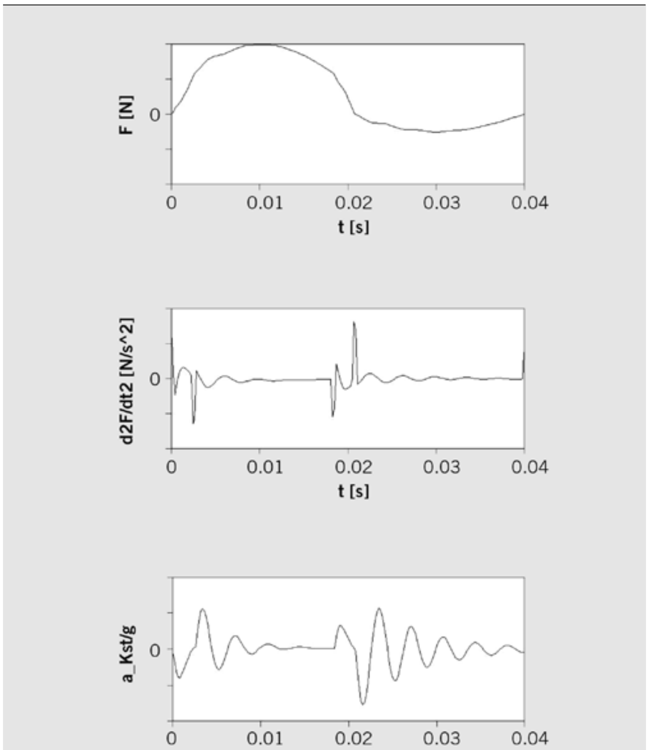


❽ Time response of module induced piston rod vibrations